REGULATION OF FIBRINOLYSIS BY S100A10 *IN VIVO*

by

Alexi P. Surette

Submitted in partial fulfilment of the requirements
for the degree of Doctor of Philosophy

at

Dalhousie University
Halifax, Nova Scotia
October 2011

DALHOUSIE UNIVERSITY

DEPARTMENT OF BIOCHEMISTRY AND MOLECULAR BIOLOGY

The undersigned hereby certify that they have read and recommend to the Faculty of Graduate Studies for acceptance a thesis entitled "REGULATION OF FIBRINOLYSIS BY S100A10 *IN VIVO*" by Alexi P. Surette in partial fulfilment of the requirements for the degree of Doctor of Philosophy.

Dated: October 13, 2011

External Examiner: _____

Research Supervisor: _____

Examining Committee: _____

_____

_____

Departmental Representative: _____

DALHOUSIE UNIVERSITY

DATE: October 13, 2011

AUTHOR: Alexi P. Surette

TITLE: REGULATION OF FIBRINOLYSIS BY S100A10 *IN VIVO*

DEPARTMENT OR SCHOOL: Department of Biochemistry and Molecular Biology

DEGREE: PhD CONVOCATION: May YEAR: 2012

_____

Signature of Author

...Dedicated to Tia

TABLE OF CONTENTS

LIST OF TABLES

LIST OF FIGURES

ABSTRACT

Endothelial cells form the inner lining of vascular networks and maintain blood fluidity by inhibiting blood coagulation and promoting blood clot dissolution (fibrinolysis). Plasmin, the primary fibrinolytic enzyme, is generated by the cleavage of the plasma protein, plasminogen, by its activator, tissue plasminogen activator (tPA). This reaction is regulated by plasminogen receptors at the surface of the vascular endothelial cells. Previous studies have identified the plasminogen receptor protein, S100A10 as a key regulator of plasmin generation by cancer cells and macrophages. Here we examine the role of S100A10 and its annexin A2 binding partner in endothelial cell function using a homozygous S100A10-null mouse. Compared to wild-type mice, S100A10-null mice displayed increased deposition of fibrin in the vasculature and reduced clearance of batroxobin-induced vascular thrombi, suggesting a role for S100A10 in fibrinolysis *in vivo*. Compared to WT cells, endothelial cells from S100A10-null mice demonstrated a 40% reduction in plasminogen binding and plasmin generation *in vitro*. Furthermore, S100A10-deficient endothelial cells demonstrated impaired neovascularization of Matrigel plugs *in vivo* suggesting a role for S100A10 in angiogenesis. These results establish an important role for S100A10 in the regulation of fibrinolysis and angiogenesis *in vivo*, suggesting S100A10 plays a critical role in endothelial cell function.

LIST OF ABBREVIATIONS AND SYMBOLS USED

ε-ACA – ε-aminocaproic acid

AIIt – annexin A2 heterotetramer

ADP – adenosine di-phosphate

APC – activated protein C

aPTT – activated partial thromboplastin time

bFGF – basic fibroblast growth factor

BSA – bovine serum albumin

cDNA – complementary deoxyribonucleic acid

CpB – carboxypeptidase B

CSF – colony-stimulating factor

Cys – cysteine

DAPI – 4',6-diamidino-2-phenylindole

DMEM – Dulbecco's minimal eagle media

DNA – deoxyribonucleic acid

DNase – deoxyribonuclease

dNTP – deoxyribonucleotide triphosphate

DPBS – Dulbecco's phosphate buffered solution

DTT – dithiothreitol

EBM-2 – endothelial basal medium 2

EDTA – ethylenediaminetetraacetic acid

EGTA – ethylene glycol tetraacetic acid

eNOS – endothelial nitric oxide synthase

ERK – extracellular signal-regulated kinase

FACS – fluorescence activated cell sorting

FBS – fetal bovine serum

Fg - fibrinogen

FITC - fluorescein isothiocyanate

GAPDH - glyceraldehyde 3-phosphate dehydrogenase

Glu-pg – glutamate plasminogen

Glu-Pm – glutamate plasmin

GPCR – G-protein coupled receptor

HBSS – Hanks buffered salt solution

Hci - homocystine

Hcy – homocysteine

HEPES – 4-(2-hydroxyethyl)-1-piperazineethanesulfonic acid

HIF – hypoxia inducible factor

HTL – homocysteine thiolactone

IL – interleukin

LDL – low density lipoporotein

LPS – lipopolysaccharide

Lys-Pg – lysine plasminogen

Lys-Pm – lysine plasmin

MMEC – murine microvascular endothelial cell

MMP – matrix metalloproteinase

NO – nitric oxide

PA – plasminogen activator

PAGE – polyacrylamide gel electrophoresis

PAI – plasminogen activator inhibitor

PAN – plasminogen apple nematode

PAP – plasmin-antiplasmin

PARs – protease-activated receptors

PBS – phosphate buffered solution

PCR – polymerase chain reaction

Pg - plasminogen

PGI_2 – prostacyclin

Pm - plasmin

PT – prothrombin time

qPCR – quantitative real time polymerase chain reaction

RNA – ribonucleic acid

s.c. – sub cutaneous

sc-tPA – single chain tissue type plasminogen activator

sc-uPA – single chain urokinase type plasminogen activator

SD – standard deviation

SDS – sodium dodecyl sulfate

SEM – standard error of the mean

shRNA – short hairpin ribonucleic acid

TAFI – thrombin activatable fibrinolysis inhibitor

TF – tissue factor

TGF – transforming growth factor

TIME – telomerase immortalized microvascular endothelial

TLR – toll-like receptor

TNF – tumor necrosis factor

tPA – tissue type plasminogen activator

tc-tPA – two chain tissue type plasminogen activator

uPA – urokinase type plasminogen activator

uPAR – urokinase type plasminogen activator receptor

UCLA – University committee on laboratory animals

VE – vascular endothelial

VEGF – vascular endothelial growth factor

vWF – von Willebrand factor

WPB – Weibel-Palade bodies

WT – wild type

ACKNOWLEDGEMENTS

I would like to thank Dr. David Waisman for the mentorship and support he has provided over the past five years. I am also thankful to my fellow Waisman lab members Kyle, Pat, Vicky, Paul, Mike, Yi, Rob, Erta and Tracy for providing an enjoyable work atmosphere and for lending a helping hand whenever one was needed. You have all helped make the past five years memorable and our conversations, though usually not scientific, helped me persevere through this degree.

Also, I wish to thank my supervisory committee, Dr. Kirill Rosen, Dr. Brent Johnston and Dr. Andrew Issekutz, for their advice and encouragement.

I also would like to thank Andrew, Brian, Kyle (again), Tyler, Craig, Matt and Tom for all of the sports and non-sport related conversations and activities we have had over the years. These have helped keep me sane over the years and I have truly enjoyed all of them.

Finally, I would like to thank my family for all of their love and support during this degree. Maman, je t'aime beaucoup et j'apprécie tous les sacrifices que tu as fait pour moi. Sans toi, ceci ne serai pas possible. Papa, j'adore nos conversations sur le sport et la politique et nos discussions sur la science m'ont donné de l'inspiration et m'ont aidé à persévérer. Sans ton support et ton exemple, je n'aurai pas accomplis ce doctorat. Merci. Sophie et Amélie, vous êtes les meilleures sœurs du monde. J'apprécie toujours êtres avec vous et votre support est grandement apprécié. Hailey, you have been an incredible addition to my life and I really enjoy all of the time I have spent with you over the last few years. Last, but not least, I want to thank Tia. Without your love, support, encouragement and patience, this degree would have been immensely more difficult. I love you and thank you so much for becoming part of my life during this degree.

CHAPTER 1: INTRODUCTION

1.1 Coagulation

Blood clots (thrombi) are formed in the vasculature in order to stop blood loss following damage to blood vessels. Tissue factor is sequestered from circulation under normal conditions, primarily by endothelial cells, adventitial fibroblasts, pericytes and smooth muscle cells.[1] Following vessel injury, a clotting cascade involving circulating inactive serine proteases (pro-enzymes) with specific targets is initiated. Tissue factor is exposed to the clotting factors present in the blood. Tissue factor is now able to interact with Factor VII to activate it into Factor VIIa. Factor VIIa activates Factor X into Factor Xa, which in turn activates prothrombin into the active protease thrombin. Circulating fibrinogen (Fg) is cleaved by thrombin into fibrin to form the main protein component of blood clots.[2] This mechanism for initiation of coagulation is known as the tissue factor pathway (Figure 1A). Another mechanism for initiating coagulation is known as the contact activation pathway. Similar to the tissue factor pathway, the contact activation pathway can also be initiated by damage to cell surfaces. In this pathway, the damaged cell surface along with exposed collagen provides a matrix for the activation of various factors leading to clot formation. Following damage, Factor XII interacts with high-molecular-weight kininogen and prekallikrein, resulting in the active Factor XIIa, which activates Factor XI to Factor XIa. Factor XIa activates Factor IX to Factor IXa. Factor IXa then interacts with Factor VIIIa to activate Factor X. Following Factor Xa activation, thrombin is activated to cleave fibrinogen into fibrin (Figure 1B).[3-5] Damage to the endothelium also results in the exposure of collagen in the sub-endothelial matrix. Exposed collagen activates circulating platelets, which also contribute to the formation of

the clot.[6] However, blood clots do not only form in order to prevent blood loss following injury. Blood clots are continually forming due to sluggish blood flow, the presence of tissue debris in the blood, or lipids.[7-9] Certain pathological conditions such as atherosclerosis[10] and cancer[11] may also result in undesirable formation of clots. An inability to clear clots in a proper fashion may result in myocardial infarction and stroke.[12] It is therefore necessary to have a system capable of degrading clots when they are unwanted or no longer necessary.

Figure 1. Coagulation pathways. The two predominant coagulation pathways are shown. The tissue factor (extrinsic) pathway relies on the exposure of tissue factor following blood vessel damage to initiate coagulation (A) while the contact activation (intrinsic) pathway is tissue factor independent and relies on a cascading activation of serine proteases to initiate coagulation (B). Abbreviations used: Tissue factor (TF), factor (F), prekallikrein (PK), high-molecular-weight kininogen (HK), activated protein C (APC), thrombomodulin (Tm), endothelial cell (EC).

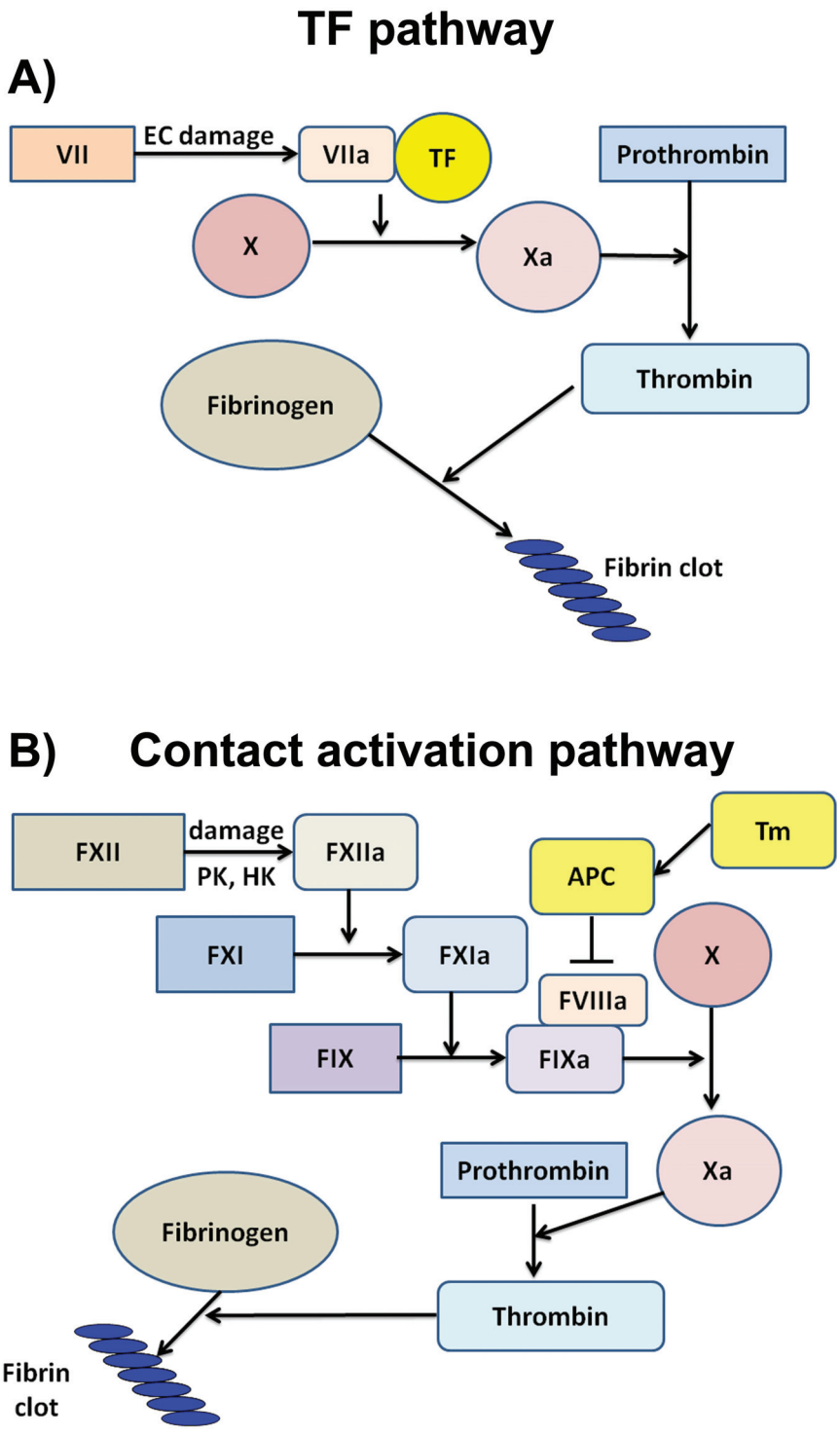
TF pathway
A)
VII
EC damage
VIIa
TF
Prothrombin
X
Xa
Thrombin
Fibrinogen
Fibrin clot
B) Contact activation pathway
FXII
damage
PK, HK
FXIIa
Tm
APC
FXI
FXIa
X
FVIIIa
FIX
FIXa
Prothrombin
Xa
Fibrinogen
Thrombin
Fibrin clot

1.2 The Plasminogen/Plasmin Fibrinolytic System

In order to degrade blood clots in the vasculature, the inactive zymogen plasminogen (Pg) is converted to the active protease plasmin. The primary function of plasmin is to degrade fibrin, the protein component of blood clots, in a process known as fibrinolysis.[13] Activation of Pg by the Pg activators (PAs), the tissue-type plasminogen activtor (tPA) and the urokinase-type plasminogen activator (uPA), is tightly regulated, as is regulation of plasmin once it has been activated.

1.2.1 Plasminogen

N-terminal glutamic acid plasminogen (Glu-Pg), a single-chain 92 kDa glycoprotein, is secreted from the liver and circulates in the plasma at a concentration of 1.5 μM.[14] Glu-Pg is composed of seven domains: an N-terminal plasminogen-apple-nematode (PAN) domain, five kringle domains (K1-K5) and a serine protease domain (Figure 2).[15] The PAN domain, consisting of the first 77 amino acid residues of the N-terminus, interacts with the kringle domains to regulate its activity.[16] The PAN-kringle interaction results in a closed conformation that is more resistant to activation.[17,18] Removal of the PAN domain generates Lys^{77}-plasminogen (Lys-Pg), which results in an open conformation that is more susceptible to activation. Cell bound Glu-Pg is converted to Lys-Pg by plasmin, increasing the rate of Pg activation by PAs.[19]

The kringle domains of Pg serve as docking sites for protein-protein interactions as well as playing a critical role in regulating Pg conformation. Most importantly, they serve as docking sites for interactions with fibrinogen and cell surface Pg receptors containing C-

terminal lysines. Of the five kringle domains, only K3 lacks a lysine-binding site while K1 and K4 have the highest affinity binding sites for lysine (Figure 2).[15,20-23]

Figure 2. Structure of plasminogen. The full length structure of human Pg is shown, with one letter amino acid code representing the amino acid sequence. Pink coloured wavy lines represent glycosylation sites while black lines connecting cysteine residues indicate disulfide bonds. Kringles 1-3 are orange, kringle 4 is red, kringle 5 is purple and the plasmin catalytic domain in gray. Adapted from[24].

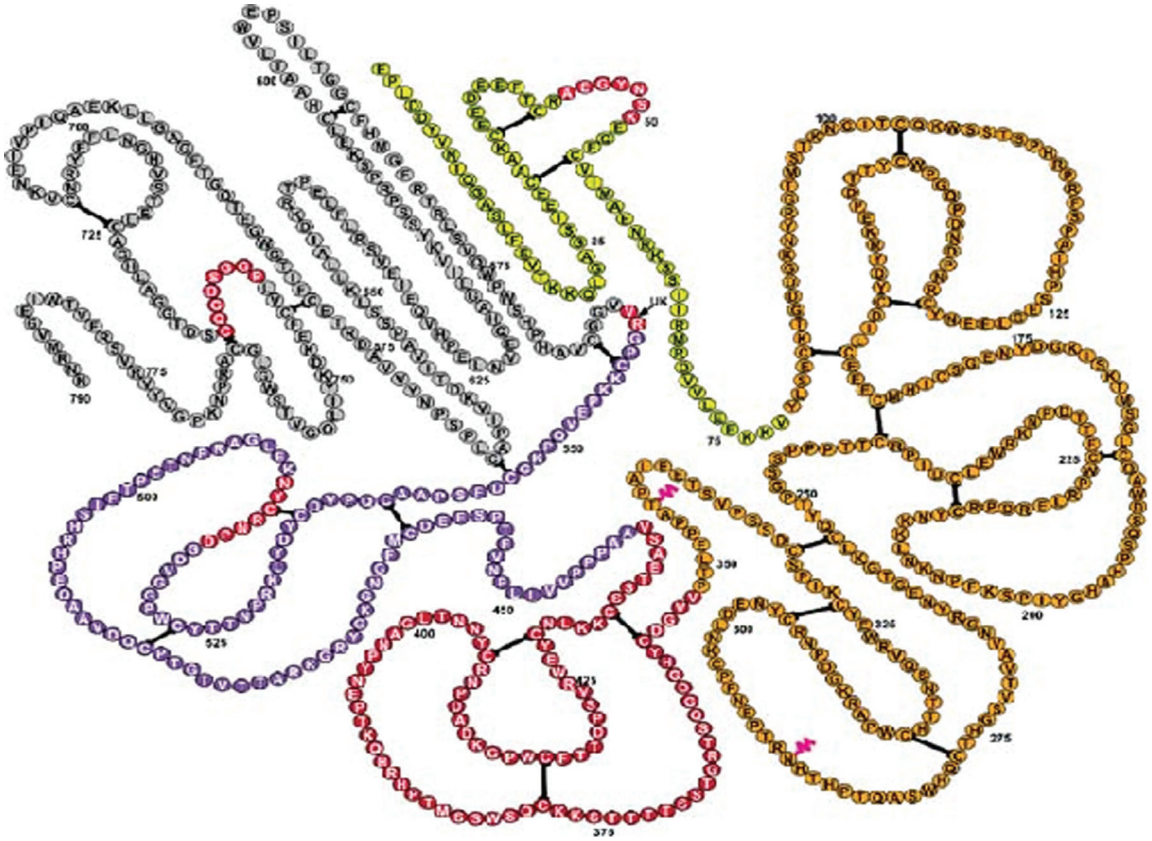

1.2.2 Plasmin

Plasmin (Pm), formed following the activation of Pg by Pg activators, is a serine protease primarily responsible for cleaving the fibrin component of clots. In addition to cleaving fibrin, plasmin is also capable of cleaving other extracellular matrix proteins, including fibronectin,[25] laminin,[26] thrombospondin[27] and von Willebrand factor (vWF).[28] Binding of Pg and plasmin occurs on a multitude of different cell types, including endothelial cells, fibroblasts, leukocytes, cancer cells, platelets, epidermal cells, neuronal cells and hepatocytes.[6,29-32] Localization of Pg and Pm on the cell surface allows Pm to be present at sites requiring blood clot dissolution, as well as in the invasiveness of various cell types.[29,33-39] Such spatio-temporal plasmin generation therefore allows Pm to participate in various cell-specific proteolytic events.

Plasmin is also capable of initiating a proteolytic cascade by activating several matrix metalloproteases (MMPs),[40,41] which are capable of degrading other components of the extracellular matrix. The development of the Pg null mouse has demonstrated that plasmin activity is critical in several physiological processes, including wound healing,[42,43] liver repair,[44] adipose tissue development[45] and breast feeding.[46] Experiments conducted using the $Pg^{-/-}$ mouse have established that Pm is the key fibrinolytic enzyme. $Pg^{-/-}$ mice display spontaneous fibrin deposits due to decreased fibrinolysis and have an impaired ability to clear thrombi experimentally lodged in the lungs.[34] Administration of a bolus of Pg results in restoration of thrombolytic potential in $Pg^{-/-}$ mice as fibrin deposits disappeared and experimentally lodged thrombi were cleared following Pg injection.[47] Induction of vascular injuries in $Pg^{-/-}$ mice demonstrated that Pm is involved in proper

vascular remodelling in response to injury.[48-50] Further proof that the effects observed in the $Pg^{-/-}$ mouse were due to impaired fibrinolysis was obtained by crossing the $Pg^{-/-}$ mouse with the $Fg^{-/-}$ mouse. In addition to increased fibrin deposition, the $Pg^{-/-}$ also suffered from progressive wasting syndrome, which is characterized by runting, weight loss and premature death.[34] Interestingly, the $Pg^{-/-}Fg^{-/-}$ mouse did not suffer from progressive wasting syndrome.[51] Adverse health effects associated with loss of Pg were therefore due, at least in large part, to an inability to deal with fibrin deposits which occur normally.[51] Loss of Pg also impaired macrophage infiltration in response to inflammatory stimuli.[37] Plasmin is also involved in the development of several pathologies, including cancer growth[52-54] and metastasis,[55] acute promyelocytic leukemia,[56] angiogenesis,[38,57,58] atherosclerosis[59] and neurodegeneration.[60] A role for Pm in the progression of antigen-induced arthritis was also observed in the $uPA^{-/-}$ mouse, as the inability to clear fibrin deposits within the joints exacerbated the progression of the disease.[61] Plasmin contributes to angiogenesis[38] by releasing and activating growth factors stored in the extracellular matrix.[40,62] Regulation of plasmin generation is therefore critical since insufficient, excessive and improper localization of plasmin activity can result in severe pathological outcomes.

1.2.3 Plasminogen Activation

Activation of Pg into plasmin is catalyzed by the Pg activators, tPA and uPA. Highly specific serine proteases, tPA and uPA activate Pg into Pm by cleaving Pg between Arg^{561}-Val^{562}. As a result of this cleavage, Glu-Pg becomes two-chained Glu-Pm, which consists of a 561 amino acid heavy chain linked by two disulfide bonds to a 230 amino acid light

chain. Plasmin is stabilized by a salt bridge that is formed between the N-terminal Val^{562} created by the cleavage and Asp^{740}. The oxyanion hole and substrate binding pocket of the active site of plasmin, found in the serine protease domain, is stabilized by this salt bridge. The catalytic triad of His^{603}, Asp^{646} and Ser^{741} is found within the serine protease domain in the light chain of Pm.[63,64] Since systemic plasmin activity would lead to excessive fibrinolysis, active plasmin is highly regulated. α2-antiplasmin binds free plasmin with high affinity in the blood and forms the irreversible, covalently linked plasmin-antiplasmin complex which inhibits plasmin activity.[65-67] Plasmin in the serum is also inhibited by α2-macroglobulin.[68] These plasmin inhibitors ensure that plasmin activity is localized to sites requiring plasmin mediated proteolysis and prevent systemic plasmin activity.

1.2.4 Plasminogen Activators

Pg is activated into plasmin by two PAs: tissue-type Pg activator (tPA) and urokinase-type Pg activator (uPA). tPA, which is primarily synthesized by endothelial cells, keratinocytes and in the brain, is the primary PA responsible for vascular fibrinolysis. Produced as a single-chain 72 kDa protein (sctPA), it is converted into the more active two-chain (tctPA) by plasmin, kallikrein and factor Xa.[68] This conversion of sctPA to tctPA increases tPA activity by 15-fold.[69] Binding of sctPA to fibrin results in a conformational change which increases its activity to levels comparable to that of tctPA.[70] tPA also binds to cell surface receptors with C-terminal lysines via its kringle domains in a manner similar to the way Pg binds to cell receptors.[71,72] tPA has the ability to bind both fibrin and endothelial cells, allowing co-localization of tPA and Pg for optimal Pg activation at sites requiring Pm activity.

uPA is secreted by many cell types, including leukocytes, fibroblasts, keratinocytes, epithelial cells, endothelial cells and cancer cells.[29] uPA is secreted as an inactive single-chain polypeptide termed pro-uPA (or scuPA). Binding of pro-uPA to its cellular receptor, urokinase PA receptor (uPAR) facilitates the activation of pro-uPA to active uPA by several proteases including plasmin, cathepsin B, factor VIIa and certain MMPs.[68,73,74] Increased uPA expression and activity is associated with increased invasiveness of various cell types, including cancer cells.[75-77] uPA activity can be correlated with cancer metastasis and can be an indicator of disease recurrence. For these reasons, uPA-uPAR have been targets for various targeted cancer therapies.[52,77-79]

Plasmin is capable of activating both of its activators in a process termed reciprocal zymogen activation.[80,81] This allows a sudden burst of localized plasmin activity at sites requiring plasmin proteolysis. The regulation of PAs is therefore also important to prevent unnecessary fibrinolysis and ensure proper spatio-temporal plasmin activity.

1.2.5 Plasminogen Activator Inhibitors

Inhibition of the PAs is mediated by the Pg activator inhibitors (PAIs). PAI-1 is the primary PAI and is produced and secreted in the vasculature by the liver, smooth muscle cells, adipocytes and platelets. PAI-1 has a short half life when circulating in plasma but binding of PAI-1 to vitronectin in the extracellular matrix (ECM) significantly prolongs its half life.[82] Binding of PAI-1 to the uPA-uPAR complex results in endocytosis of the complex, removing active uPA from the cell surface and decreasing uPA dependent Pg activation.[83] Following the binding of tPA and PAI-1, the tPA-PAI-1 complex is internalized by the low-density lipoprotein-related and very low-density lipoprotein receptors and degraded.[84,85] PAI-1 is therefore capable of decreasing plasmin mediated proteolytic capacity by mediating the removal and degradation of plasmin activators found in circulation.

1.2.6 Cell Surface Receptors for Plasminogen and Plasminogen Activators

In order to localize Pg activation to the surface of cells requiring proteolysis, cells utilize a variety of molecules that have the ability to bind to Pg with low affinity (Kd = 1 μM) and high capacity (10^4-10^7 receptors per cell).[86-89] Cell surface receptors for Pg include several proteins and gangliosides.[13] Extensive work has demonstrated that binding of Pg to eukaryotic cells is blocked by peptides containing C-terminal lysines, lysine and lysine analogs such as ε-aminocaproic acid (ε-ACA). These experiments led to the conclusion that cell surface proteins containing C-terminal lysines interact with the kringle domains of Pg to mediate binding of Pg to cell surfaces (Figure 3).[30,90,91] A list of cell surface Pg receptor proteins can be found in table 1. Among the proteins with C-terminal lysines

which function as cell surface Pg receptors are α-enolase,[91] Plg-R_{TK},[92] cytokeratin 8,[93] histone H2B[94] and the annexin A2 heterotetramer (AIIt).[95] Of particicular interest to this thesis is AIIt, which will be discussed in detail in sections 1.3 and 1.4.

Figure 3. Interaction between the lysine binding kringle domain of plasminogen and the carboxyl-terminal lysine residue of the plasminogen receptors. Lysine-binding sites in the Pg kringle domain interacts with a carboxyl-terminal lysine on the Pg receptor. The anionic, cationic and hydrophobic nature of the carboxyl-terminal lysine interacts with three distinct regions within the kringle: the cationic center, the anionic center and the hydrophobic groove.

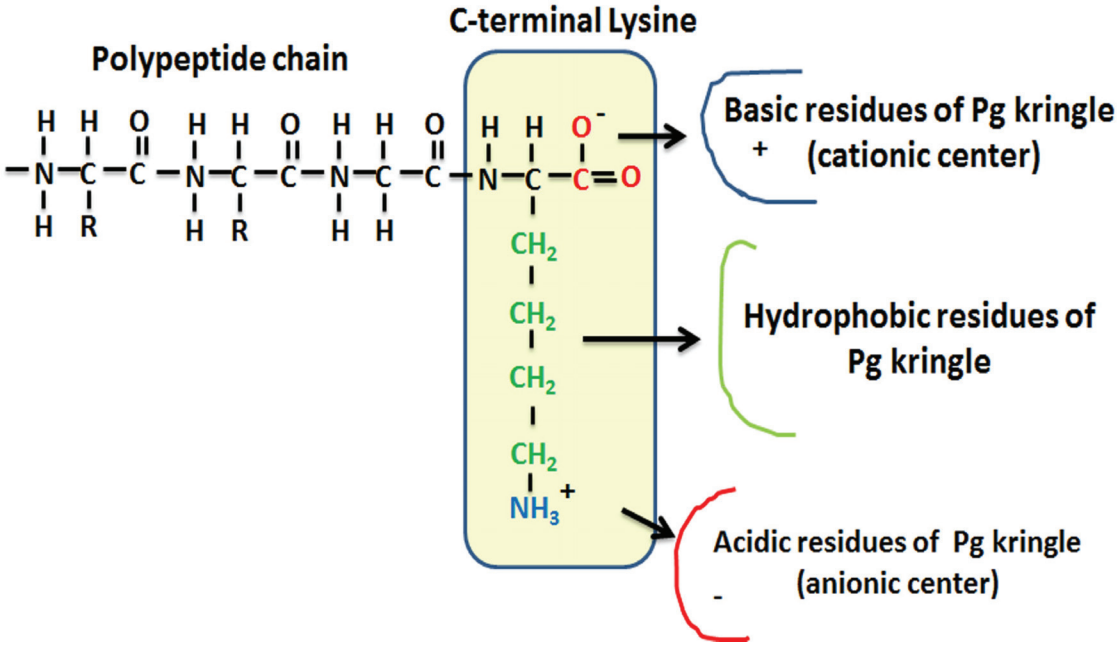
C-terminal Lysine
Polypeptide chain
Basic residues of Pg kringle
(cationic center)
Hydrophobic residues of
Pg kringle
Acidic residues of Pg kringle
(anionic center)

Table 1. Identified cell-surface receptor proteins for plasminogen

Receptor	Cell type	Contains C-terminal lysine
Annexin A2[93]	Various	No
Annexin A2 heterotetramer[94]	Various	Yes
Histone 2B[95]	Various	Yes
Integrin αMβ2[96]	Leukocytes	No
GAPDH[97]	Streptococcus pyogenes 64/14	Yes
Actin[98]	Endothelial cell	No
Gp330[99]	Kidney epithelial	No
α-enolase[100]	U-937	Yes
Cytokeratin 8[90]	Epithelial cell	Yes
Histone-proline rich glycoprotein (HPRG)[101]	Various	Yes
Plg-R_{TK}[102]	Catecholaminergic cells	Yes

1.2.7 Plasminogen Receptor Inhibitors

Activation of Pg may also be regulated by Pg receptor inhibitors, which remove C-terminal lysine from Pg receptors, preventing binding of Pg. Some of the more prevalent Pg receptor inhibitors are thrombin-activated fibrinolysis inhibitor (TAFI), carboxypeptidase B and carboxypeptidase N.[96-100] Hydrolysis of the C-terminal lysine by these enzymes prevents C-terminal lysine dependent Pg and tPA binding to cell surfaces, which results in decreased co-localization between Pg and PAs. Additionally, since PAs and Pm are no longer protected by being bound to cell surface receptors, there are increased interactions between PA and PAIs and Pm and α2-antiplasmin.[101] Regulation of Pg activation is therefore a complex process that limits plasmin mediated proteolysis to sites requiring plasmin activity (Figure 4).

Figure 4. Regulation of Plasmin Activation and Activity. Activation of Pg into the active serine protease plasmin is catalyzed by two Pg activators, the tissue-type Pg activator (tPA) and the urokinase-type Pg activator (uPA). tPA and uPA are inhibited by the Pg activator inhibitors (PAIs), while active plasmin is inhibited by α2-antiplasmin and α2-macroglobulin. Plasmin degradation of fibrin clots is inhibited by thrombin-activated fibrinolysis inhibitor (TAFI). Inhibitors are shown in brown boxes and PAs in green boxes.

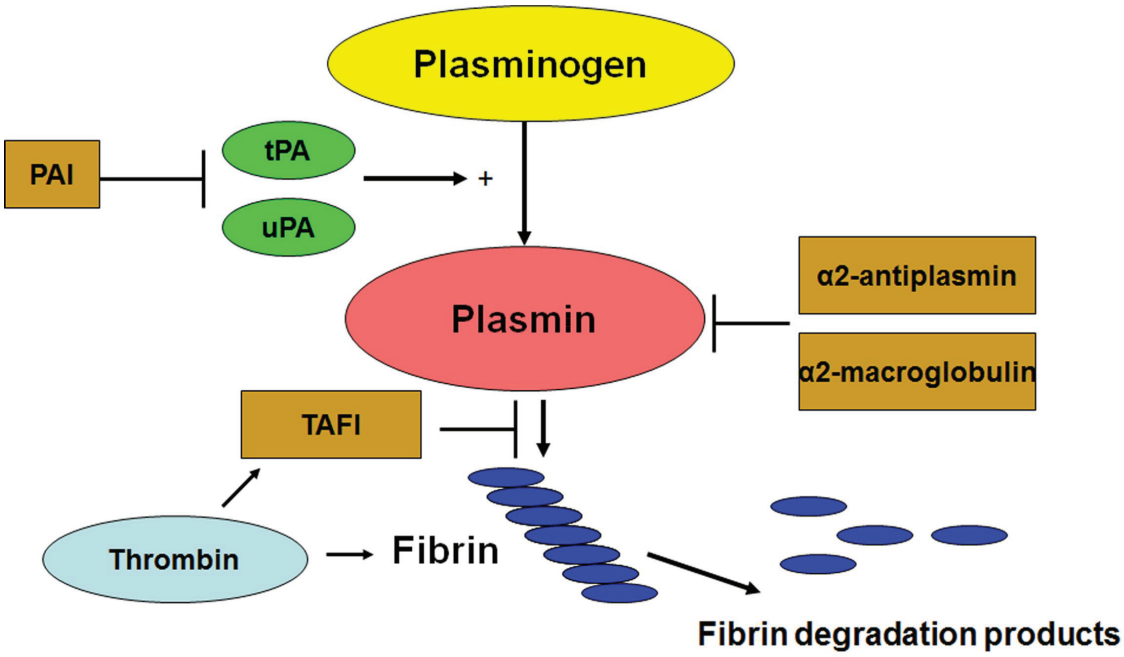
Plasminogen
PAI
tPA
uPA
+
Plasmin
α2-antiplasmin
α2-macroglobulin
TAFI
Thrombin
Fibrin
Fibrin degradation products

1.3 Annexin A2 Heterotetramer

The annexin A2 heterotetramer (AIIt) is composed of two annexin A2 subunits and two S100A10 subunits (figure 5).

1.3.1 Annexin A2

Annexin A2 belongs to the annexin family of proteins. The annexins are characterized by the presence of conserved annexin repeats, which are approximately 70 amino acids in length, and by an ability to bind to negatively charged phospholipids in a Ca^{2+} dependent fashion.[102] Annexins have been shown to participate in numerous cellular processes, including endocytosis,[103] exocytosis,[104] vesicle trafficking,[105] inter-cellular interactions,[106] cellular interactions with the extracellular matrix,[107] ion channel formation[108] and inhibition of phospholipase A2.[109] Annexin A2 exists in both a monomeric and heterotetrameric form with S100A10. The ratio of heterotetrameric/monomeric annexin A2 varies from cell-type to cell-type. Overall, approximately 90% of annexin A2 is present in the heterotetrameric form within cells[110] but can range from nearly 100% heterotetrameric in intestinal epithelial cells to 50% monomeric in fibroblasts.[111] Annexin A2 is predominantly localized in the cytoplasm,[112] the plasma membrane,[113-116] in the nucleus[117,118] and associated with the cytoskeleton.[119] Several studies have observed that AIIt is associated with caveolae.[120-122] A planar curved molecule, annexin A2 has opposing concave and convex sides (Figure 5). The concave side contains the amino- and carboxy-terminals of the protein while the convex side contains the phospholipid and Ca^{2+} binding sites.[123,124] Several regulatory sites exist on the concave side of the annexin A2. The N-terminal regions contains the S100A10 binding site (S1-G14)[110] along with several sites

for post-translational modifications, including a redox sensitive cysteine (C8) which is glutathionylated,[125] three phosphorylation sites (S11, Y23 and S25) which have regulatory functions[126-130] and a nuclear export signal.[118] Annexin A2 may be phosphorylated by pp60src,[131] c-src and protein kinase C.[127,129] Such phosphorylation events can be controlled by growth factor signaling cascades[132-134] and regulate cellular processes such as Rho-mediated actin rearrangement,[130] cell surface AIIt localization [128] and annexin A2 nuclear entry.[135]

Figure 5. Structure of annexin A2 heterotetramer (AIIt). An illustration of the structure of AIIt. Two annexin A2 subunits interact with two S100A10 subunits.

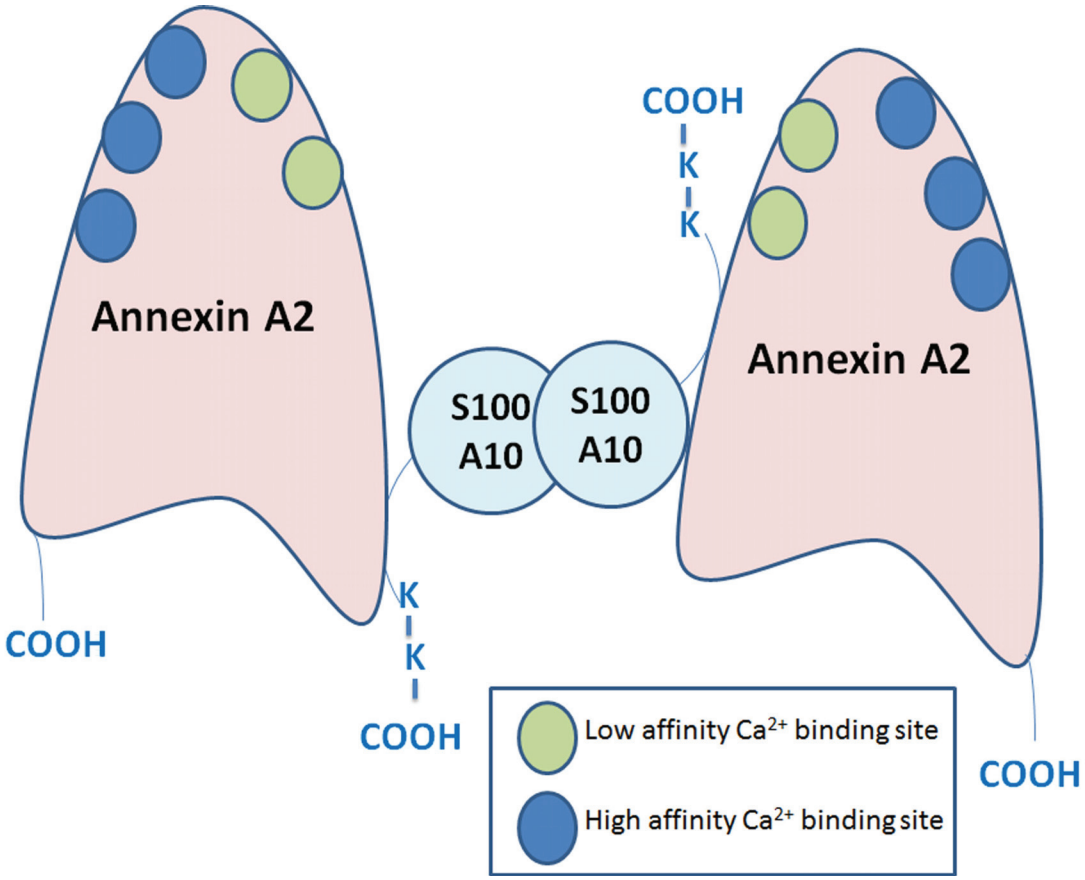
Annexin A2
COOH
K
K
COOH
S100
A10
S100
A10
Annexin A2
COOH
K
K
COOH
Low affinity Ca2+ binding site
High affinity Ca2+ binding site

Annexin A2 may also be ubiquitinated, yet this modification does not appear to target the protein for proteasomal dependent degradation. Instead, it possibly regulates actin binding.[136] The C-terminal region of the protein has another redox sensitive cysteine (C132), which is also susceptible to glutathionylation. Reversible glutationylation at C8 and C132 regulates annexin A2 binding to F-actin and phospholipids.[137] Also located in the C-terminal region are binding sites for F-actin,[138] Ca^{2+} and phospholipids,[110,139] heparin[140] and fibrin.[141] The region between F32 and D338 of the protein contains Ca^{2+} binding sites with the sequence GxGT-[38 aa]-D/E[123] and consists of four 68-69 amino acid long homologous repeats containing five helices.

Functionally, annexin A2 has been shown to participate in a variety of cellular processes. Of particular interest to this thesis is that annexin A2 serves to anchor AIIt to the extracellular cell surface, allowing the Pg receptor S100A10 to regulate the conversion of Pg into plasmin.[95,110,115,116,142,143] Annexin A2 lacks a typical signal peptide for transport to the extracellular membrane. Phosphorylation of annexin A2 at tyrosine 23 is necessary for translocation of AIIt from the cytoplasm to the extracytoplasmic plasma membrane. Transport to the extracellular membrane as a result of this phosphorylation occurs independently of the classical endoplasmic reticulum-golgi pathway.[144] In addition, binding of annexin A2 to intracellular S100A10 blocks polyubiquitinylation of S100A10 and subsequent proteosomal dependant degradation.[145] Loss of annexin A2 therefore also results in loss of S100A10[146] and the annexin $A2^{-/-}$ mouse can in fact be considered an $AIIt^{-/-}$ mouse. Like other annexins, annexin A2 has been demonstrated to play a role in endocytosis,[103,147-151] exocytosis [152,153] and vesicular transport. [102,110,154] Additionally, annexin

A2 binds with F-actin to modulate the cytoskeleton,[130,138,155,156] interacts with various cell-adhesion molecules including E-cadherin,[157] CD-44,[158] tenascin-C[159] and AHNAK,[160] regulates several ion channels[161,162] and modulates lipid raft organization.[163-165] Annexin A2 has been reported to be overexpressed in a variety of different cancers.[106,166-171] This upregulation may provide several advantages to tumor growth. Increased annexin A2 levels may lead to increased AIIt levels at the cell surface and increase cancer cell proteolytic activity, which increases metastatic and angiogenic potential by providing a mechanism for ECM remodelling required for these processes.[39,58,77,128,172] Additionally, a role for annexin A2 in cellular transformation was first suggested following the observation that annexin A2 was a phosphorylation target of v-Src in transformed fibroblasts.[173] Recent studies have demonstrated that annexin A2 may not only be target of v-Src, but may play a role in proper v-Src cellular localization and may be required for v-Src dependent transformation.[174] Annexin A2 has also been shown to play a role in increased cell motility by modulating rho-dependent actin remodelling.[175] Phosphorylation of S25 localizes annexin A2 to the nucleus and has been shown to associated with nuclear entry, DNA synthesis and cell proliferation.[135] A role in cancer cell redox regulation has also been demonstrated,[176] indicating that annexin A2 may modulate tumorigenesis in a multitude of fashions. Recently, annexin A2 has been described as a receptor in plasmin mediated signaling in monocytes.[177-179] Further investigation into the role annexin A2 and AIIt may play in cell signaling will be described in chapters 4 and 5.

1.3.2 S100A10

S100A10 is a member of the S100 family of proteins, which are small (approximately 10 kDa) usually acidic polypeptides characterized by the presence of an EF-hand calcium binding motif on the N- and C-terminal regions, connected by an unstructured linker region.[180,181] Binding of calcium to the EF-hand domains result in conformational changes, usually resulting in the ability to bind to effector proteins. Therefore, S100 proteins respond to changes in Ca^{2+} concentrations within cells and participate in signaling events in response to these alterations.[182,183] S100 proteins are usually located in the cytoplasm and nucleus, though some are secreted and act as chemoattractants in metastatic disease.[184] S100 proteins are involved in a multitude of cellular processes, including differentiation, cell cycle progression, metabolic regulation and inflammation.[181] S100A10, the primary focus of this thesis, is different from other S100 family members in that a mutation in the EF-hand domain has rendered it insensitive to calcium and is maintained in a constitutively active state.[185-187] S100A10, which was initially discovered with its binding partner, annexin A2[187,188] is therefore able to bind annexin A2 in a Ca^{2+} independent fashion. Expression of S100A10 has been observed in most cell types and tissues. Lung, kidney and intestine have the highest S100A10 levels while expression levels are very low in the liver and absent in red blood cells.[110,189,190] S100A10, usually as part of AIIt, interacts with various other cellular components, including the Rho GTPase-activating protein DLC1,[191] cytosolic phospholipase A2,[192] the potassium channel TASK-1,[193] the sodium channel Na(V)1.8,[194] the calcium channels TRPV5 and TRPV6[195] and the serotonin 1B receptor (5-HT1B receptor).[196,197] Interaction between S100A10 and these trans-membrane proteins is necessary for proper localization and function. S100A10

therefore appears required for proper surface presentation of some receptors and ion channels. Cathepsin B, a lysosomal cysteine-protease, interacts with the S100A10 in AIIt on the cell surface.[198] Subsequent work from the Sloane laboratory showed that caveolin-1 may participate in localization of S100A10 and AIIt to the extracellular membrane and that this was important in localization of cathepsin B to the cell surface.[199] AIIt in caveolae may therefore promote proteolysis in multiple ways: by mediating Pg activation and interacting with another protease, cathepsin-B. Our laboratory has demonstrated that S100A10 on the cell surface directly binds Pg and tPA, thus promoting conversion of Pg into the active serine protease plasmin.[39,95,115,116,143]

1.3.3 Role of AIIt in fibrinolysis

Initially, annexin A2 was identified as a cell surface Pg and tPA receptor.[200-202] More recently, our laboratory has expanded on the original model to demonstrate that annexin A2 serves to localize AIIt to the cell surface and that it is the S100A10 portion of the heterotetramer that acts as the Pg and tPA receptor.[95,116,143] Surface plasmon resonance studies have demonstrated that S100A10 binds Pg (K_d=1.81 μM), tPA (K_d=0.45 μM) and plasmin (K_d=0.36 μM) while AIIt binds to Pg (K_d=0.11 μM), tPA (K_d=0.68 μM) and plasmin (K_d=77 nM). Annexin A2, on the other hand, failed to bind to Pg and tPA but displayed binding affinity for plasmin (K_d=0.78 μM). Treatment with carboxypeptidase B (CpB) removed C-terminal lysines of S100A10 and abrogated Pg and tPA binding to S100A10 and AIIt.[95,203] In AIIt, only S100A10 contains a C-terminal lysine, fulfilling a requirement for Pg binding. Characterization of the ability of the components of AIIt to activate Pg into plasmin in a tPA dependent fashion support these binding studies.

S100A10 itself was able to increase the rate of tPA dependent plasmin generation 46 fold, while AIIt increased the rate 77 fold. Annexin A2, on the other hand, was only able to increase the rate of generation 2 fold. The presence of S100A10 and AIIt also protected plasmin from inactivation by α2-antiplasmin and tPA inactivation by PAI-1.[143] AIIt also promotes plasmin activation by co-localizing on the cell surface with uPAR, bringing cell bound Pg into close proximity with its other activator.[39,143,172] Loss of S100A10 and/or AIIt from the cell surface results in decreased plasmin activation in several cell types, including macrophages,[142,204] fibrosarcoma (HT-1080),[39] colorectal cancer (colo 222),[172] breast cancer,[205] leukemic[206,207] and endothelial cells.[208,209] Depletion of S100A10 in HT-1080 fibrosarcoma cells by transfection with antisense S100A10 also significantly reduced tumor growth in SCID mice.[39] Loss of S100A10 and/or AIIt in these cells also results in impaired invasiveness through extracellular matrices, indicating that AIIt dependent plasmin activation is critical in cellular invasion in processes such as fibrinolysis, angiogenesis, tumor growth and macrophage infiltration. AIIt, through S100A10, is therefore a critical regulator of plasmin activation at the cell surface.

1.4 Endothelial Cells

Endothelial cells line blood vessels and participate in a wide range of physiological processes (Figure 6). One of the primary functions of the endothelium is to control thrombotic and fibrinolytic systems to ensure proper blood flow is maintained under normal physiological conditions. Endothelial cells from different parts of the body vary in function. For example, endothelial cells in the liver, spleen and bone marrow sinusoids are lined in a discontinuous fashion as to allow cellular trafficking between them while

endothelial cells in endocrine glands and in peritubular capillaries of the kidney are fenestrated as to allow selective permeability.[210] Endothelial cells from large vessels like the aorta and the umbilical vein also differ from endothelial cells isolated from smaller vessels and capillaries. Microvascular endothelial cells are considerably more proteolytically active than macrovascular endothelial cells since they express higher levels of tPA[211] and MMPs.[212] Consequently, microvascular endothelial cells are more active in fibrinolysis and angiogenesis than macrovascular endothelial cells.[213] The roles of the endothelium in angiogenesis will be described in detail later in this section and in the maintenance of vascular patency will be discussed in further detail in section 1.5. Endothelial cells form a semi-permeable barrier that regulates the passage of nutrients, fluids and leukocytes between the blood and interstitial space. This allows nutrients to flow through the body in a regulated fashion and nourish tissues and organs while also participating in controlling inflammatory responses. In order to regulate this barrier, endothelial cells interact with one another and with other vascular cells using cadherin and tight junctions. Cadherin junctions are primarily regulated by vascular endothelial (VE-) cadherin. A transmembrane protein, VE-cadherin links adjacent endothelial cells together to prevent vascular leakage.[214] Alterations of VE-cadherin may result in increased vascular leakage. Among the factors which increase vascular permeability by altering VE-cadherin via phosphorylation are histamine,[215] lipopolysaccharides (LPS)[216] and vascular endothelial growth factor (VEGF).[217] The cadherin junctions are located immediately basal to the tight junctions.[218] Tight junctions form the barriers that are responsible for the blood-brain barrier and the blood-testis barrier.[219] Tight junctions are more developed in the macrovasculature than in the microvasculature since greater nutrient exchange occurs

in microvascular endothelial cells. Leukocyte infiltration into tissues also normally occurs in post-capillary venules, requiring less developed tight junctions to ease infiltration.[220] Claudins are the major consituent of the tight junctions and, like VE-cadherin, are transmembrane proteins that can be altered by phosphorylation. Transforming growth factor (TGF-) β1 in fact induces phosphorylation of VE-cadherin and claudin-5 to increase vascular permeability in the nervous system.[221] Both cadherin and tight junctions link the extracellular environment with the intracellular environment with the use of transmembrane proteins. The intracellular portions of VE-cadherin and claudins are linked to other protein complexes inside the cell which are linked to the actin cytoskeleton.[222-224]

Figure 6. Endothelial cell functions. Illustration of the various endothelial cell functions.

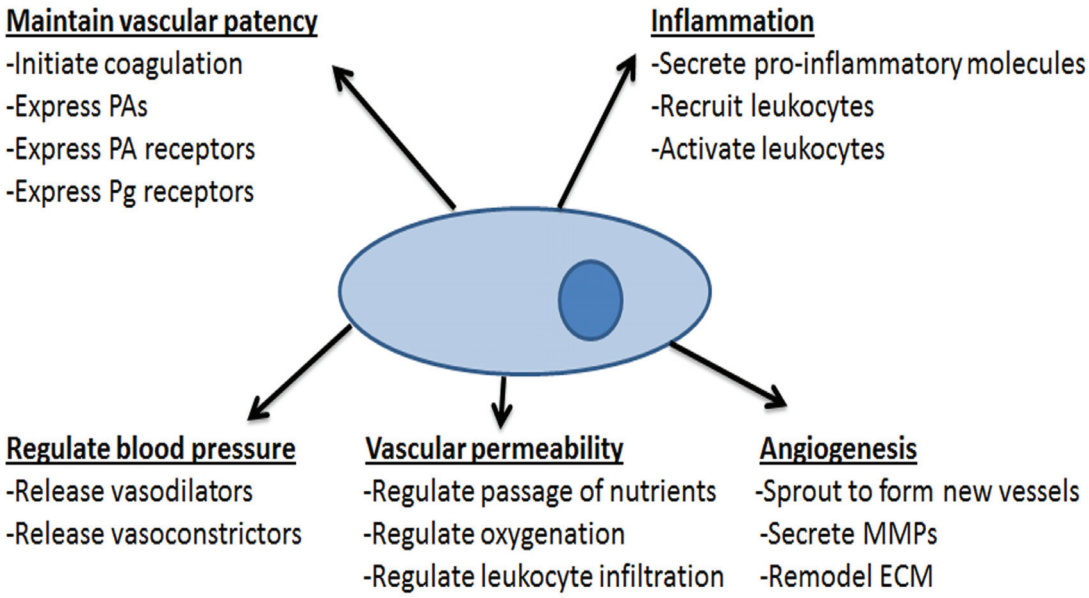
Maintain vascular patency
-Initiate coagulation
-Express PAs
-Express PA receptors
-Express Pg receptors
Inflammation
-Secrete pro-inflammatory molecules
-Recruit leukocytes
-Activate leukocytes
Regulate blood pressure
-Release vasodilators
-Release vasoconstrictors
Vascular permeability
-Regulate passage of nutrients
-Regulate oxygenation
-Regulate leukocyte infiltration
Angiogenesis
-Sprout to form new vessels
-Secrete MMPs
-Remodel ECM

Endothelial cells contribute to the regulation of blood pressure and flow by secreting factors that promote either vasodilation or vasoconstriction. Nitric oxide (NO), a free radical that is produced in endothelial cells via endothelial NO synthase (eNOS) oxidation of L-arginine to L-citrulline,[225] is a vasodilator that is released constitutively by endothelial cells. Basal eNOS activity is triggered by the shear stress produced by flowing blood.[226] eNOS activity may be enhanced by a variety stimuli, including thrombin, histamine,[227] acetylcholine[228] and bradykinin,[229] resulting in increased NO production and secretion. NO mediates vasodilation by relaxing vascular smooth muscle cells by interacting with guanylyl cyclase.[230] Additionally, NO participates in the maintenance of proper blood flow by inhibiting platelet aggregation, promoting platelet disaggregation[231] along with inhibition of leukocyte adhesion to endothelial cells.[232] Endothelial cells also secrete another potent vasodilator, prostacyclin (PGI_2), which also aides in the maintenance of proper blood fluidity by relaxing vascular smooth muscle cells and by inhibiting platelet activation.[233,234] Endothelial cells also secrete molecules that trigger vasoconstriction. Endothelin is produced by endothelial cells and interacts with vascular smooth muscle cells to trigger vasconstriction.[235] Endothelin expression is inhibited by NO[236] and is stimulated by epinephrine, thrombin, angiotensin II, hypoxia, insulin and cytokines.[237] Disruption in blood flow results in decreased NO production and subsequent increased endothelin activity. Endothelial cell dysfunction results from failure to produce sufficient NO, leading to vessel constriction. Prolonged endothelial dysfunction as a result of diminished NO secretion and impaired blood flow may result in chronic inflammation.[238]

Leukocytes, which circulate in the vasculature, are predominantly responsible for immune reactions. In order to mediate inflammatory responses outside of the blood, leukocytes must interact with endothelial cells to extravasate from the circulating blood into the extravascular space where the immune reaction is taking place. Therefore, endothelial cells play a critical role during inflammatory responses. During inflammatory responses, endothelial cells at the site of inflammation are activated in two types of responses. Type I activation is transcription independent and allows a rapid response to extracellular ligands through G-protein coupled receptors (GPCRs) and increased intracellular Ca^{2+} levels.[238,239] Type II activation is transcription dependent and takes longer to develop but allows a for sustained activation in response to factors secreted by leukocytes like tumor-necrosis factor (TNF) and interleukin-1 (IL-1).[238] Activation of endothelial cells results in secretion of NO and PGI_2 to increase blood flow to the affected area.[232,240] While resting endothelial cells do not support efficient leukocyte recruitment since they do not express high levels of adhesion molecules on the cell surface, activated endothelial cells recruit leukocytes to the site of inflammation by exocytosing Weibel-Palade bodies (WPBs), resulting in presentation of P-selectin on the cell surface to interact with leukocytes and release of chemoattractants that induce adhesion.[241-243] Other adhesion molecules like E-selectin, ICAM-1 and VCAM-1 are also expressed by activated endothelial cells to mediate leukocytes recruitment.[238,244,245] Once leukocytes are sequestered by the endothelium, they interact with other adhesion molecules on the endothelial cells (CD31 and CD99) to extravasate between adjacent endothelial cells into the extravascular space.[246,247]

Endothelial cell dysfunction plays a critical role in the progression of atherosclerosis. Elevated native low density lipoprotein (LDL) and modified LDL levels in the blood have been demonstrated to induce endothelial cell dysfunction, in part by reducing NO bioavailability.[248] The combination of endothelial cells dysfunction and elevated LDL levels result in an accumulation of LDL within the arterial wall.[249] Free radicals created by endothelial cells and leukocytes react with LDL to create oxidized-LDL (oxLDL).[250] Increased leukocyte adhesion and infiltration occurs as a result of endothelial dysfunction. As monocytes infiltrate into the intimal space, they are transformed into macrophages by colony-stimulating factor (CSF).[249] Macrophages engulf oxLDL using scavenger LDL receptors and turn into foam cells following overwhelming lipid ingestion and metabolism.[251] Foam cells release more inflammatory stimuli, perpetuating the inflammatory response and increasing the likelihood of thombotic events and plaque formation, eventually creating an atherosclerotic lesion.[249,250]

In adults, the quiescent vasculature does not produce new blood vessels under normal situations. Angiogenesis, or the growth of new blood vessels, normally only occurs in adults in a highly regulated fashion during the female reproductive cycle.[252] During development, angiogenesis is tightly controlled and the resulting vasculature is highly structured and organized. Angiogenesis may also occur following tissue injury in order to re-vascularize damaged areas.[253] Several pathological disorders trigger the quiescent vasculature to become mitotically active and sprout to develop new blood vessels.[254] Of particular interest to this thesis is the requirement for endothelial cell proteolytic activity during angiogenesis to remodel the extracellular environment. Excessive abnormal

angiogenesis can contribute to tumor growth, adiposity and chronic inflammation while suppression of angiogenesis is associated with cardiac failure and diabetic nephropathy.[255] As a tumor grows, it reaches a size where simple oxygen diffusion is insufficient to allow sufficient metabolism to occur to permit continued growth. The key transcriptional regulator hypoxia inducible factor-α (HIF-α) becomes stabilized in low oxygen conditions and induces the transcription of several pro-angiogenic genes, including VEGF, angiopoietins, fibroblast growth factor, MMPs and PAs.[256] HIF-α induces the expression of these genes in the tumor and in endothelial cells themselves during periods of oxygen deprivation. Endothelial cells respond to these growth factors by sprouting towards the area of oxygen deprivation in order to restore proper oxygenation.[257,258] During this process, adhesion molecules on endothelial cells become altered to allow migration of the endothelial cells.[254,259] MMPs and plasmin play important roles in this migration since the extracellular matrix must be degraded in a specific way to clear a path for the sprouting endothelial cells.[255,260] Regulation of Pg activation is therefore important in angiogenic regulation[58] and a role for AIIt is this processes has been demonstrated.[208]

1.5 Maintenance of Vascular Patency by Endothelial Cells

The vascular system provides a network for blood flow through the body. As described previously, blood contains a system that is capable of initiating rapid coagulation. Endothelial cells, which line the interior of blood vessels, are primarily responsible for controlling the processes that mediate coagulation and fibrinolysis. Impairment in the ability of endothelial cells to regulate either of these processes can have lethal consequences. Endothelial cells regulate fibrinolysis by expressing cell surface Pg receptors (including AIIt) and secreting PAs and their inhibitors.[36,261] Additionally, endothelial cells regulate the initiation of coagulation. Thrombomodulin, a transmembrane protein expressed by endothelial cells, binds and inactivates thrombin.[262] The thrombomodulin-thrombin complex activates protein C to activated protein C (APC).[263,264] APC, whose zymogen is produced by the liver and circulates in plasma,[265] is a serine protease that exhibits anti-coagulatory effects by degrading Factor Va and Factor VIIIa. Activation of APC is further stimulated by the endothelial cell protein C receptors.[266]

Endothelial cells also play an important role in the initiation of coagulation. Tissue factor is expressed in low levels by the resting endothelium and is maintained beneath the cell surface or between cells.[267] Following endothelial injury, tissue factor becomes exposed to coagulation factors in the plasma and initiates coagulation.[268] Tissue factor expression in endothelial cells is also induced in response to stimulation from pro-inflammatory mediators like endotoxin,[269] thrombin,[270] cytokines,[271] VEGF,[272] hypoxia[273] and oxLDL.[274] Endothelial cells also express thrombin receptors, the protease-activated receptors

(PARs), on the cell surface. Binding of thrombin to PAR1, a GPCR, triggers endothelial cell activation and induces the expression of pro-thrombotic factors and inflammatory mediators.[227,275] During inflammation, TNF and IL-1 trigger leakage of plasma proteins (including fibrinogen) to provide a matrix for cells invading out of the vasculature. Fg that has leaked is cleaved to fibrin to provide structure for the matrix. Prolonged inflammation can therefore lead to the development of fibrin clots in the area surrounding the vasculature.[238,276]

Under normal circumstances, endothelial cells do not interact with platelets present in the blood. However, as is the case in endothelial-leukocyte interactions, endothelial cells may be triggered to interact with platelets and participate in their activation. Following endothelial injury, platelets adhere to the exposed endothelial compartments to initiate coagulation.[277] Platelets interact with vWF and collagen that has been exposed due to injury.[277] This interaction, in conjuction with exposure to adenosine di-phosphate (ADP) from endothelial cells and thrombin, triggers platelet activation.[278] Activated platelets mediate further platelet aggregation and bind fibrinogen to promote thrombus formation.[278] Activated platelets also release growth factors like VEGF and basic fibroblast growth factor (bFGF) that recruit inflammatory cells, fibroblasts and endothelial cells to participate in wound healing.[279,280] The fibrin clot formed with the aid of platelets stems blood loss due to injury while also serving as a matrix for the cells that migrate to the site of injury to participate in wound healing. In normal physiological wound healing, these cells will regulate plasmin activation to break down the fibrin clot as wound healing progresses.[268]

1.6 Homocysteine

Elevated levels of homocysteine (Hcy) in plasma (hyperhomocystenemia) have been identified as a significant independent risk factor for cardiovascular diseases, stroke, thrombosis and dementia.[281] Hcy is an amino acid which contains a sulfhydryl group. It is formed by demethylation of methionine, a reaction catalyzed by S-adenosyl-methionine synthetase.[282] Homocysteine can either be remethylated to form methionine in a vitamin B12-dependent reaction or undergo transsulphuration into cysteine in a vitamin B6 dependent reaction, a reaction catalyzed by Cystathionine β-synthase.[282] Mutations in the enzymes which catalyze these reactions as well as a diet insufficient in folate, vitamin B12 or vitamin B6 may result in elevated plasma homocysteine levels.[283] In circulation, homocysteine is primarily bound to serum proteins via a hcy-cysteine disulfide linkage.[282] It may also exist as a monomer, as a homocystine (Hci) homodimer linked by a disulfide bond, as a homocysteine-cysteine dimer or as cyclic homocysteine thiolactone (HTL).[284,285] Even though Hcy and cysteine (Cys) vary by one carbon group (Figure 7), the pKa of the sulfhydryl group of Hcy is more elevated than that of Cys.[286] As a result, disulfide bonds formed between Hcy and cysteine residues on proteins are much more stable and are less likely to be displaced by other thiols than disulfide bonds formed with other thiols.[287]

1.7 Role of homocysteine in endothelial cell dysfunction.

One mechanism by which Hcy may contribute to cardiovascular disease is by contributing to endothelial cell dysfunction.[288-295] Elevated homocysteine levels induce

endothelial cell dysfunction by increasing vascular oxidant stress, resulting in decreased nitrous oxide (NO) bioavailability.[296-298] Hcy has also been shown to induce ERK phosphorylation through an unknown G protein-coupled receptor.[299] ERK activation by homocysteine results in increased expression of MMP-9,[281,300] which also contributes to homocysteine mediated endothelial dysfunction. AIIt has been shown to play a role in similar signaling events in response to plasmin,[301] β2-glycoprotein I[302] and may trigger signaling events itself through Toll-like receptor 4 (TLR4).[303] Annexin A2 is present in lipid rafts,[154,304] and may therefore participate in signaling initiation that may occur in lipid rafts.[305]

1.8 Interaction of Homocysteine and AIIt

Another mechanism by which Hcy may contribute to cardiovascular disease and stroke is by inhibiting endothelial cell fibrinolytic activity.[291] Conflicting reports exist in the literature as to where tPA binds on AIIt. Our group has reported that tPA binding occurs on the C-terminal lysine of S100A10[95] while the Hajjar group has reported that tPA binding occurs at Cys8 of Annexin A2.[202] The Hajjar group has reported that binding of Hcy to Cys8 prevents binding of tPA to Annexin A2, resulting in a decrease in AIIt dependent plasmin activation on the cell surface of endothelial cells.[291] Interestingly, other groups report that Hcy also exists as homocysteine-thiolactone (HTL) (Figure 7) in the blood. HTL may also modify proteins. Unlike Hcy, which attacks free thiols, HTL binds to proteins through acylation of the ε-amino group of lysine by the activated carboxyl group of HTL.[306] Given the importance of the C-terminal lysine of S100A10 in plasmin activation, binding of HTL to S100A10 could provide an alternative mechanism to Hcy

inhibition of AIIt dependent plasmin activation. Elucidating the mechanism by which Hcy impairs AIIt dependent fibrinolysis can therefore offer insight into how hyperhomocysteinemia increases the risk of cardiovascular disease and stroke.

Figure 7. Structures of homocysteine, homocystine, homocysteine thiolactone and cysteine. Chemical structures of homocysteine, homocystine, homocysteine thiolactone and cysteine are drawn.

Homocysteine

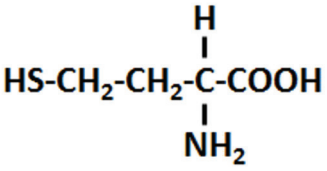

Homocystine

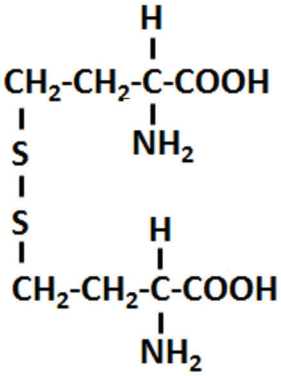

Homocysteine thiolactone

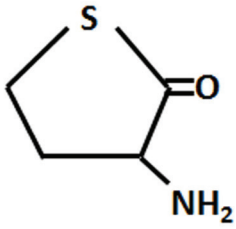

Cysteine

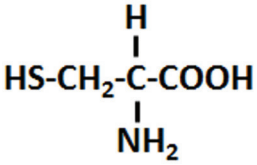

1.9 Conceptual Framework

The primary objective of this study was to elucidate the role of endothelial cell S100A10 in regulating the active serine protease plasmin. The primary function of plasmin is to maintain vascular patency by degrading the fibrin-rich blood clots, a process called fibrinolysis. Fibrinolysis is a normal vascular process that occurs continuously and is required to prevent naturally occurring blood clots from growing and causing vascular occlusions which would result in heart attack and stroke. A number of studies have demonstrated the importance of AIIt in regulating plasmin activation. However, most of the literature has focused on the role of the annexin A2 monomer in endothelial plasmin activation instead of the role of the heterotetramer. Based on the work presented in this thesis, we hypothesize that S100A10 plays a key role in the fibrinolytic and angiogenic response of endothelial cells *in vivo*.

CHAPTER 2: MATERIALS AND METHODS

2.1 Mice

The S100A10-deficient (S100A10$^{-/-}$) mice, along with their wild type (WT) counterparts, are on a 129SV x a C57BL/6 background and were a generous gift from Dr Per Svenningsson.[196] The annexin A2-deficient mice (annexin A2$^{-/-}$), along with their WT counterparts, are on a 129SVj x a C57BL/6J background and were a generous gift from Dr Katherine Hajjar.[208] Experimental mice were typically 6 to 8 weeks of age and of mixed gender. All animal experiments performed were in accordance with protocols approved by the University Committee on Laboratory Animals at Dalhousie University.

2.2 Isolation of murine microvascular endothelial cells

Primary murine microvascular endothelial cells (MMECs) were isolated from lungs of S100A10$^{-/-}$ and WT mice. Lungs were removed from 6 mice and washed in Hank's buffered saline solution (HBSS) without Ca^{2+} and Mg^{2+}. Lungs were then minced into 1-2mm^2 pieces in HBSS without Ca^{2+} and Mg^{2+} and washed twice. The HBSS was aspirated and minced lungs were placed in 5 ml Dulbecco's minimal eagle medium (DMEM) (Gibco) with 0.18 U/ml Blendzyme Liberase (Roche Diagnostic) and 0.1 mg/ml DNase 1 (Invitrogen) for 1 hour at 37 ºC for digestion. The supernatant after digestion was collected and pooled with the collection of supernatants of washing the minced lungs 3 times with 5 ml HBSS without Ca^{2+} and Mg^{2+}. The cell suspension was centrifuged for 8 minutes at 600 x g and washed twice with 30 ml HBSS without Ca^{2+} and Mg^{2+}. The cell pellet was re-suspended in 5 ml Trypsin/EDTA (Gibco) for 10 minutes at 37 ºC followed

by passage through a 70 μm filter and washed with HBSS with 1% BSA (Sigma-Aldrich). The cell suspension was Fc blocked by incubation with 5 μg in 500 μl mouse IgG for 20 minutes at 4 ºC followed by a 20 minute incubation at 4 ºC with magnetically labelled anti-CD144 antibody (Miltenyi Biotec). The cell pellet was washed 3 times with HBSS with 1% BSA and labelled cells were separated using a miniMAC separation column (Miltenyi Biotec) according to manufacturers directions. Purified cells were plated on gelatin-coated flasks. Purity of endothelial cells was determined by visualizing Dil-Ac-LDL (Biomedical Technologies) stained cells by microscopy.

2.3 Cell culture

Telomerase Immortalized Microvascular Endothelial (TIME) cells, a generous gift from Dr M. McMahon (UCSF)[307], and MMECs were maintained in endothelial basal medium-2 (EBM-2) media (Lonza) supplemented with 10% fetal bovine serum (FBS; Gibco). T241 fibrosarcoma cells were a generous gift from Dr Y. Cao (Karolinska Institute) and were maintained in DMEM with 10% FBS.

2.4 Plasmids

pSUPER-retro-S100A10 shRNA1 was constructed by cloning the dsDNA oligo 5′-GAT CCC CGT GGG CTT CCA GAG CTT CTT TCA AGA GAA GAA GCT CTG GAA GCC CAC TTT TTA-3′ and 5′-AGC TTA AAA AGT GGG CTT CCA GAG CTT CTT CTC TTG AAA GAA GCT CTG GAA GCC CAC GGG-3′ into the pSUPER.retro.puro vector

(OligoEngine), pSUPER-retro-S100A10 shRNA5 was constructed by cloning the dsDNA oligo 5′-GAT CCC CAG AGT ACT CAT GGA AAA GGT TCA AGA GAC CTT TTC CAT GAG TAC TCT TTT TTA-3′ and 5′-AGC TTA AAA AAG AGT ACT CAT GGA AAA GGT CTC TTG AAC CTT TTC CAT GAG TAC TCT GGG-3′ into the pSUPER.retro.puro vector (OligoEngine), pSUPER-retro-annexin A2 shRNA4 was constructed by cloning the dsDNA oligo 5′-GAT CCC CGT GCA TAT GGG TCT GTC AAT TCA AGA GAT TGA CAG ACC CAT ATG CAC TTT TTA-3′ and 5′-AGC TTA AAA AGT GCA TAT GGG TCT GTC AAT CTC TTG AAT TGA CAG ACC CAT ATG CAC GGG-3′ into the pSUPER-retro.puro vector (OligoEngine) and the pSUPER-retro-S100A10 scramble was constructed by cloning the dsDNA oligo 5′-GAT CCC CGT GGG AGT TCA GAG CTT CTT TCA AGA GAA GAA GCT CTG AAC TCC CAC TTT TTA-3′and 5′-AGC TTA AAA AGT GGG AGT TCA GAG CTT CTT CTC TTG AAA GAA GCT CTG AAC TCC CAC GGG-3′into the pSUPER.retro.puro vector (OligoEngine).

2.5 Transfections and Transductions

Phoenix-Ampho packaging cells plated to 80-90% confluence in 25 cm^3 flasks were transfected with 5 μg of pSUPER-retro plasmids described above using Lipofectamine 2000™ transfection reagent (Invitrogen) according to manufacturers instructions. After 48 hours, supernatants were collected and filtered with a 45μm filter and 8 μg/ml polybrene (Sigma) and added to infect TIME cells plated to 60% confluence in 25 cm^3 flasks for 24 hours. TIME cells were allowed to recover for 48 hours in complete EBM-2 before being selected with 2 μg/ml of puromycin (Invitrogen) in complete EBM-2 for at least one

week. Cells were maintained in the presence of puromycin while in culture.

2.6 Western blot analysis and immunostaining

Proteins, obtained by lysing cells with cell lysis buffer (1% NP-40, 150 mM NaCl, 20 mM Tris-HCl, 1 mM EDTA, 1 mM EGTA, and proteinase inhibitor cocktail (1:500; Sigma-Aldrich)) were loaded into each well mixed with SDS sample buffer (60 mM TrisHCl (pH 6.8), 10% glycerol, 2% SDS and 0.1 M β-mercaptoethanol) and resolved by 12% SDS-polyacrylamide gel electrophoresis (PAGE) following the method described by Laemmli [308] and electroblotted onto nitrocellulose membranes.[309] Murine tissues were lysed by dissociating the tissues using a polytron in phosphate buffered solution (PBS) (137 mM NaCl, 2.7 mM KCl, 8.1 mM Na_2HPO_4, 1.76 mM KH_2PO_4, pH 7.4), 1% Triton X-100, 5 mM EDTA, 100 mM ε-aminocaproic acid, 10 mM benzamidine, 1 mM pefabloc and protease inhibitor cocktail, mixed with SDS sample buffer and resolved by SDS-PAGE and electroblotted onto nitrocellulose membranes. Membranes were fixed with 4% formaldehyde, blocked with Odyssey blocking buffer (LI-COR Biosciences) followed by incubation with primary antibodies. Primary antibodies used were monoclonal mouse anti-human S100A10 (BD Biosciences), monoclonal goat anti-mouse S100A10 (R&D Systems), mouse monoclonal anti-annexin A2 (BD Biosciences), fibrin(ogen) (Abcam), mouse monoclonal anti-actin (loading control; Sigma Aldrich), monoclonal rabbit anti-phospho-p42/p44 (Cell Signaling Technology), monoclonal rabbit anti-p42/p44 (Cell Signaling Technology), rabbit monoclonal anti-phospho-p38 (Cell Signaling Technology), rabbit monoclonal anti-p-Jnk (Cell Signaling Technology), polyclonal goat anti-tissue

factor (American Diagnostica), rabbit polyclonal anti-αtubulin (loading control; Santa-Cruz), polyclonal rabbit anti-Pg (American Diagnostica) and monoclonal mouse anti-fibrinogen (American Diagnostica). Membranes were then incubated with the species appropriate secondary IRdye-800 antibody (LI-COR Biosciences). Antibody complexes were viewed using the Odyssey IR imaging system (LI-COR Biosciences). Protein expression was quantified using the Odyssey quantification software. Proteolyzed annexin A2 was prepared according to Kassam *et al.*[143] while bovine AIIt was prepared according to Khanna *et* al.[311]. Briefly, bovine lung was homogenized and AIIt purified from the homogenate using a Diethylaminoethyl (DEAE) sepharose column. Proteolyzed annexin A2 was obtained by incubating bovine AIIt with 50 nM plasmin, resulting in removal of 27 amino acids from the amino-terminal.

2.7 Cell Surface Biotinylation

Endothelial cells were plated to 80% confluence in 100 cm^3 cell culture plates, washed 3X with incubation buffer (IB: 20 mM HEPES, 150 mM NaCl, 3 mM $CaCl_2$ and 1 mM $MgCl_2$, pH 7.4) and then scraped in 150 μL IB. The cell suspension was then incubated with 20 μL of 10 mM Sulfo-NHS-SS-biotin (Pierce, Rockford IL) to label surface proteins for 30 minutes at room temperature, washed 2X with IB and lysed with cell lysis buffer. Total protein (100 μg) from the cell lysis was incubated with 30 μL of Dynabeads M-280 streptavidin (Invitrogen) for 2 hours at 4 ºC with rotation and washed 5X with cell lysis buffer (1% NP-40, 150 mM NaCl, 20 mM Tris-HCl pH 7.4, 1 mM EDTA, 1 mM EGTA, 1 mM $NaVO_4$, 10 mM NaF and protease inhibitor cocktail (1:500; Sigma-

Aldrich)). Biotinylated surface proteins bind to the streptavidin from the Dynabeads and were separated from unlabelled proteins using a magnet since Dynabeads carry a magnetic charge. Beads were re-suspended in 2x SDS-PAGE loading buffer with β-mercaptoethanol, boiled for 10 minutes and removed from the SDS-PAGE loading buffer using the magnet. Once the Dynabeads were removed, surface proteins were resuspended in 2x SDS-PAGE loading buffer, electrophoresed and immunostained for S100A10 and annexin A2.

2.8 Analysis of tissue fibrin deposition by western blot analysis

WT and S100A10$^{-/-}$ mice were anaesthetized with isolflurane. Heparin sodium (500U; Sigma-Aldrich) was injected iv via the tail vein and sacrificed by transcardial perfusion 10 minutes later with ice cold PBS followed by cervical dislocation. Lung, liver, spleen and kidneys were harvested and homogenized in 10 mM sodium phosphate buffer (pH 7.5), 0.1 M ε-aminocaproic acid, 5 mM trisodium EDTA, 10 U/ml aprotinin, 10 U/ml heparin and 2 mM PMSF using a polytron. The homogenate was incubated with rotation for 14 hours at 4 ºC, centrifuged at 10,000 x g for 15 minutes and resuspended in 3 M urea. The suspension was incubated with rotation for 2 hours at 37 ºC, vortexed vigorously and centrifuged at 14,000 x g for 15 minutes. The supernatant was discarded and the sediment was dissolved at 65 ºC in reducing SDS sample buffer before being resolved by 7.5% SDS-PAGE and immunostained by western blot analysis.

2.9 Analysis of tissue fibrin deposition by immunohistochemistry

Lung, liver, kidney and spleen tissues were removed from the WT and S100A10$^{-/-}$ mice following sacrifice by transcardial perfusion with 4% formaldehyde. Tissues were fixed in 10% formalin, dehydrated in ethanol and embedded in paraffin. Paraffin sections were deparaffinized, blocked with horse serum (1:20, Invitrogen) and incubated with an antibody against fibrin (Dako) or normal rabbit IgG1 (as control, BD Biosciences) at room temperature overnight. A peroxidase DAB detection system (Dako) was applied according to manufacturers detection to visualize fibrin staining and sections were counter-stained with Meyer's Hematoxylin (Sigma-Aldrich). Sections were mounted using Cytoseal 60 mounting media (Richard-Allen Scientific) and viewed using a 20×/0.5 NA objective lens. Images were captured by the Nikon Eclipse E600 microscope using a Nikon DXM1200F camera. Digital acquisition of the images was performed using ACT-1 v2.7 software (Nikon). Figures were generated using Adobe Photoshop CS3 v10 (Adobe Systems Incorporated).

2.10 Batroxobin induced fibrin deposition

WT and S100A10$^{-/-}$ mice were injected with 25 μCi ^{125}I-fibrinogen (MP Biomedicals) followed by 25 U/kg batroxobin (Pentapharm) using tail vein catheters (Braintree Scientific). Two hours later, blood and tissues were collected and weighed. Gamma counts for the tissues and blood were measured with a Beckman LS 5000TA scintillation counter and corrected for weight.

2.11 Tail vein clip assay

WT and S100A10$^{-/-}$ mice were anaesthetized with isoflurane and the bottom 3 mm of the tail was clipped off with a scalpel and the bleeding tail was placed in 37 °C saline. Time until bleeding stoppage and re-bleeding were recorded.

2.12 Histochemistry and immunohistochemistry of murine tails

Sections of tails from WT and S100A10$^{-/-}$ mice were fixed in 10% formalin, dehydrated in ethanol and embedded in paraffin. Paraffin sections were deparaffinized, blocked with horse serum (1:20, Gibco, Grand Island, NY) and incubated with an antibody against S100A10 (R&D Systems) or normal goat IgG1 (as control, BD Biosciences) at room temperature overnight. A peroxidase DAB detection system (Dako) was applied according to manufacturers detection to visualize fibrin staining and sections were counter-stained with Meyer's Hematoxylin (Sigma). Masson's trichrome staining was then performed to ensure tail morphology was not altered by loss of S100A10. For Masson's trichrome staining, sections were deparaffinized, fixed in Bouin's fixative for 1 hour, rinsed in water, stained with celestine blue for 5 minutes and hematoxylin for 8 minutes. The sections were then rinsed in water, placed in Scott's tap water substitute until sections turned blue, rinsed in water again and stained with ponceau 2R/Acid fuchsin mixture for 10 minutes and with 1% phosphomolybdic acid until red stain is removed from collagen but remains in muscle, red blood cells and fibrin. Subsequently, the sections were rinsed in water, stained with 2% light green SF yellowish in 2% acetic acid until the connective elements are stained green, rinsed in water, 100% ethanol and then xylene. Sections were

mounted using Cytoseal 60 mounting media (Richard-Allen Scientific) and viewed using a 20×/0.5 NA objective lens. Images were captured by the Nikon Eclipse E600 microscope using a Nikon DXM1200F camera. Digital acquisition of the images was performed using ACT-1 v2.7 software (Nikon). Figures were generated using Adobe Photoshop CS3 v10 (Adobe Systems Incorporated).

2.13 Murine blood parameters

Blood was collected from WT and S100A10$^{-/-}$ mice by cardiac puncture using a 25-gauge needle into 100 μL EDTA (2% w/v, Sigma-Aldrich). Platelet levels in whole blood were measured using a LH 755 analyzer (Beckman Coulter). Fibrinogen and Pg levels were determined by Western Blot analysis of murine plasma. Murine plasma was obtained following centrifugation (1500 x g) of whole blood collected with EDTA.

2.13.1 Coagulation assays

The prothrombin time (PT) and activated partial thromboplastin time (aPTT) were determined using an ACL TOP (Beckman Coulter). Citrated blood collected from the mice was used for both coagulation assays. PT and aPTT were determined by clot formation, measuring turbidity.

2.13.2 Clot lysis assay

In vitro clot lysis was determined using a modification of the aPTT assay. In a 96-well, flat bottom plate, 50 µL citrated plasma, 50 µL APTT reagent (STA®-PTT A, Stago) and 100µL HBS-Tw80 (40 mM HEPES pH 7.0, 150 mM NaCl and 0.01% Tween 80) were added to wells containing 2.5 µL of 5.8 µM sc-tPA (Genentech). Duplicate reactions were carried out in wells lacking sc-tPA. After incubation at 37 °C for 3 minutes, 100 µL of 25 mM $CaCl_2$ was added, the solution mixed and absorbance was monitored at 405 nm every minute for 60 minutes using a BioTek ELx808 plate reader. Clot lysis time was defined as the time required to achieve the absorbance that was one-half of the difference between the maximum absorbance reached after clotting and the minimum absorbance value achieved after complete lysis.

2.13.3 Antiplasmin activity and plasmin-antiplasmin complex levels

Antiplasmin activity was assessed using a Coamatic © Plasmin Inhibitor chromogenic kit (generously provided by Diapharma, West Chester OH), following manufacturer's direction. Antiplasmin activity was measured by loss of plasmin activity. Citrated blood collected from the mice was used. The assay was calibrated using standardized human plasma, HemosIL Calibration plasma (Instrumentation Laboratory, Lexington, MA). Plasmin-antiplasmin levels were determined using Imuclone® PAP ELISA (American Diagnostica Inc, Montréal QC) following manufacturer's direction.

2.13.4 Thrombin potential assay

Endogenous Thrombin Potential was determined using Technothrombin ® TGA (Technoclone, Vienna, Austria), utilizing a modification of the procedure as directed by the manufacturer. Briefly, citrated murine plasma samples collected with 20 mM Benzamidine and 2000 KIU/mL aprotinin were diluted ½ with TGA-buffer prior to addition of the trigger reagent and substrate. This assay measures thrombin potential by initiating coagulation following addition of TF and negatively charged phospholipids. Activation of prothrombin to thrombin is determined using a colourimetric thrombin substrate.

2.14 Endothelial cell plasminogen activation with tPA

TIME cells and MMECs were trypsinized with EDTA-free trypsin (Invitrogen) and washed 3X with DPBS. For carboxypeptidase B (CpB; Worthington Biochemical) treatment, cells were incubated for 20 minutes at 37 °C in the presence of 5 U/ml CpB. $1x10^5$ cells were then incubated with 5 nM tPA in IB for 20 minutes at 4 °C. The cells were then washed 3X with IB and incubated with 0.5 μM Glu-Pg and 250 μM Pm substrate S2251 (Chromogenix, Diapharma Group) with or without 100 mM ε-aminocaproic acid (ε-ACA). The rate of plasmin generation was measured at absorbance 405 nm every minute for 2 hours using a BioTek ELx808 plate reader.

2.15 Endothelial cell plasminogen activation with uPA

TIME cells were trypsinized with EDTA-free trypsin and washed 3X with Dulbecco's PBS (DPBS) (Hyclone). Cells were then washed with 0.05M glycine, pH 3.0, 0.1 M NaCl for 3 minutes followed by neutralization with an equal volume of 0.5 M HEPES pH 7.5, 0.1 M NaCl to dissociate potential endogenously bound ligands. $1x10^5$ cells were then incubated with 25 nM uPA (Sigma-Aldrich) for 30 minutes at 37 °C in DPBS containing 0.2% BSA, washed 3X in DPBS with 0.2% BSA and incubated with 0.5 μM Glu-Pg and 250 μM Pm substrate S2251 (Chromogenix, Diapharma Group) in 0.05 M Tris-HCl, pH 7.4, 0.1 M NaCl, 0.01% Tween 80. The rate of plasmin generation was measured at absorbance 405 nm every minute for 2 hours using a BioTek ELx808 plate reader.

2.16 FITC-Plasminogen preparation

Glu-Pg (2-5 mg/mL) was dialyzed against 0.1 M carbonate buffer (pH 9), and a 50 M excess of fluorescein isothiocyanate (FITC) (Sigma) was added after being dissolved in dimethyl sulfoxide. Pg and FITC were mixed for 16 hours in the dark and treated with 0.01% hydroxylamine to remove all labile FITC-Pg bonds. Unincorporated FITC was removed by gel filtration through an NAP-10 column using HBSS (20 mM HEPES, 1 mM CaCl2, and 1 mM MgCl2; pH 7.4). Typically, 2 FITC molecules were bound to each Pg molecule as determined by the A_{280}/A_{495} ratio.

2.17 Plasminogen binding assay

TIME cells and MMECs were washed and cultured in the absence of serum for 2 hours prior to assay. Cells were trypsinized with EDTA-free trypsin and washed 3X with DPBS. For carboxypeptidase B treatment, cells were incubated for 20 minutes at 37 °C in the presence of 5 U/ml CpB. CpB treatment was performed to remove C-terminal lysines in order to observe C-terminal lysine dependant Pg binding. Cells were then incubated with 200 nM FITC Glu-Pg, with or without ε-ACA (100 mM), for 1 hour at 4 °C in HBSS. Pg binding was measured by FACS analysis (FACSCalibur, BD Biosciences).

2.18 Matrigel plug assay

Growth Factor-reduced Matrigel (BD Biosciences) containing 200 ng/ml basic fibroblast growth factor (bFGF) (Invitrogen) and 60 U/mL heparin (Calbiochem) added was injected subcutaneously (750 µL) into WT and S100A10$^{-/-}$ C57BL/6 mice. After 7 days, the Matrigel plug was removed and embedded in Tissue Tek Cryo-OCT (Andwin Scientific).

2.19 T241 tumors

T241 tumors were established by subcutaneous injection of 2x10^6 T241 fibrosarcoma cells, suspended in 100 µL DMEM (Invitrogen), containing 10% FBS (Hyclone), in the right flank of female 6-8 week old mice. Tumors were removed from the mice after 3 weeks and embedded in Tissue Tek Cryo-OCT (Andwin Scientific). T241 cells are

obtained from a C57Bl/6 derived fibrosarcoma.[311]

2.20 Immunofluorescence

Matrigel plug and T241 tumor sections were blocked with horse serum (1:20; Gibco) and incubated with monoclonal rat anti-CD31 (MEC13.3, 1:250; BD Biosciences) or normal mouse IgG1 (as control; BD Biosciences) at room temperature overnight. Sections were then stained with Alexa-Fluor 488 conjugated rabbit anti-rat (1:2500; Invitrogen) and DAPI. Vessel density was quantified using Image J v1.42q software (National Institutes of Health).

2.21 Matrigel invasion and cell migration

Murine WT or S100A10$^{-/-}$ endothelial cells and control shRNA, S100A10-depleted or annexin A2-depleted TIME cells were loaded (1x10^5 cells/well) into the upper chamber of Transwell chambers with 8 μm pores, coated with Matrigel (invasion assays) or uncoated (migration assays) (BD Biosciences). Pg (0.5 μM; American Diagnostica) and CpB (5 U/mL) were added to serum-free media in the upper chamber where indicated, while media containing 20% FBS was added to the bottom chamber as chemoattractant. After 48 hours, cells on the underside of the membrane were stained with hematoxylin and eosin (Sigma-Aldrich) and counted.

2.22 Aortic ring assay

Aortas were isolated from the WT, S100A10$^{-/-}$ and annexin A2$^{-/-}$ mice. All connective tissue was removed from the aortas, which were then cut into segments 1 mm in length and embedded into 250 μL of collagen (1.5 mg/ml; Worthington Biochemical) in a 48 well plate. Collagen was formed by mixing 7.5 volumes of 2 mg/ml collagen , 1 volume of 10x MEM (Gibco), 1.5 volumes of $NaHCO_3$ (15.6 mg/ml), and ~0.1 volume 1 M NaOH to adjust the pH to 7.4. Once the collagen had solidified around the aortic rings, 200 μL of complete EBM-2 was added to each well. After 7 days, images of the aortic sprouts were obtained using a Zeiss Axiovert 200M (2×/0.08 NA objective lens) using a Hamamatsu ORCA-R2 digital camera.

2.23 Tube formation assay

100 μL of Matrigel was placed in 96 well plates and allowed to solidify. Control, S100A10-depleted or annexin A2-depleted TIME cells were placed on top of the Matrigel or fibrin in the presence of complete EBM-2. After 24 hours, tube formation was viewed using a Zeiss Axiovert 200M (2×/0.08 NA objective lens) using a Hamamatsu ORCA-R2 digital camera.

2.24 Zymography

Gelatin zymography was performed in 10% SDS-PAGE in the presence of 0.1% gelatin. WT MMECs, S100A10$^{-/-}$ MMECs, control shRNA, S100A10 and annexin A2 depleted TIME cells were plated in 96 well plates. Cells were cultured at 37 ºC in the presence or absence of Pg in EBM-2 with 1% FBS. Conditioned media was collected after 6 hours, mixed with gel loading buffer (without β-mecaptoethanol, without boiling) and resolved by SDS-PAGE. Following electrophoresis, gels were washed twice for 30 minutes in renaturing buffer (50 mM Tris-HCl, pH 7.5, 2.5 % Triton X-100) to remove SDS. Gels were then incubated overnight at 37 ºC in substrate buffer (50 mM Tris-HCl pH 8, 200 mM NaCl, 5 mM $CaCl_2$, 0.02% Brij-35), stained with 0.1% Coomassie Blue R250 in 50% methanol and 10% glacial acetic acid for 30 minutes and destained.

2.25 RNA isolation and cDNA synthesis

Total RNA was isolated from lungs, livers, spleens and kidneys obtained from the WT or S100A10$^{-/-}$ mice. Tissues were homogenized in Trizol (Invitrogen) using a blender. Total RNA was isolated from WT or S100A10$^{-/-}$ endothelial cells and control, S100A10-depleted or annexin A2-depleted TIME cells by lysing cells in Trizol. All RNA extraction using Trizol was performed according to manufacturer's instructions. 1 μg total RNA was pre-incubated with random hexamer primers at 70 ºC for 10 min prior to incubation at 42 ºC for 60 min with 5X FS buffer (Invitrogen), 1 mM dNTP, 40 U RNaseOUT (Invitrogen), 20 mM DTT (Invitrogen), 100 pM random hexamer primers (Invitrogen) and 200 U Super Script II reverse transcriptase (Invitrogen) to create cDNA.

2.26 Quantitative real-time PCR

For quantitative real-time PCR (qPCR) reactions, specific primers for murine and human S100A10, annexin A2 and GAPDH were designed using IDT Primer Quest software (PE Applied Biosystems) and synthesized by IDT. qPCR reactions were performed using the Roto-Gene™ 6000 (Corbett Life Science). Each qPCR reaction was carried out in a total volume of 20 µL containing 8 µL SsoFast™ EvaGreen® Supermix (Bio-Rad, CA), 1 µL each of 3ˈ and 5ˈ primer (IDT) and 10 µL of cDNA. Amplification was performed with an initial incubation of 95 ºC for 10 min followed by 45 cycles of the following 3 step procedure: denaturation at 95 ºC for 10 min, annealing at 65 ºC for 15 seconds and extension at 72 ºC for 20 seconds, with a ramp rate of 2 ºC/second.

Primer sequences were as follows:

S100A10 forward primer: 5′-AAA TGC CAT CCC AAA TGG AGC ACG-3′

S100A10 reverse primer: 5′-TCA GGT CCT CCT TTG TCA AGT GGT-3′

Annexin A2 forward primer: 5′-CAT CCT GAC AAA CCG CAG CAA TGT-3′

Annexin A2 reverse primer: 5′-AGC ATC ATC CTG GGC AGG TGT CTT-3′

GAPDH forward primer: 5′-TGT GAT GGG TGT GAA CCA CGA GAA-3′

GAPDH reverse primer: 5′-GAG CCC TTC CAC AAT GCC AAA GTT-3′

S100A10 and annexin A2 expression was normalized against expression of the control gene GAPDH to adjust for variations in mRNA quality and cDNA synthesis efficiency.

2.27 Plasmin and homocysteine induced signaling

TIME cells were plated in 12 well plates and incubated overnight with serum reduced (1% FBS) EBM-2. Cells were then incubated with either 0.43 Committee of thrombolitic agents unit (CTA)/mL plasmin (Sigma-Aldrich) or 100 μM homocysteine, scraped into cell lysis buffer at 15 min intervals and proteins were analyzed by Western Blot.

2.28 Tissue factor activity assay

TIME cells were lysed by repeated freeze thawing in a buffer of 50 mM Tris-HCl, 100 mM NaCl, 0.1% Triton X-100, pH 7.4. Tissue factor activity of the cell lysates was assayed using the Actichrome TF assay (American Diagnostica) according to manufacturers instructions. Activity is measured using a colourimetric TF substrate.

2.29 AIIt plasminogen activation assay

1 μM bovine AIIt was incubated with 5 mM homocysteine (Hcy), homocystine (Hci) or cysteine (Cys) or 1 mM homocysteine thiolactone (HTL) overnight at 37 ºC. Pg activation was then assayed by incubating the AIIt with 0.5 μM Glu-Pg, 2 nM tPA and 250 μM Pm substrate S2251. The rate of plasmin generation was measured at absorbance 405 nm every minute for 2 hours using a BioTek ELx808 plate reader.

2.30 Statistical analysis

Statistical analysis was performed using GraphPad Prism. Analysis performed were Student's T test and ANOVA with Tukey test.

CHAPTER 3: REGULATION OF FIBRINOLYSIS BY S100A10 *in vivo*

3.1 S100A10$^{-/-}$ mice accumulate fibrin in their tissues.

S100A10 has been proposed to be an important regulator of cellular Pm generation.[116] Mice with inactivation of the Pg gene do not generate Pm and develop spontaneous fibrin deposition in the tissues due to impaired fibrinolysis.[312,313] Therefore, we compared the fibrin content of freshly isolated tissues from WT and S100A10$^{-/-}$ mice. Tissue homogenates were prepared and the fibrin levels were determined by Western blot analysis using an anti-fibrin antibody. As shown in Figure 8, tissues from S100A10$^{-/-}$ mice contain significantly higher amounts of fibrin than their WT litter mates. Quantification of band intensity revealed a 1.8-fold increase in fibrin in lung (Figure 8A), 2.2 fold increase in the liver (Figure 8B), 4.4 fold increase in the spleen (Figure 8C) and 4 fold increase in the kidney (Figure 8D) from the S100A10$^{-/-}$ mice compared with WT controls. Fibrin immunohistochemistry of tissue sections demonstrated areas of fibrin deposition in the S100A10$^{-/-}$ lung (Figure 9A), liver (Figure 9B), spleen (Figure 9C) and kidney (Figure 9D) while fibrin positive staining was not observed in sections from the WT mice. Since this increased accumulation of fibrin in the tissues of the S100A10-/- mice could be due to either enhanced coagulation or reduced fibrinolytic activity, we further investigated the potential role of S100A10 in coagulation and fibrinolysis. The PT and aPTT values were identical between the WT and S100A10$^{-/-}$ mice (Figure 10), suggesting that S100A10 depletion does not affect the coagulation pathway.

Previous reports have demonstrated that loss of annexin A2 results in loss of S100A10 in

murine tissues.[208] The loss of S100A10 was observed to affect annexin A2 levels in a tissue specific fashion. Loss of S100A10 decreased annexin A2 levels in the lung, spleen and kidney (Figure 11A,C,D), annexin A2 protein was not detectable in WT and $S100A10^{-/-}$ liver (Figure 11B) and annexin A2 levels were not altered in the small intestine (Figure 11E). While annexin A2 protein levels were decreased in lung, spleen and kidney from the $S100A10^{-/-}$ mouse, annexin A2 mRNA levels were not altered in these tissues (Figure 12A-C), suggesting that loss of S100A10 results in decreased annexin A2 protein stability in lung, spleen and kidney.

Figure 8. Western blot analysis reveals that loss of S100A10 results in increased tissue fibrin deposition. Lung (A), liver (B), spleen (C) and kidney (D) tissues from 6 WT and 6 S100A10$^{-/-}$ mice were collected, and the fibrin content of tissue lysates was determined by SDS-PAGE and Western blot analysis. 10 ng of each tissue were loaded. Quantification of fibrin deposition was normalized to WT levels. Statistical analysis was performed using Student's t-test and and the data are expressed as the mean (±) SEM of 6 independent experiments (** $p < 0.01$, *** $p < 0.001$).

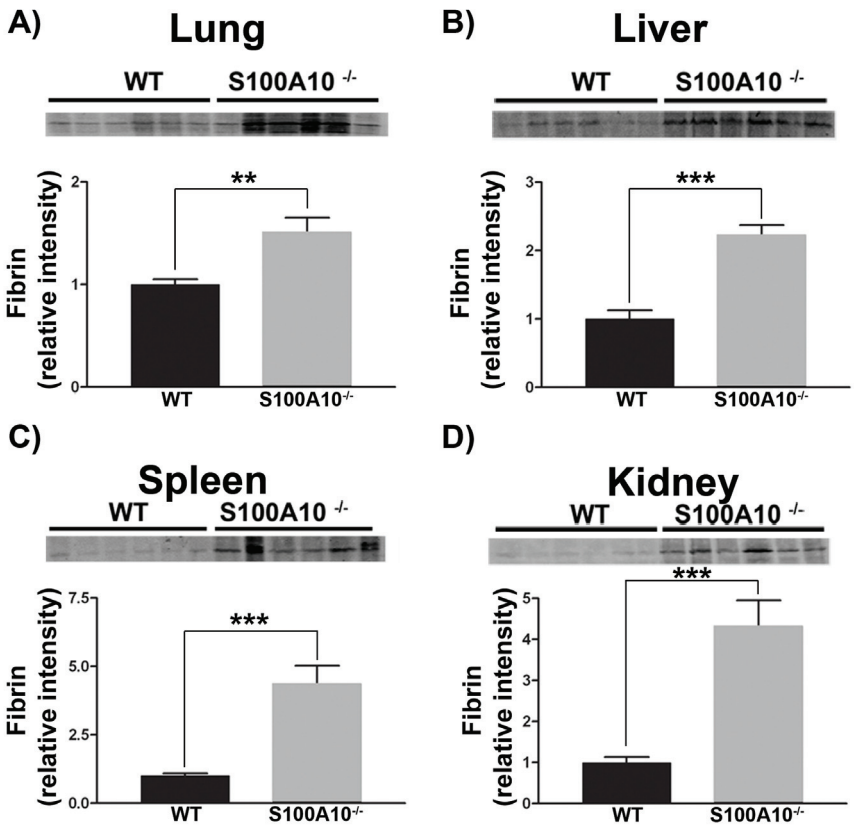
A)
Lung
WT
S100A10 -/-
Fibrin (relative intensity)
**
WT
S100A10-/-
B)
Liver
WT
S100A10 -/-
Fibrin (relative intensity)
***
WT
S100A10-/-
C)
Spleen
WT
S100A10 -/-
Fibrin (relative intensity)
***
WT
S100A10-/-
D)
Kidney
WT
S100A10 -/-
***
Fibrin (relative intensity)
WT
S100A10-/-

Figure 9. Immunohistochemical analysis reveals loss of S100A10 results in elevated fibrin deposits in tissues. Immunohistochemistry for fibrin was performed on perfused sections of formalin fixed tissues. Sections were deparaffinized and incubated with anti-fibrin antibody followed by anti-rabbit HRP. Arrows indicate areas with fibrin deposition. Tissues observed were lung (A), liver (B), spleen (C) and kidney (D).

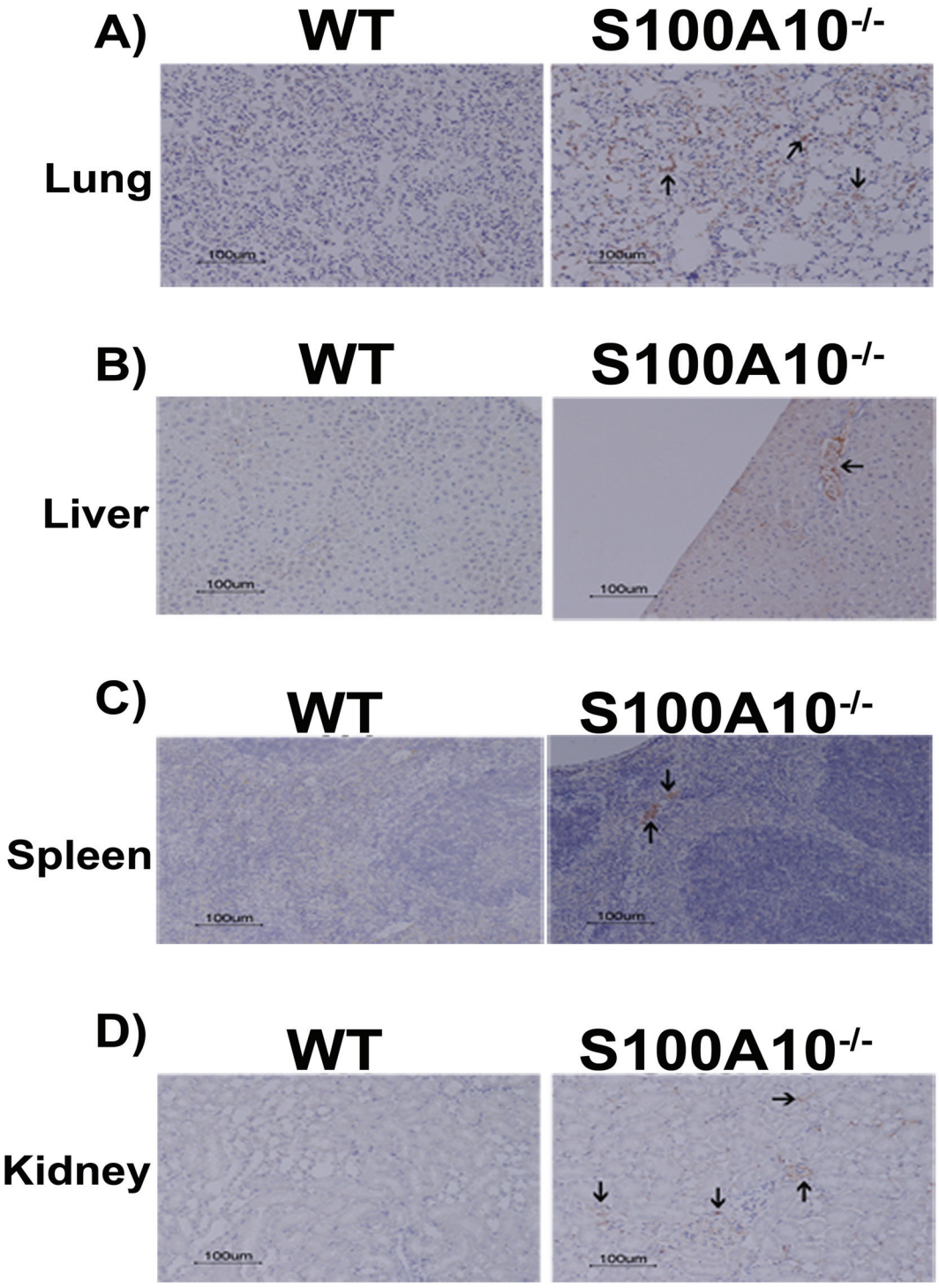
A)
WT
S100A10-/-
Lung
100um
100um
B)
WT
S100A10-/-
Liver
100um
100um
C)
WT
S100A10-/-
Spleen
100um
100um
D)
WT
S100A10-/-
Kidney
100um
100um

Figure 10. Comparison of coagulation pathways. Murine blood was obtained by cardiac puncture and treated with sodium citrate to prevent clotting. The activated partial thromboplastin time (aPTT) (A) and prothrombin time (PT) (B) in the S100A10$^{-/-}$ mice were observed to be comparable with their WT counterparts. Statistical analysis was performed using Student's t-test and and the data are expressed as the mean (±) SEM of 6 independent experiments. Coagulation assays performed by Victoria Miller, samples were collected by Alexi Surette.

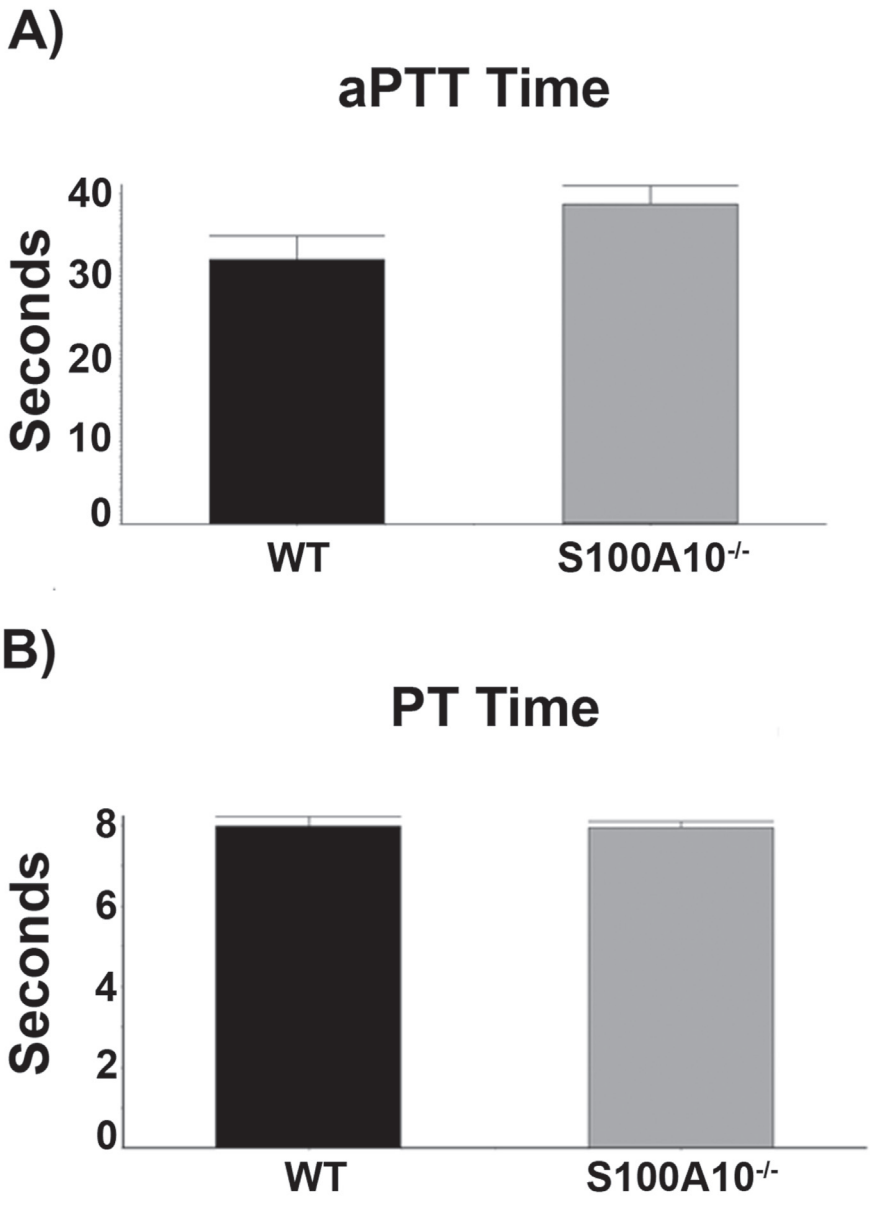
A)
aPTT Time
Seconds
40
30
20
10
0
WT
S100A10-/-
B)
PT Time
Seconds
8
6
4
2
0
WT
S100A10-/-

Figure 11. Annexin A2 levels in tissues from S100A10$^{-/-}$ mice. Annexin A2 and S100A10 protein levels were analyzed by Western Blot in tissues isolated from WT and S100A10$^{-/-}$ mice. Annexin A2 protein levels decreased in lung (A), kidney (C) and spleen (D), were not detectable in liver (B) and were unaltered in the small intestine (E). As expected, S100A10 protein levels were not detected in tissues isolated from S100A10$^{-/-}$ mice.

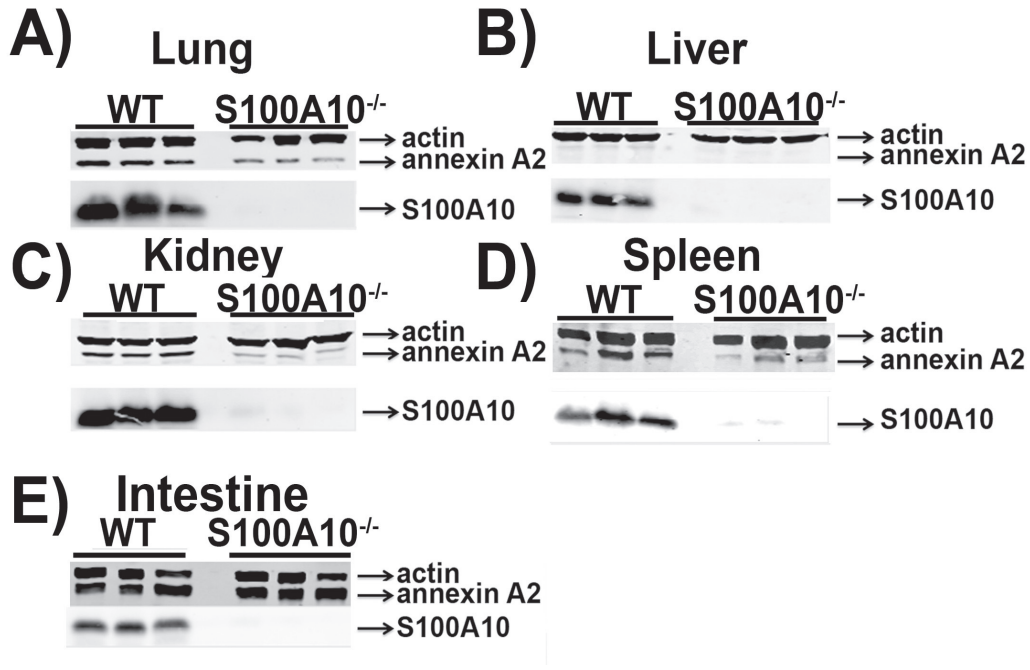
A)
Lung
WT
S100A10-/-
actin
annexin A2
S100A10
B)
Liver
WT
S100A10-/-
actin
annexin A2
S100A10
C)
Kidney
WT
S100A10-/-
actin
annexin A2
S100A10
D)
Spleen
WT
S100A10-/-
actin
annexin A2
S100A10
E)
Intestine
WT
S100A10-/-
actin
annexin A2
S100A10

Figure 12. Annexin A2 mRNA levels in tissues from S100A10$^{-/-}$ mice. Annexin A2 mRNA levels were analyzed in tissues isolated from WT and S100A10$^{-/-}$ mice. Loss of S100A10 did not affect annexin A2 mRNA levels in lung (A), kidney (B) and spleen (C). Statistical analysis was performed using Student's t-test and and the data are expressed as the mean (±) SEM of 6 independent experiments.

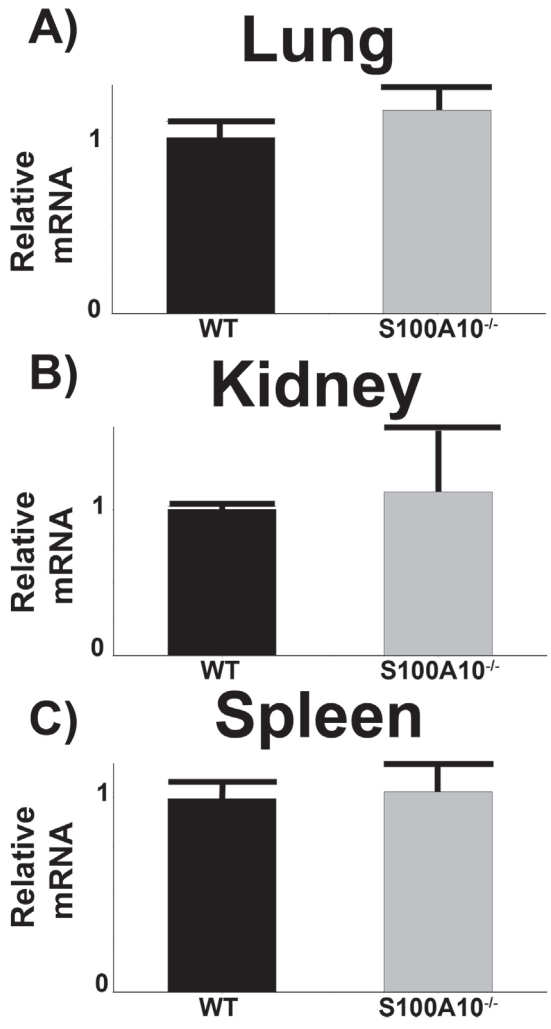
A)
Lung
Relative mRNA
1
0
WT
S100A10-/-
B)
Kidney
Relative mRNA
1
0
WT
S100A10-/-
C)
Spleen
Relative mRNA
1
0
WT
S100A10-/-

3.2 S100A10$^{-/-}$ mice have impaired fibrinolysis

To evaluate fibrinolysis in WT and S100A10$^{-/-}$ mice, tissues and blood were collected following ^{125}I-fibrinogen and batroxobin injection via the tail vein into WT and S100A10$^{-/-}$ mice (Figure 13). Batroxobin is a thrombin like enzyme isolated from the venom of the snake *Bothrops atrox*. Batroxobin cleaves fibrinogen to release fibrinopeptide A, resulting in the formation of fibrin. However, fibrin formed by batroxobin is more likely to form microclots than fibrin formed by thrombin since thrombin will cleave fibrinogen to release fibrinopeptides A and B, resulting in fibrin that is more cross-linked and more stable.[314] We observed that the tissues of the S100A10$^{-/-}$ mice had significantly greater accumulation of ^{125}I-label than the WT mice and less ^{125}I-label in the blood (Figure 14). For example, the residual radioactivity in the lung tissue of the S100A10$^{-/-}$ mouse was 2.5-fold higher than the WT lung tissue and 5-fold lower in the blood. The dramatic loss in the ability of the S100A10$^{-/-}$ mouse to degrade a batroxobin-induced clot could be due to alterations in plasma components of the clotting system or the fibrinolytic activity of the endothelium. Therefore, we compared the plasma components of the clotting and fibrinolytic systems. The platelet and protein levels of plasma Pg and fibrinogen of WT and S100A10$^{-/-}$ mice were similar (Figure 15A,B). Plasma clots prepared from WT and S100A10$^{-/-}$ mice were then evaluated for their susceptibility to tPA-mediated clot lysis. We observed that neither the time to clot nor the time of clot lysis differed between the WT and S100A10$^{-/-}$ mice (Figure15 C,D). Additionally, no differences were observed in antiplasmin levels, plasmin-antiplasmin (PAP) complex levels and thrombin potential between the WT and S100A10$^{-/-}$ mice

(Figure 15E,F,G).

Figure 13. Schematic design of *in vivo* clot induction. WT and S100A10$^{-/-}$ mice were injected with ^{125}I-fibrinogen and batroxobin. After 2 hours, tissues were collected, weighed and radioactivity was measured in a gamma counter.

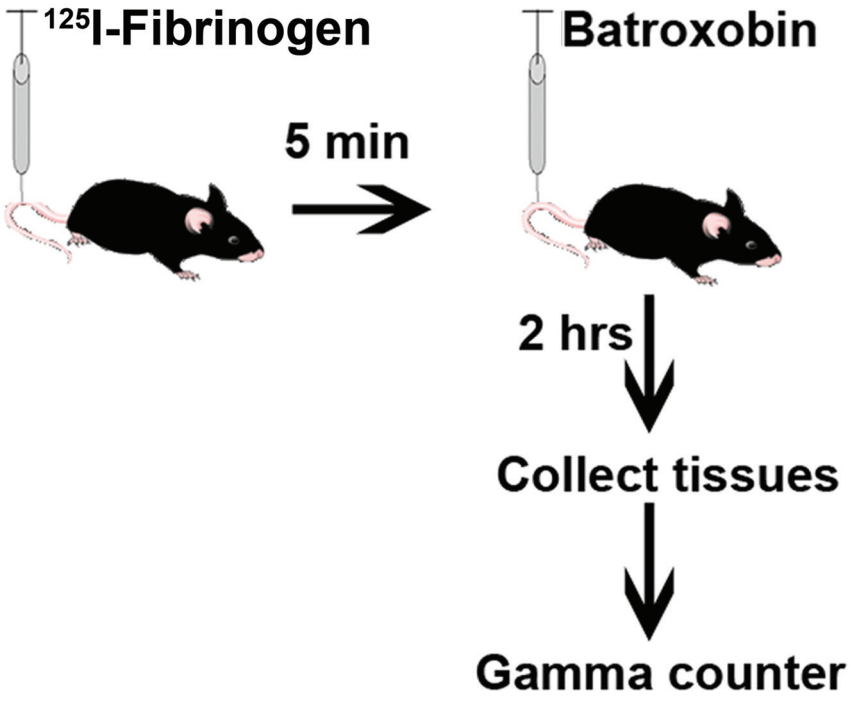
^{125}I-Fibrinogen
5 min
Batroxobin
2 hrs
Collect tissues
Gamma counter

Figure 14. S100A10$^{-/-}$ mice have impaired ability to clear induced fibrin clots. The data are expressed as counts per gram of tissue. Statistical analysis was performed using Student's t-test and and the data are expressed as the mean (±) SEM of 6 independent experiments (* $p < 0.1$, ** $p < 0.01$, *** $p < 0.001$).

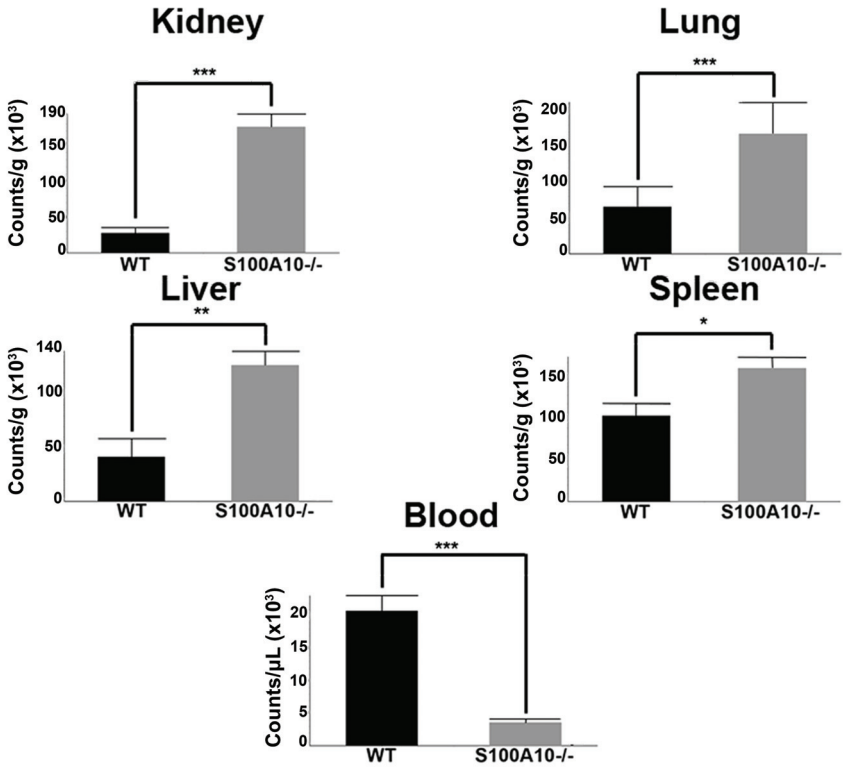
Kidney
***
Counts/g (x10³)
190
150
100
50
0
WT
S100A10-/-
Lung
***
Counts/g (x10³)
200
150
100
50
0
WT
S100A10-/-
Liver
**
Counts/g (x10³)
140
100
50
0
WT
S100A10-/-
Spleen
*
Counts/g (x10³)
150
100
50
0
WT
S100A10-/-
Blood
***
Counts/µL (x10³)
20
15
10
5
0
WT
S100A10-/-

Figure 15. Comparison of clotting parameters and components. Murine blood was obtained by cardiac puncture and treated with sodium citrate to prevent clotting. Platelet levels (A), Fg and Pg levels (B), clotting time (C), clot lysis time (D), antiplasmin activity (E), plasmin-antiplasmin levels (F) and endogenous thrombin potential (G) in the S100A10$^{-/-}$ mice were observed to be comparable with their WT counterparts. Statistical analysis was performed using Student's t-test and and the data are expressed as the mean (±) SEM of 6 independent experiments for A, C-G while B was obtained from 3 independent experiments. Clotting time, clot lysis time, antiplasmin activity, plasmin-antiplasmin levels and endogenous thrombin potential assays were performed by Victoria Miller with samples collected by Alexi Surette.

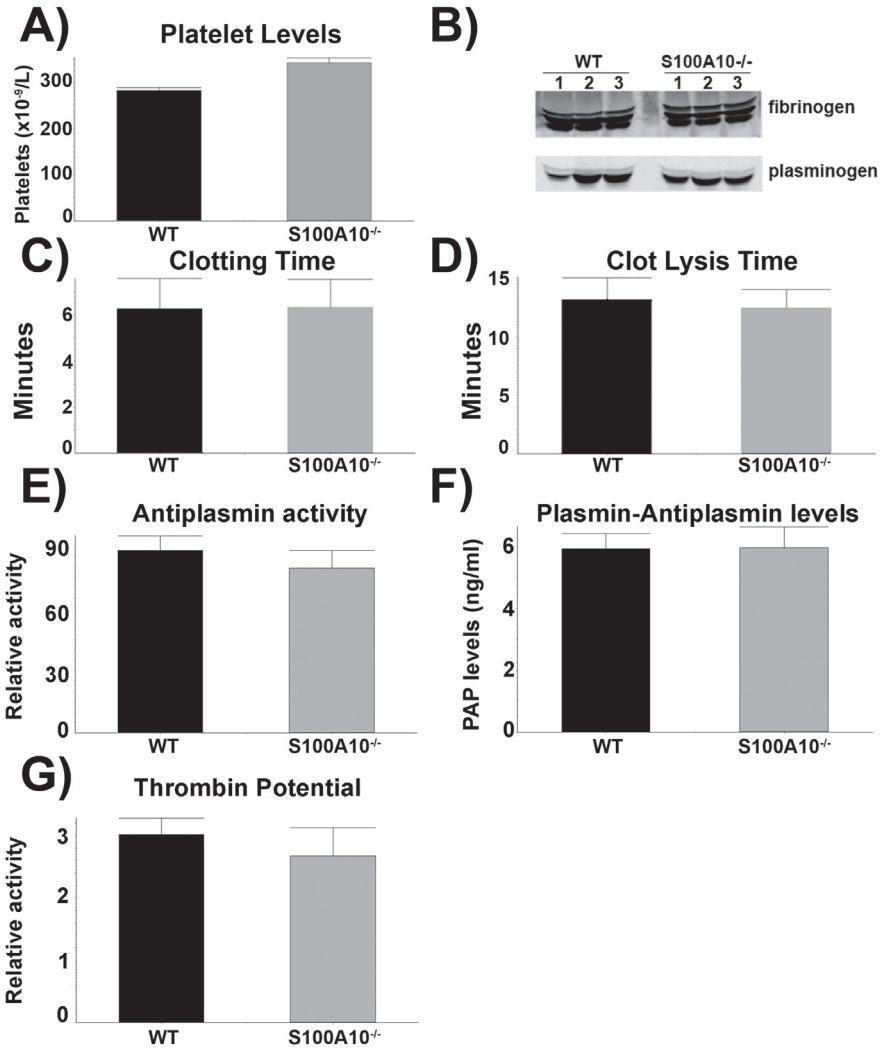
A)
Platelet Levels
Platelets (x10⁻⁹/L)
300
200
100
0
WT
S100A10-/-
B)
WT
S100A10-/-
1 2 3
1 2 3
fibrinogen
plasminogen
C)
Clotting Time
Minutes
6
4
2
0
WT
S100A10-/-
D)
Clot Lysis Time
Minutes
15
10
5
0
WT
S100A10-/-
E)
Antiplasmin activity
Relative activity
90
60
30
0
WT
S100A10-/-
F)
Plasmin-Antiplasmin levels
PAP levels (ng/ml)
6
4
2
0
WT
S100A10-/-
G)
Thrombin Potential
Relative activity
3
2
1
0
WT
S100A10-/-

3.3 Tail bleeding-re-bleeding assay

A short segment of the tail of WT and S100A10$^{-/-}$ mice was clipped and the time until cessation of bleeding was determined. We observed that mice lacking S100A10 had a 4-fold reduction in the bleeding time after the tail clip compared to the WT mice (Figure 16). Since we observed a decrease in fibrinolysis in the S100A10$^{-/-}$ mouse (Figure 14), and a similar coagulation rate (Figure 10A,B), the observed reduction in bleeding time by the S100A10$^{-/-}$ mice was likely due to decreased fibrinolysis of the tail clip-induced blood clot. We also observed that the time between cessation of bleeding and the initiation of subsequent episodes of bleeding, the re-bleeding time, was of shorter duration and also occurred with less frequency with the S100A10$^{-/-}$ mice (Table 2). This suggested that the clots formed by the S100A10$^{-/-}$ mice were more stable than the WT mice, presumably again due to a decreased rate of fibrinolysis.

We also examined the tails of the mice for other differences that might explain the variations in the bleeding and re-bleeding values. Sections of the tails were stained for collagen with Masson's trichrome (Figure 17A) and obvious qualitative differences were not observed, thus suggesting that the collagen levels and architecture of the tails were similar. Since the tail collagen is the major platelet adhesive substratum for initiation of coagulation, these results further support our data suggesting that decreased fibrinolytic activity by the endothelium of the S100A10$^{-/-}$ mice was responsible for the decreased bleeding times. Sections of the tail from the WT and S100A10$^{-/-}$ mice were also stained

for S100A10 (Figure 17B). As expected, S100A10 did not stain the tail section obtained from the S100A10$^{-/-}$ mouse while S100A10 staining in observed throughout the WT sections, including on the endothelium of the vessels.

Figure 16. Bleeding time in WT and S100A10$^{-/-}$ mice. The last 3 mm of the tail of anaesthetized WT and S100A10$^{-/-}$ mice was clipped using a scalpel blade. The clipped tails of the anaesthetized mice were placed in 37 ºC saline and the time for first cessation of bleeding was recorded. Statistical analysis was performed using Student's t-test and the data are expressed as (±) SEM of 6 independent experiments (*** $p < 0.001$).

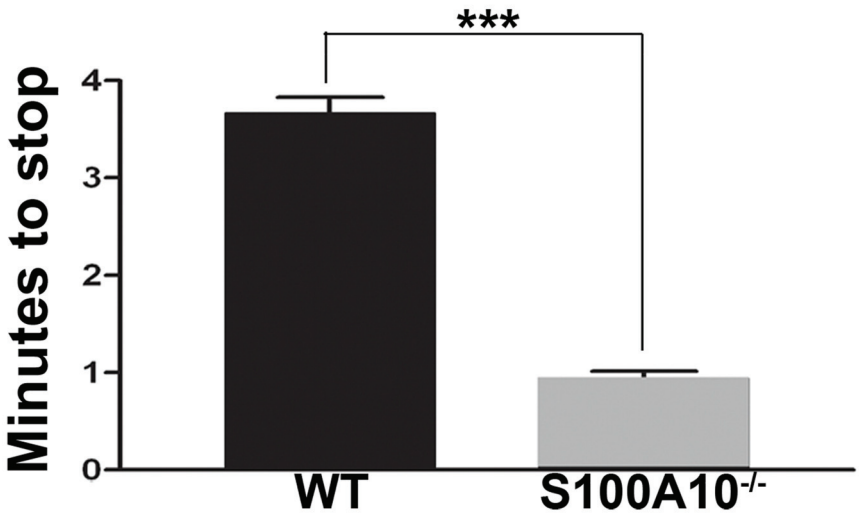
***
Minutes to stop
4
3
2
1
0
WT
S100A10-/-

Table 2. Time of bleeding stops and starts.

	Stop	Start	Stop	Start	Stop	Start	Stop	Start	Stop	Start	Stop	Start	Stop	Start	Stop	Start	Stop	Start	Stop	Start
WT 1	3:30	4:50	7:40	9:36	10:23															
WT 2	3:09	3:20	4:15	5:40	6:11	8:20	9:11	11:10	12:10	13:20	14:15	15:01	21:00	22:30						
WT 3	3:38	4:55	7:11	7:40	8:35	8:50	11:47	12:25												
WT 4	3:30	5:54	6:28	7:20	8:05	9:00	9:41	11:36	12:03	13:50	14:39	15:50	17:04	18:12	18:40	18:56	23:23	26:12	27:33	29:13
WT 5	4:17	6:14	7:40	8:54	11:01	12:06	15:45	17:20	19:50	21:33										
WT 6	2:57	6:29	11:03	13:16	17:37	20:04	21:50													
-/- 1	0:45																			
-/- 2	0:50	2:30	4:00																	
-/- 3	0:51	4:30	5:00																	
-/- 4	0:58	10:40	11:02																	
-/- 5	1:15	6:08	7:07	11:30	11:58	17:00	17:17													
-/- 6	1:01	5:31	5:55																	

The last 3 mm of the mouse tail was clipped and the tail was placed in 37 ºC saline. Time until cessation and re-initiation of bleeding was recorded. Bleeding-re-bleeding was followed for 30 minutes.

Figure 17. Masson's trichrome and S100A10 staining of tail clip sections. Masson's trichrome stain was used to observe the morphology of tail sections from WT and S100A10$^{-/-}$ mice (A). Immunohistochemistry for S100A10 was also performed on tail sections from WT and S100A10$^{-/-}$ mice (B). Sections were deparaffinized and either subjected to Masson's trichrome or anti-S100A10 antibody followed by anti-goat HRP. Sections were mounted using Cytoseal 60 mounting media (Richard-Allen Scientific) and viewed using a 20×/0.5 NA objective lens. Images were captured by the Nikon Eclipse E600 microscope using a Nikon DXM1200F camera. Digital acquisition of the images was performed using ACT-1 v2.7 software (Nikon). Sections of tails from 3 different mice were used.

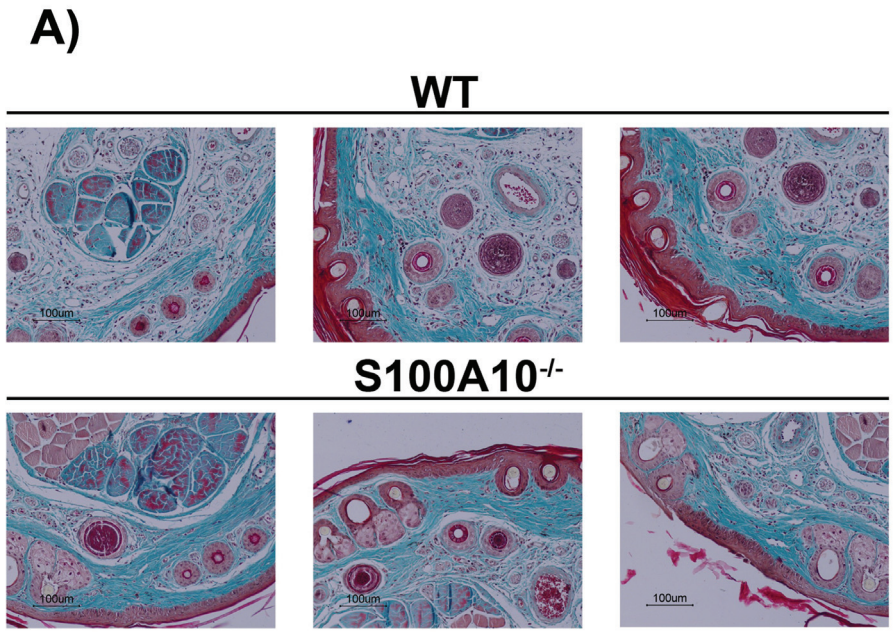
A)
WT
100um
100um
100um
S100A10-/-
100um
100um
100um

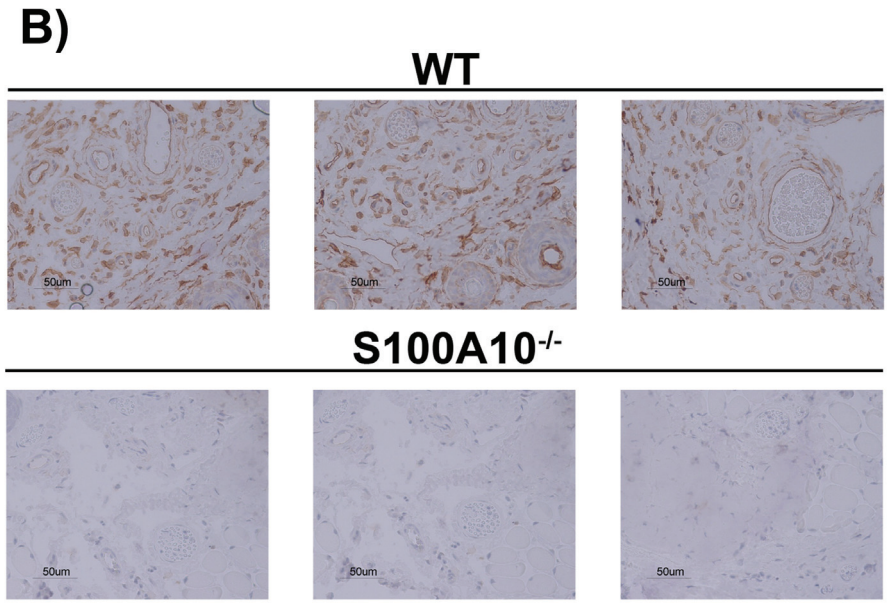
B)
WT
50um
50um
50um
S100A10-/-
50um
50um
50um

3.4 Generation of plasmin by isolated endothelial cells from WT and S100A10$^{-/-}$ mice.

We investigated the possibility that the fibrinolytic defect displayed by the S100A10$^{-/-}$ mice was due to endothelial cell dysfunction. Lung endothelial cells from WT and S100A10$^{-/-}$ mice were isolated (Figure 18). Total annexin A2 levels were unaffected by loss of S100A10 (Figure 19A) while cell-surface annexin A2 was depleted in the S100A10$^{-/-}$ cells (Figure 19C). In contrast, the cell surface levels of annexin A2 in the endothelial cell line, TIME, were unaffected by S100A10 depletion (Figure 19D), while total annexin A2 levels were also unaltered (Figure 19B). Compared to the WT mice, the endothelial cells from the S100A10$^{-/-}$ mice displayed 40% less Pg binding (Figure 20A) and Pm generation (Figure 21A). We also observed that human endothelial cells that were depleted of S100A10 by RNA interference also bound about 50% less Pg (Figure 20B) and generated 60% less Pm with both tPA and uPA (Figure 21B,D). Pretreatment of the cells with carboxypeptidase B significantly decreased Pg binding and activation, suggesting that these processes are dependent in large part on carboxyl-terminal lysine on the Pg receptors. In this regard, S100A10 was responsible for 76% and 55% of the carboxyl-terminal dependent Pg binding of the murine and human endothelial cells, respectively. This also suggests that although S100A10 is the dominant Pg-binding protein in endothelial cells, other carboxyl-terminal lysine containing Pg receptors also contribute to endothelial cell Pg binding and Pm generation. Treatment with ε-aminocaproic acid (ACA) ablated Pg binding and activation by preventing Pg interaction with cell surface Pg receptors.

Figure 18. Dil-Ac-LDL staining of primary microvascular endothelial cells from WT and S100A10$^{-/-}$ mice. Dil-Ac-LDL was incubated with the isolated lung microvascular cells to confirm their purity. Endothelial cells specifically uptake Dil-Ac-LDL and the fluorescence (red) accumulates in the intracellular membranes. Total cells were stained with 4',6-diamidino-2-phenylindole (DAPI) (blue). All cells stained positively for Dil-Ac-LDL and DAPI. Sections were mounted using Vectashield mounting medium (Vector Laboratories) and viewed using a 20×/0.5 NA objective lens. Images were captured by the Zeiss Axioplan 2 microscope using a Spot 2 digital camera. Digital acquisition of the images was performed using Axiovision 4.7 (Zeiss). Figure is representative of 3 independent experiments.

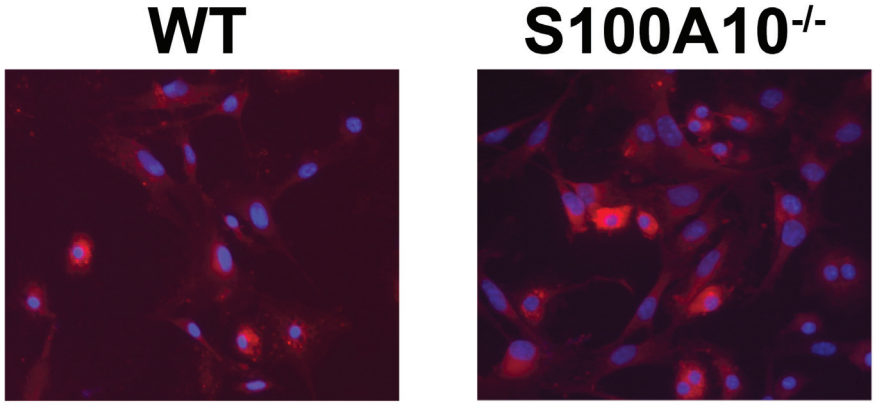
WT
S100A10-/-

Figure 19. Total and cells surface AIIt levels in S100A10 depleted endothelial cells. In order to detect the total cellular levels of annexin A2 and S100A10, primary murine endothelial cells, isolated from WT or S100A10$^{-/-}$ mice (A), as well as control and S100A10 depleted TIME cells (B), were dissociated from culture flasks, lysed, subjected to SDS PAGE and immunoblotted with anti-actin (loading control), anti-annexin A2 or anti-S100A10 antibodies. Cell surface protein levels for primary murine endothelial cells (C) and TIME cells (D), as detected by cell-surface biotinylation, are shown. Total and cell surface protein levels in annexin A2 depleted TIME cells were also analyzed (E). Data is representative of 3 independent experiments. TIME cell shRNA knockdown cell lines were prepared by Dr Patricia Madureira.

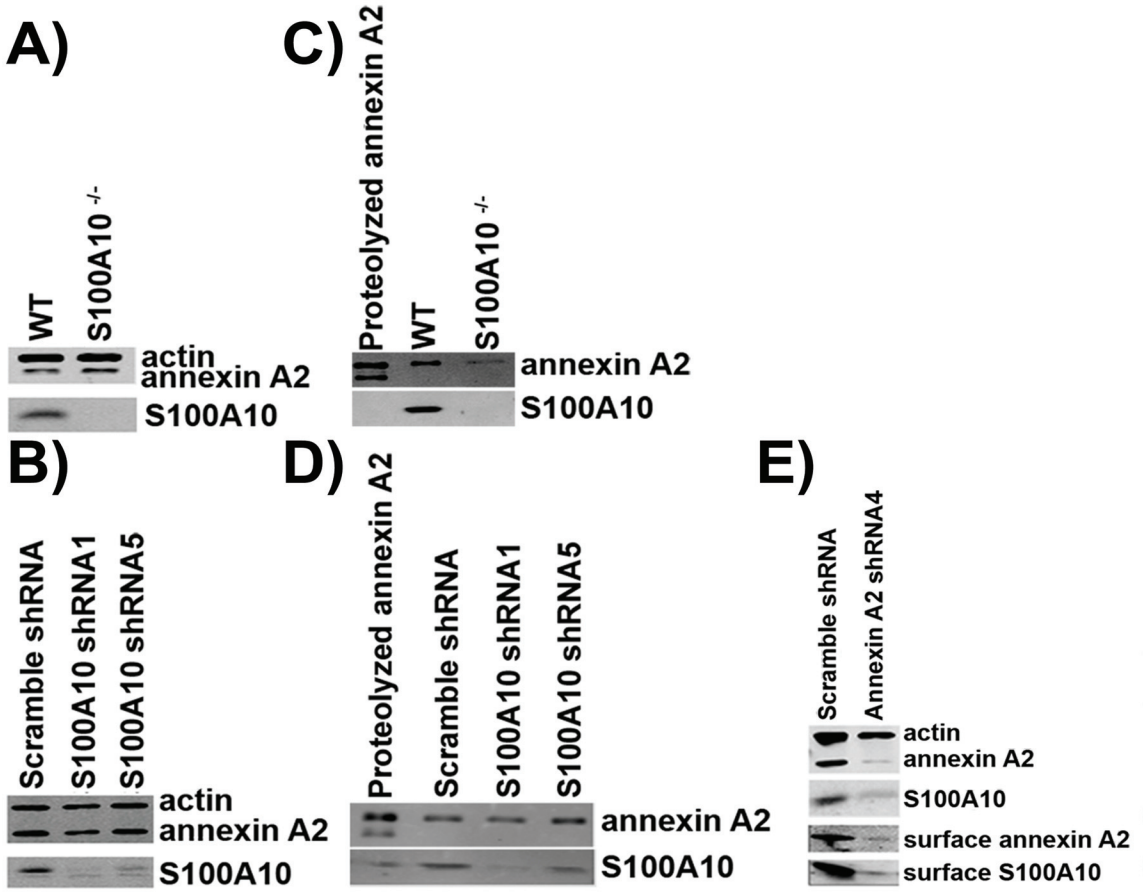
A)
WT
S100A10 -/-
actin
annexin A2
S100A10
C)
Proteolyzed annexin A2
WT
S100A10 -/-
annexin A2
S100A10
B)
Scramble shRNA
S100A10 shRNA1
S100A10 shRNA5
actin
annexin A2
S100A10
D)
Proteolyzed annexin A2
Scramble shRNA
S100A10 shRNA1
S100A10 shRNA5
annexin A2
S100A10
E)
Scramble shRNA
Annexin A2 shRNA4
actin
annexin A2
S100A10
surface annexin A2
surface S100A10

Figure 20. Depletion of S100A10 results in decreased endothelial cell plasminogen binding. FITC-Pg binding to the primary murine endothelial cells (A), S100A10 depleted TIME cells (B) and annexin A2 depleted TIME cells (C) was measured by FACS. Quantification of flow cytometric analysis of Pg binding was calculated using WinMDI software. Statistical analysis was performed using ANOVA with the Tukey test (n=3, *** $p < 0.001$). Treatment of cells with CpB decreased Pg binding by removing C-terminal lysines from cell surface Pg receptors and ε-ACA decreased Pg binding by preventing Pg binding to C-terminal lysines on Pg receptors.

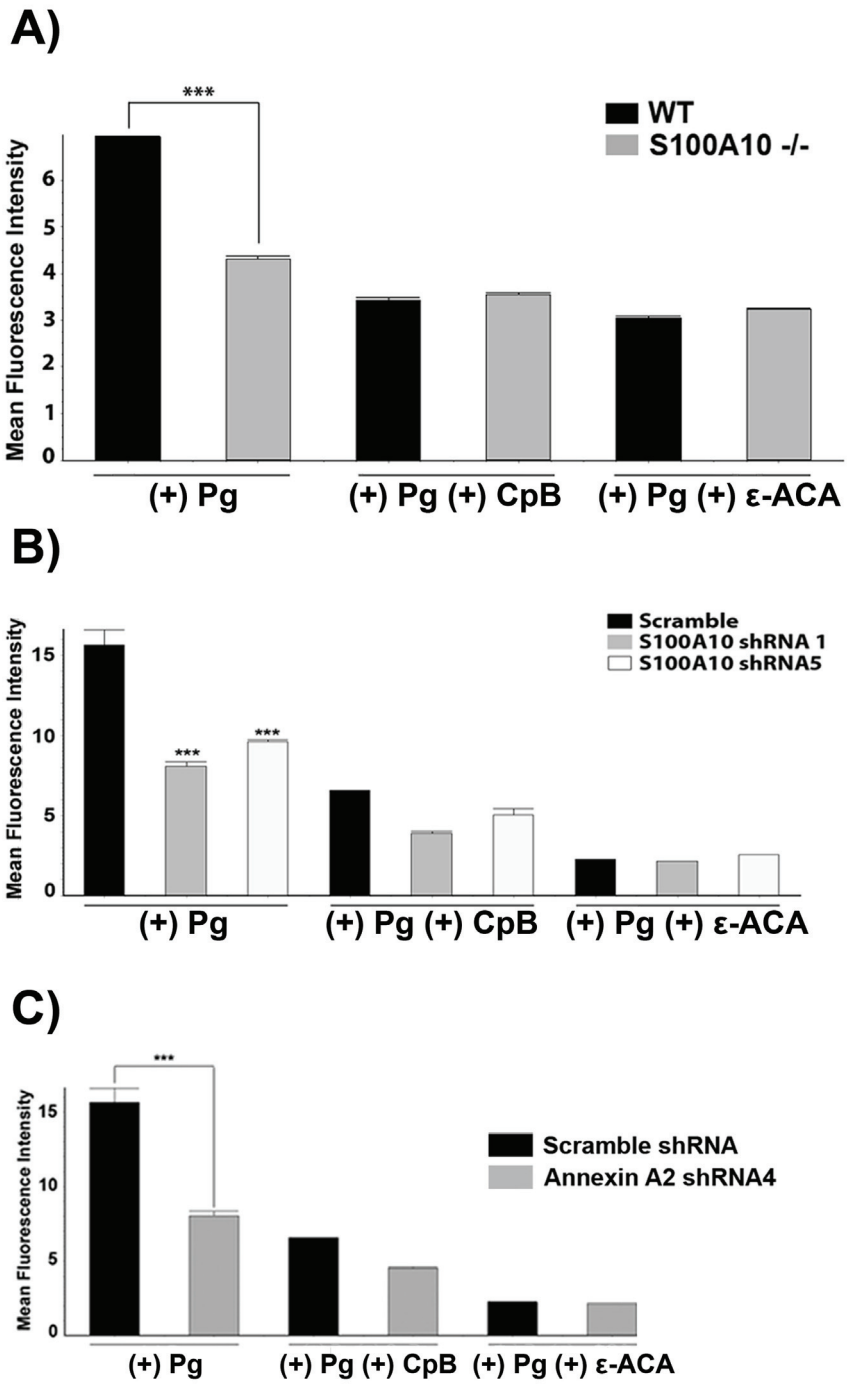
A)
***
WT
S100A10 -/-
Mean Fluorescence Intensity
0
1
2
3
4
5
6
(+) Pg
(+) Pg (+) CpB
(+) Pg (+) ε-ACA
B)
Scramble
S100A10 shRNA 1
S100A10 shRNA5
Mean Fluorescence Intensity
0
5
10
15
***
***
(+) Pg
(+) Pg (+) CpB
(+) Pg (+) ε-ACA
C)
***
Scramble shRNA
Annexin A2 shRNA4
Mean Fluorescence Intensity
0
5
10
15
(+) Pg
(+) Pg (+) CpB
(+) Pg (+) ε-ACA

Figure 21. Depletion of S100A10 results in decreased tPA dependent endothelial cell plasmin generation. Loss of S100A10 affected tPA dependent plasmin generation by primary murine endothelial cells (A) and TIME cells (B), as did loss annexin A2 (C). uPA dependent plasmin generation by TIME cells was also affected by loss of S100A10 (D) and annexin A2 (E). Statistical analysis was performed using ANOVA (n=3, *$p < 0.1$, **$p < 0.01$, ***$p < 0.001$). Treatment of cells with CpB decreased Pg activation by removing C-terminal lysines from cell surface Pg receptors and ε-ACA decreased Pg activation by preventing Pg binding to C-terminal lysines on Pg receptors.

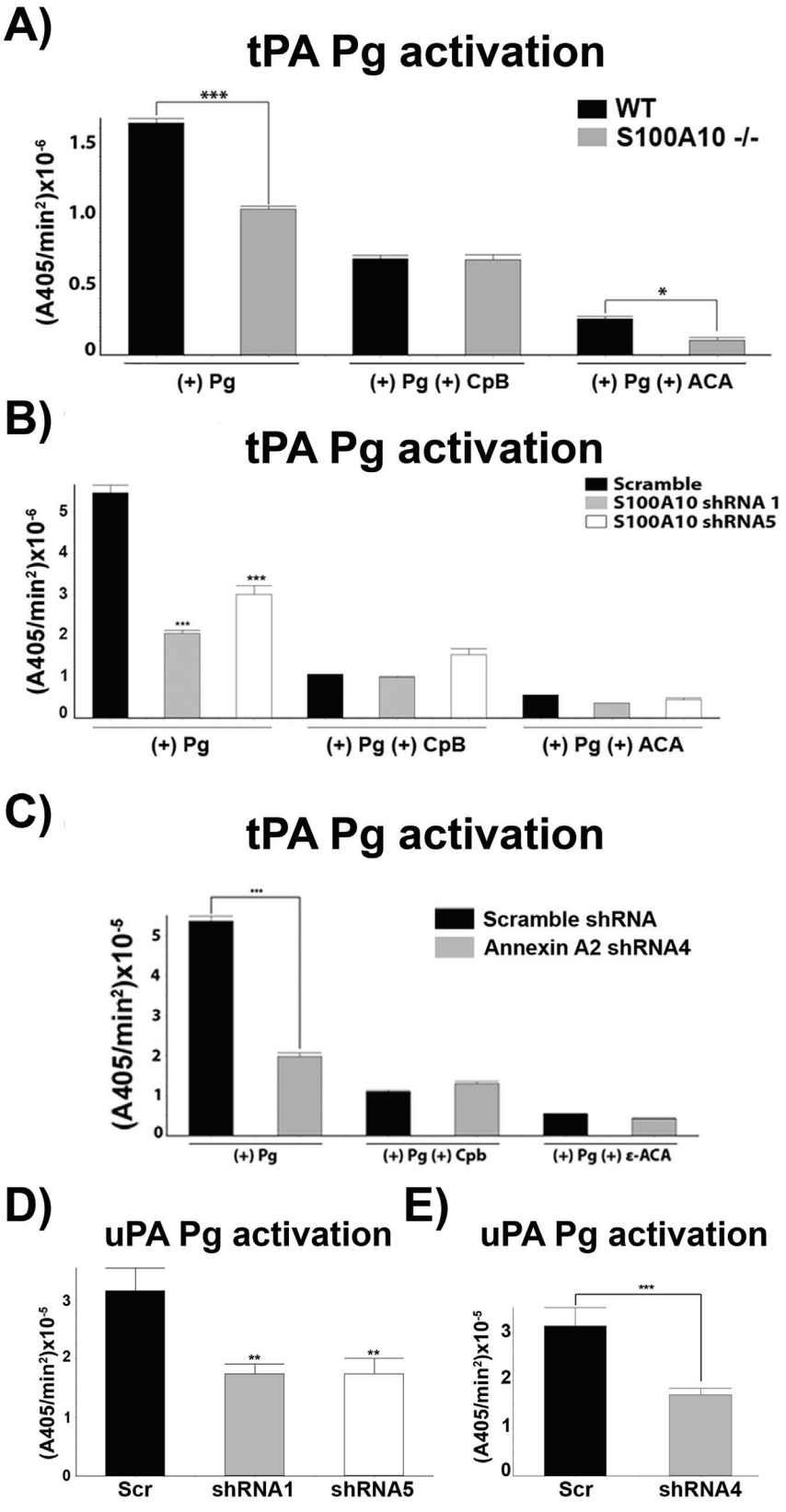
A)
tPA Pg activation
WT
S100A10 -/-
(A405/min²)x10⁻⁶
***
*
(+) Pg
(+) Pg (+) CpB
(+) Pg (+) ACA
B)
tPA Pg activation
Scramble
S100A10 shRNA 1
S100A10 shRNA5
(A405/min²)x10⁻⁶
***
***
(+) Pg
(+) Pg (+) CpB
(+) Pg (+) ACA
C)
tPA Pg activation
Scramble shRNA
Annexin A2 shRNA4
(A405/min²)x10⁻⁵
***
(+) Pg
(+) Pg (+) Cpb
(+) Pg (+) ε-ACA
D)
uPA Pg activation
(A405/min²)x10⁻⁵
**
**
Scr
shRNA1
shRNA5
E)
uPA Pg activation
(A405/min²)x10⁻⁵
***
Scr
shRNA4

We also examined the possible contribution of annexin A2 to endothelial cell Pm regulation. Depletion of annexin A2 by RNA interference reduced TIME cell Pg binding by about 50% (Figure 20C) and Pm generation with tPA and uPA (Figure 21C,E) by approximately 60%. These values were similar to the loss in Pg binding and Pm generation observed for S100A10-depleted TIME cells. As expected, the depletion of TIME cell annexin A2 by the annexin A2 shRNA also resulted in S100A10 depletion (Figure 19E). Thus, the similarity between the loss in Pg binding and Pm generation between TIME cells depleted of S100A10 by S100A10 shRNAs, but possessing unaltered levels of annexin A2 and those depleted of both annexin A2 and S100A10 by the annexin A2 shRNA suggested that annexin A2 did not significantly contribute to TIME cell Pg binding and Pm generation under these experimental conditions. Annexin A2 binds Pg via a mechanism that is absolutely dependent on the exposure of a new carboxyl-terminal lysine. The exposure of this lysine residue requires proteolytic processing and the loss of 29 amino acid residues (about 3200 Da).[114] Therefore, if annexin A2 played a significant role in Pm generation by the TIME cells, it would be expected that the truncated annexin A2 would be the predominant form of annexin A2 on the cell surface of TIME cells. Although we easily detected intact cell surface annexin A2, we were unable to detect any truncated annexin A2 at the cell surface (Figure 19D).

3.5 S100A10$^{-/-}$ mice display reduced angiogenesis

Pm, by virtue of its role in the degradation of extracellular matrix proteins, plays an important role in angiogenesis and Pg$^{-/-}$ mice show significant defects in angiogenesis.[58] To examine the possible role of S100A10 in angiogenesis, we implanted WT and S100A10$^{-/-}$ mice with Matrigel plugs containing bFGF. When known angiogenic factors, such as bFGF, are mixed with Matrigel and injected subcutaneously into mice, endothelial cells migrate into the Matrigel plug and form vessel-like structures. We observed that the Matrigel plugs obtained from the WT mice contained 4.7 fold more positive endothelial cell staining when compared to the plugs obtained from the S100A10$^{-/-}$ mice (Figure 22A,B). When T241 tumors grown in the WT and S100A10$^{-/-}$ mice were stained for the endothelial cell marker CD31, we observed 1.7 fold more positive staining in the tumors grown in the WT mice compared to those grown in the S100A10$^{-/-}$ mouse (Figure 23A,B). These results suggest that angiogenesis was severely compromised in the S100A10$^{-/-}$ mice. Interestingly, aortas isolated from the S100A10$^{-/-}$ mouse did not demonstrate impaired sprouting when embedded into collagen *ex vivo* (Figure 24A,B). Previous reports have reported that loss of annexin A2 resulted in impaired sprouting into collagen by aortas isolated from annexin A2$^{-/-}$ mice.[208] We were unable to reproduce these results since aortas isolated from the annexin A2$^{-/-}$ mice displayed similar sprouting compared to the aortas isolated from WT and S100A10$^{-/-}$ mice (Figure 24). Additionally, tube formation was not altered by S100A10 (Figure 25B,C) and annexin A2 (Figure 25D) depletion of TIME cells. Secretion and Pg dependent activation of matrix

metalloproteinase 9 (MMP-9) was not affected by loss of S100A10 or annexin A2 in TIME cells (Figure 26A-C) or in S100A10$^{-/-}$ endothelial cells (Figure 26D). Again, this result was unexpected as it differed from previously published reports[208]. Previous reports have indicated that Pm activity is not required for tube formation *in vitro*.[315] Loss of Pg activation due to loss of S100A10 may therefore not be necessary for tube formation since MMP activity may provide sufficient proteolytic activity. Pm proteolytic activity, however, is required for proper invasion through a matrigel barrier. *In vivo*, loss of S100A10 severely impacts endothelial migration into matrigel and a growing fibrosarcoma. Such angiogenesis requires the interplay between several cell types, including endothelial cells, neutrophils and macrophages. S100A10 mediated Pg activation by all of these cells may be necessary for proper angiogenesis and the compound loss of Pg activation by all these cells may result in more severe loss of endothelial cell invasion *in vivo* compared to the results observed *in vitro*.

Figure 22. Loss of S100A10 impairs invasion of endothelial cells into Matrigel *in vivo.* WT and S100A10$^{-/-}$ mice were implanted with a Matrigel plug containing 200 ng/ml basic fibroblast growth factor and 60 U/ml heparin. CD31 staining (green) of endothelial cells shows decreased invasion into the matrigel plug in S100A10$^{-/-}$ mice (A). Nuclei were stained with DAPI (blue). Tissue surrounding the matrigel plug is visible in the S100A10$^{-/-}$ sections. Quantification of positive CD31 staining of 20X fields from 3 separate matrigel plugs was performed using Image J software (B). Sections were mounted using Vectashield mounting medium (Vector Laboratories) and viewed using a 20×/0.5 NA objective lens. Images were captured by the Zeiss Axioplan 2 microscope using a Spot 2 digital camera. Digital acquisition of the images was performed using Axiovision 4.7 (Zeiss). Statistical analysis was performed using Student's t-test (n=3, *** $p<0.001$).

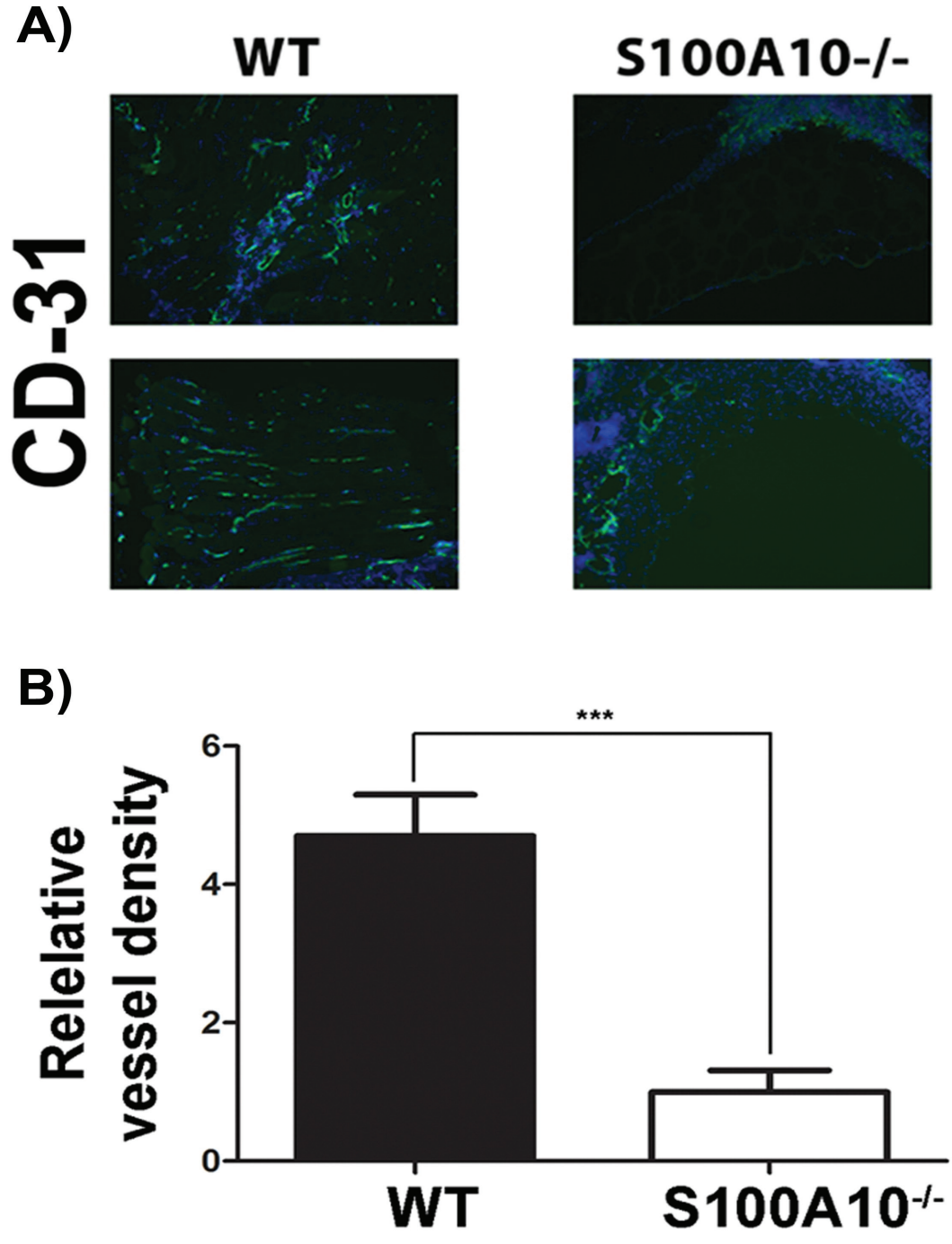
A)
WT
S100A10-/-
CD-31
B)
***
Relelative vessel density
6
4
2
0
WT
S100A10-/-

Figure 23. Loss of S100A10 impairs endothelial cell invasion into growing T241 tumors. T241 fibrosarcoma cells were injected *s.c.* into WT and S100A10$^{-/-}$. Tumors were collected after 3 weeks. CD31 staining (green) of endothelial cells shows decreased levels of endothelial cells in tumors collected from the S100A10$^{-/-}$ mice (A). Nuclei were stained with DAPI (blue). Quantification of positive CD31 staining of 20X fields from 3 separate tumors was performed using Image J software (B). Sections were mounted using Vectashield mounting medium (Vector Laboratories) and viewed using a 20×/0.5 NA objective lens. Images were captured by the Zeiss Axioplan 2 microscope using a Spot 2 digital camera. Digital acquisition of the images was performed using Axiovision 4.7 (Zeiss). Statistical analysis was performed using Student's t-test (n=3, *** $p<0.001$). T241 tumors were grown by Dr Kyle Phipps.

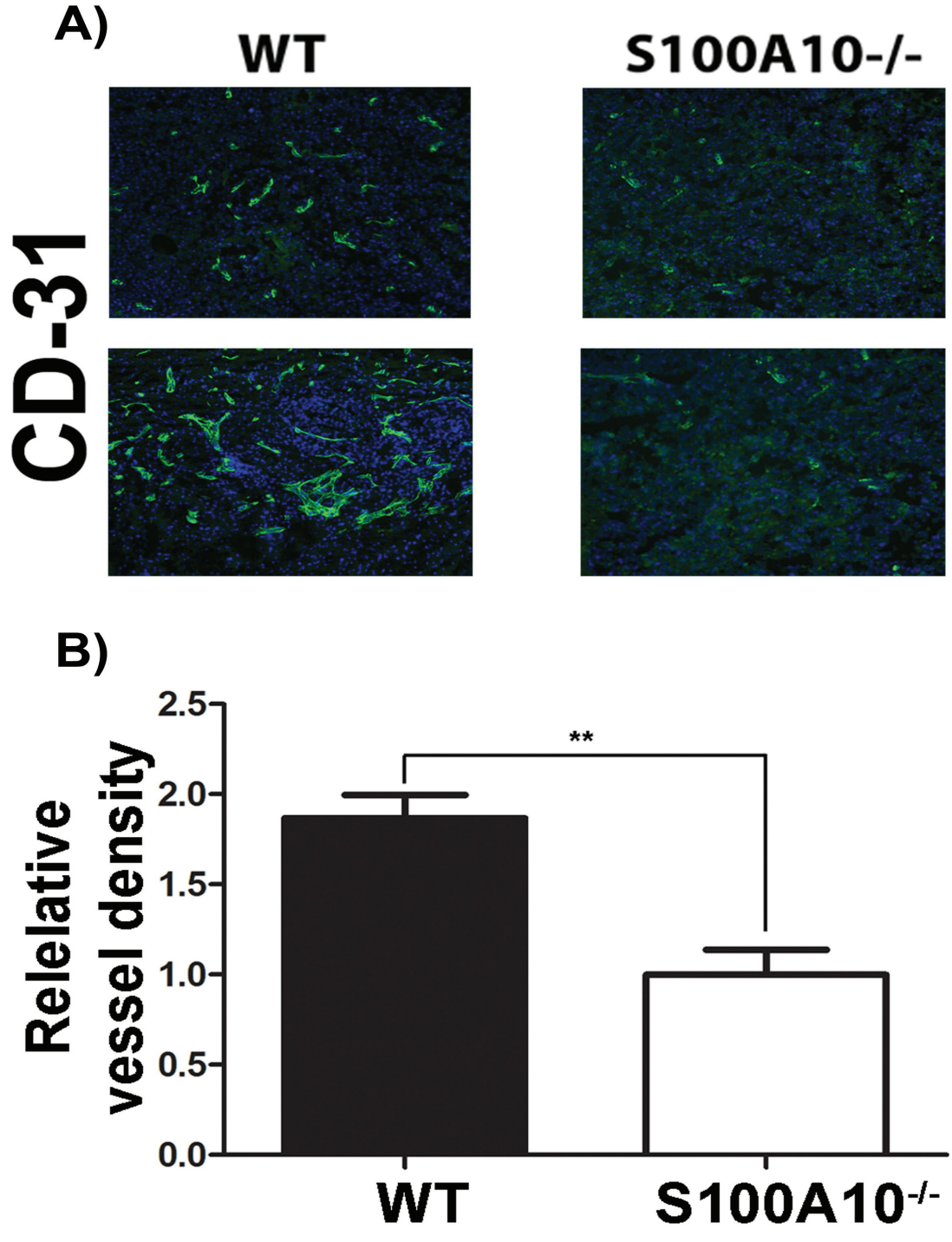
A)
WT
S100A10-/-
CD-31
B)
Relelative vessel density
2.5
2.0
1.5
1.0
0.5
0.0
**
WT
S100A10-/-

Figure 24. Aortic ring sprouting is not affected by loss of S100A10 and annexin A2. Aortas were isolated, cut and embedded into collagen to induce sprouting. Compared to aortic rings from WT mice (A), loss of S100A10 (B) and annexin A2 (C) did not alter sprouting into collagen. Representative of 3 independent experiments.

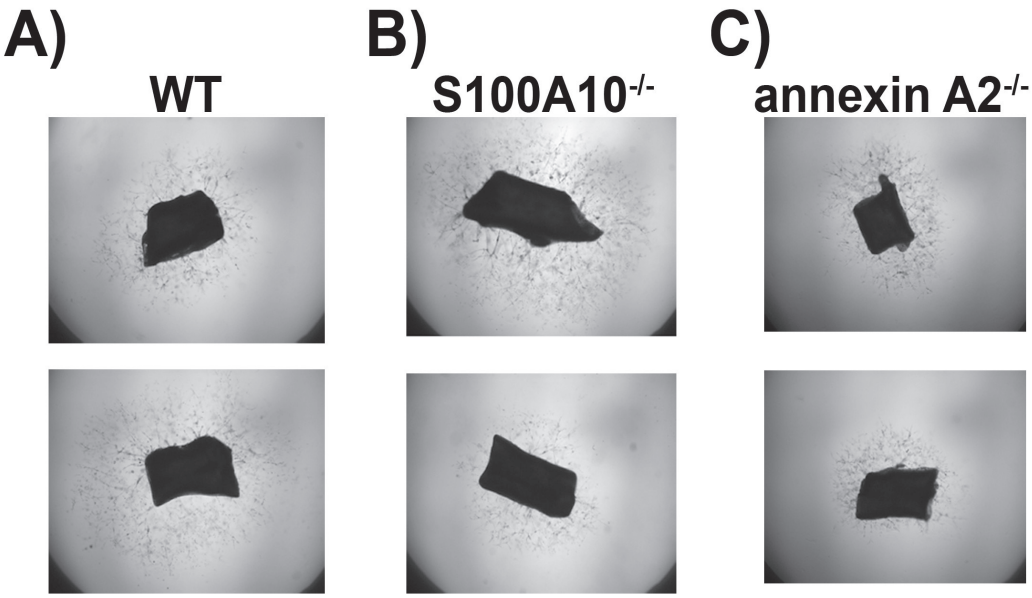
A)
WT
B)
S100A10-/-
C)
annexin A2-/-

Figure 25. Loss of S100A10 or annexin A2 does not impair endothelial cell tube formation. Control (A), S100A10 (B,C) and annexin A2 depleted (D) TIME cells were plated on top of solidified matrigel to induce tube formation. Depletion of S100A10 and annexin A2 did not alter tube formation ability. Representative of 3 independent experiments.

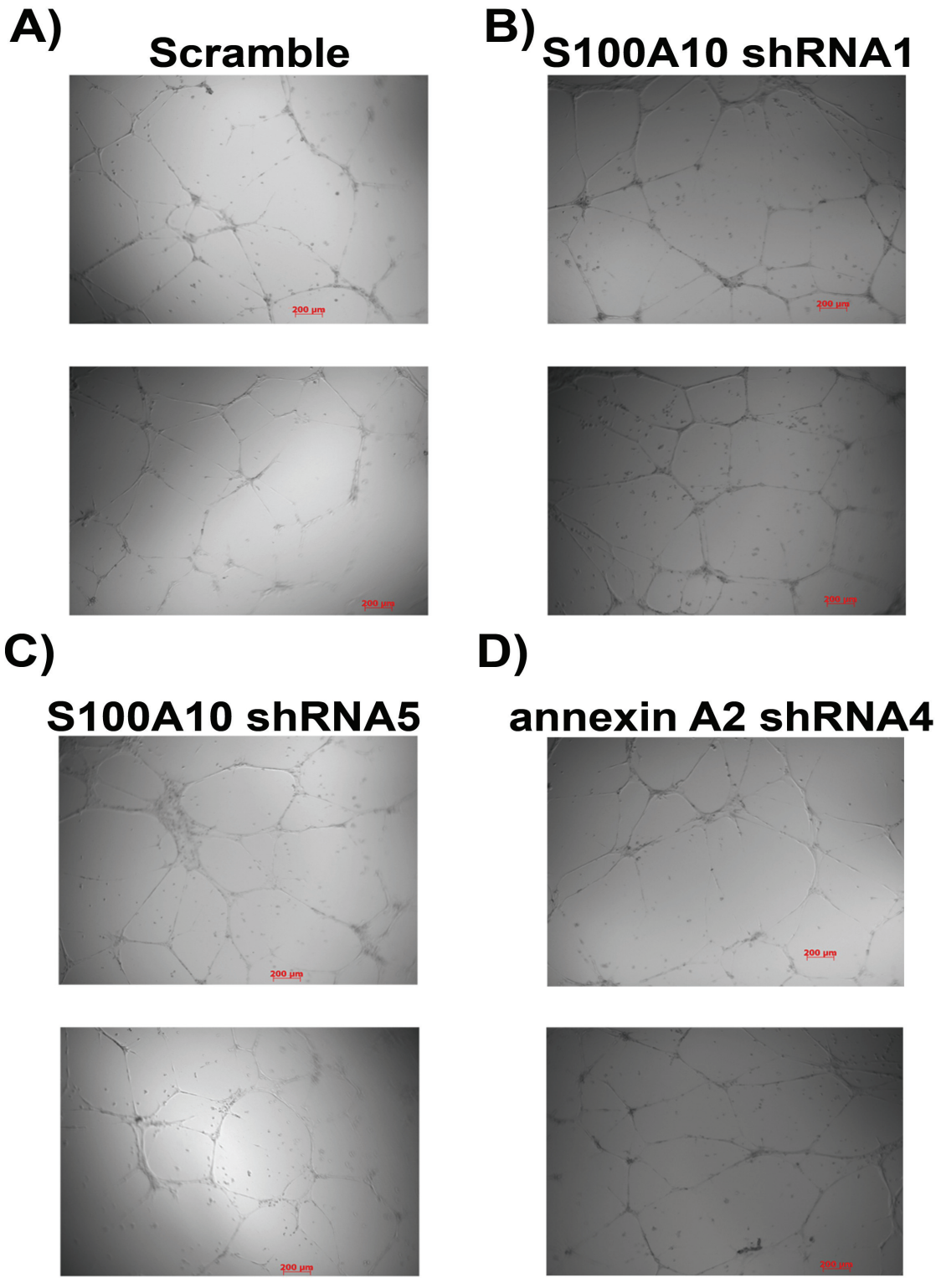
A)
Scramble
B)
S100A10 shRNA1
C)
S100A10 shRNA5
D)
annexin A2 shRNA4

Figure 26. Loss of S100A10 or annexin A2 does not affect MMP-9 secretion and Pg dependent activation as measured by gelatin zymography. MMP activity in conditioned media collected from control, S100A10 shRNA1 (A), S100A10 shRNA5 (B) and annexin A2 shRNA4 (C) TIME cells, as well as from WT and S100A10$^{-/-}$ MMECs (D) grown in the presence or absence of Pg was assayed by gelatin zymography. The addition of Pg resulted in the appearance of active MMP-9. Conditioned media collected from HT-1080 cells (HT) served as a positive control for pro-MMP-9 and MMP-2. Plasmin also served as an additional control to verify whether plasmin activity was present in the conditioned media with Pg present. Proteolytic activity is observed by negative (white) staining since the active protease will degrade gelatin and prevent staining of the gelatin. Representative of 3 independent experiments.

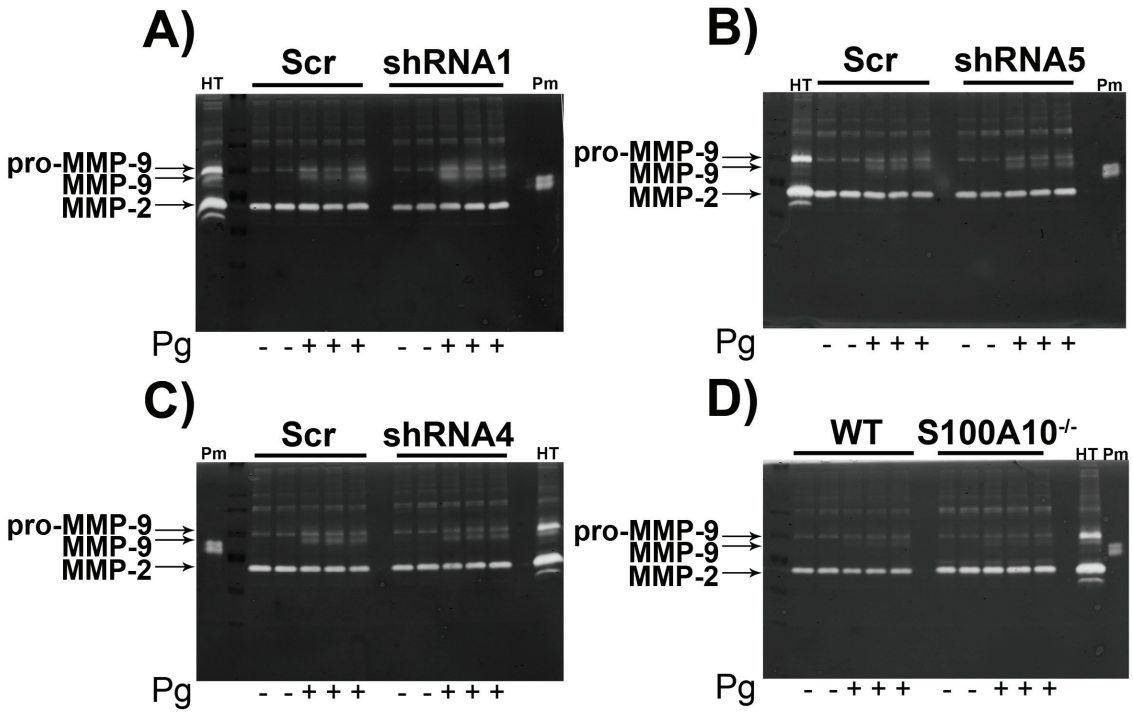
A)
Scr
shRNA1
HT
Pm
pro-MMP-9
MMP-9
MMP-2
Pg
- - + + + - - + + +
B)
Scr
shRNA5
HT
Pm
pro-MMP-9
MMP-9
MMP-2
Pg
- - + + + - - + + +
C)
Scr
shRNA4
Pm
HT
pro-MMP-9
MMP-9
MMP-2
Pg
- - + + + - - + + +
D)
WT
S100A10-/-
HT Pm
pro-MMP-9
MMP-9
MMP-2
Pg
- - + + + - - + + +

3.6 Endothelial cells from S100A10$^{-/-}$ mice show impaired chemotaxis through Matrigel

The simplest explanation for the inability of the S100A10-depleted endothelial cells to vascularize the Matrigel plug was due to the reduced capacity of these cells to generate Pm and clear a path through the Matrigel plug. We therefore directly examined the ability of the WT and S100A10$^{-/-}$ endothelial cells to migrate through a Matrigel layer. These experiments used Boyden chambers in which Pg and endothelial cells isolated from WT or S100A10$^{-/-}$ mice were placed in the upper chamber, the insert between chambers was coated with Matrigel, and serum was added to the lower chamber to act as a chemoattractant. We observed that in response to the chemoattractant, 74% fewer S100A10$^{-/-}$ endothelial cells migrated across the Matrigel barrier than WT endothelial cells (Figure 27A). Carboxypeptidase B treatment decreased migration across the Matrigel barrier of both WT and S100A10$^{-/-}$ cells. We also observed that 55% fewer S100A10-depleted TIME cells migrated across the Matrigel barrier than control TIME cells (Figure 27B) and that carboxypeptidase B treatment also decreased migration across the Matrigel barrier of both control and S100A10-depleted TIME cells. Interestingly, the chemotaxis of the WT endothelial cells was enhanced in the presence of Pg. A comparison of the chemotaxis of the S100A10$^{-/-}$ cells in the presence or absence of Pg suggested that S100A10 was responsible for 100% of this Pg-dependent chemotaxis of the S100A10$^{-/-}$ cells and similarly for 75% of the Pg dependent chemotaxis of the S100A10-depleted TIME cells. These results suggest that S100A10 plays a key role in the

regulation of endothelial cell surface protease activity. Loss of annexin A2 resulted in similar decrease in Pg dependent invasion through a matrigel barrier (Figure 27C).

Figure 27. Role of S100A10 in plasmin dependent Matrigel invasion. Primary WT or S100A10$^{-/-}$ murine endothelial cells (A), control or S100A10 depleted TIME cells (B) and annexin A2 depleted TIME cells (C) were added to the top chamber of Matrigel coated Transwell chambers in the presence of media and in the presence or absence of Pg (0.5 μM). The lower chambers contained media with 10% fetal bovine serum (FBS). Cells were incubated for 48 hours after which invading cells were stained with Haematoxylin and Eosin and counted. In some experiments cells were pretreated with carboxypeptidase B (CpB, 5 U/ml), which was added to the upper chamber where indicated. Data are expressed as mean number of cells per 40X field plus or minus SD of 3 independent experiments. Statistical analysis was performed using ANOVA (** $p<0.01$, *** $p<0.001$).

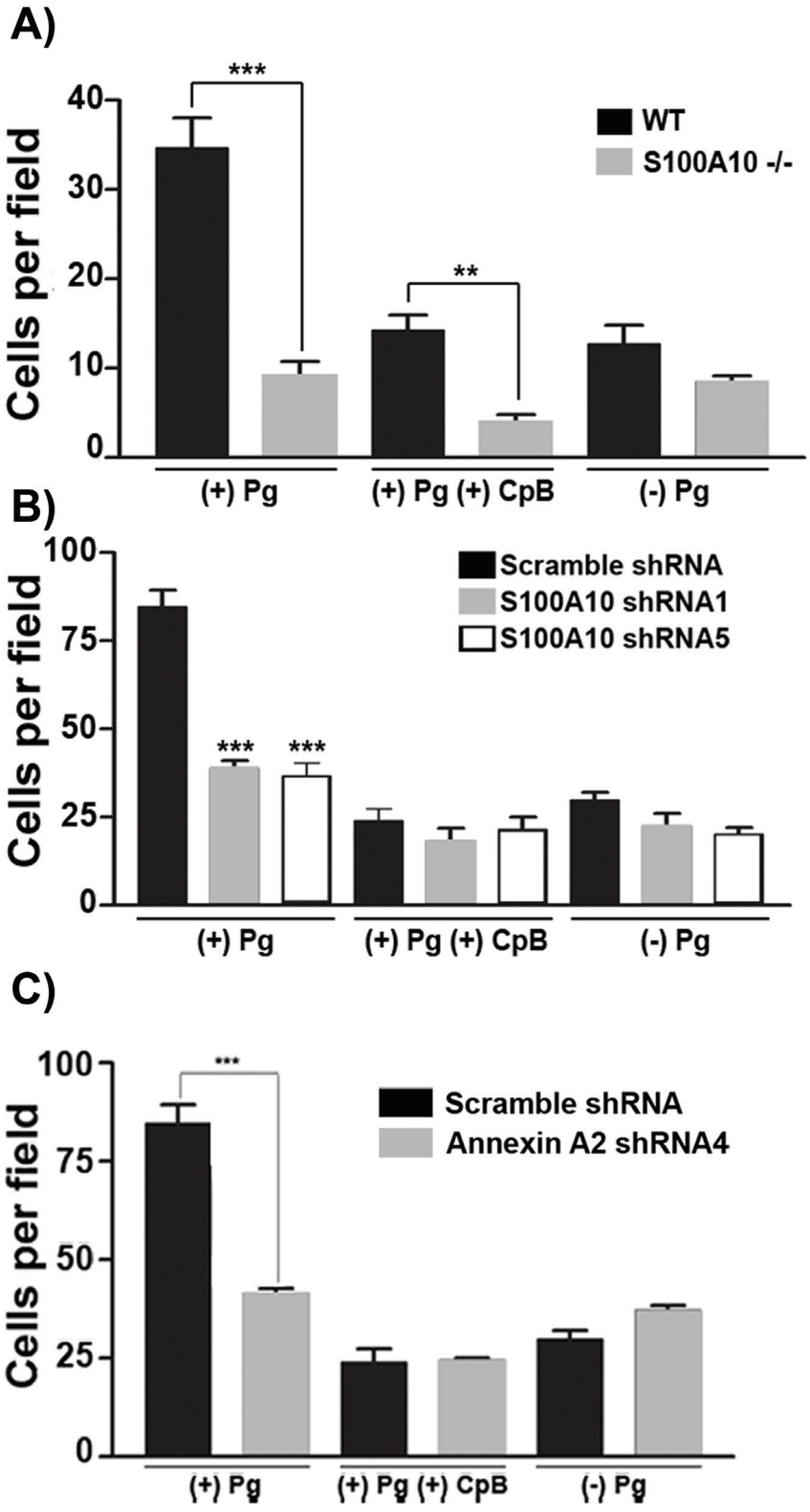
A)
***
**
40
30
20
10
0
Cells per field
WT
S100A10 -/-
(+) Pg
(+) Pg (+) CpB
(-) Pg
B)
100
75
50
25
0
Cells per field
Scramble shRNA
S100A10 shRNA1
S100A10 shRNA5
***
***
(+) Pg
(+) Pg (+) CpB
(-) Pg
C)
100
75
50
25
0
Cells per field
***
Scramble shRNA
Annexin A2 shRNA4
(+) Pg
(+) Pg (+) CpB
(-) Pg

When chemotaxis assays were repeated in the absence of a Matrigel barrier, the migration of endothelial cells from WT and S100A10-null mice through the inserts was indistinguishable (Figure 28A) as was the migration of the S100A10 depleted TIME cells (Figure 28B). Loss of annexin A2 also did not affect migration (Figure 28C). This result establishes that the ability of the S100A10$^{-/-}$ endothelial cells to migrate in response to a chemotactic stimulus was unaffected by genetic ablation of S100A10.

Figure 28. Loss of S100A10 does not affect endothelial cell migration. Primary WT or S100A10$^{-/-}$ murine endothelial cells (A), control or S100A10 depleted TIME cells (B) and annexin A2 depleted TIME cells (C) were added to the top chamber of Transwell chambers in the presence of media. The lower chambers contained media with 10% fetal bovine serum (FBS). Cells were incubated for 48 hours after which invading cells were stained with Haematoxylin and Eosin and counted. Data are expressed as mean number of cells per 40X field plus or minus SD of 3 independent experiments.

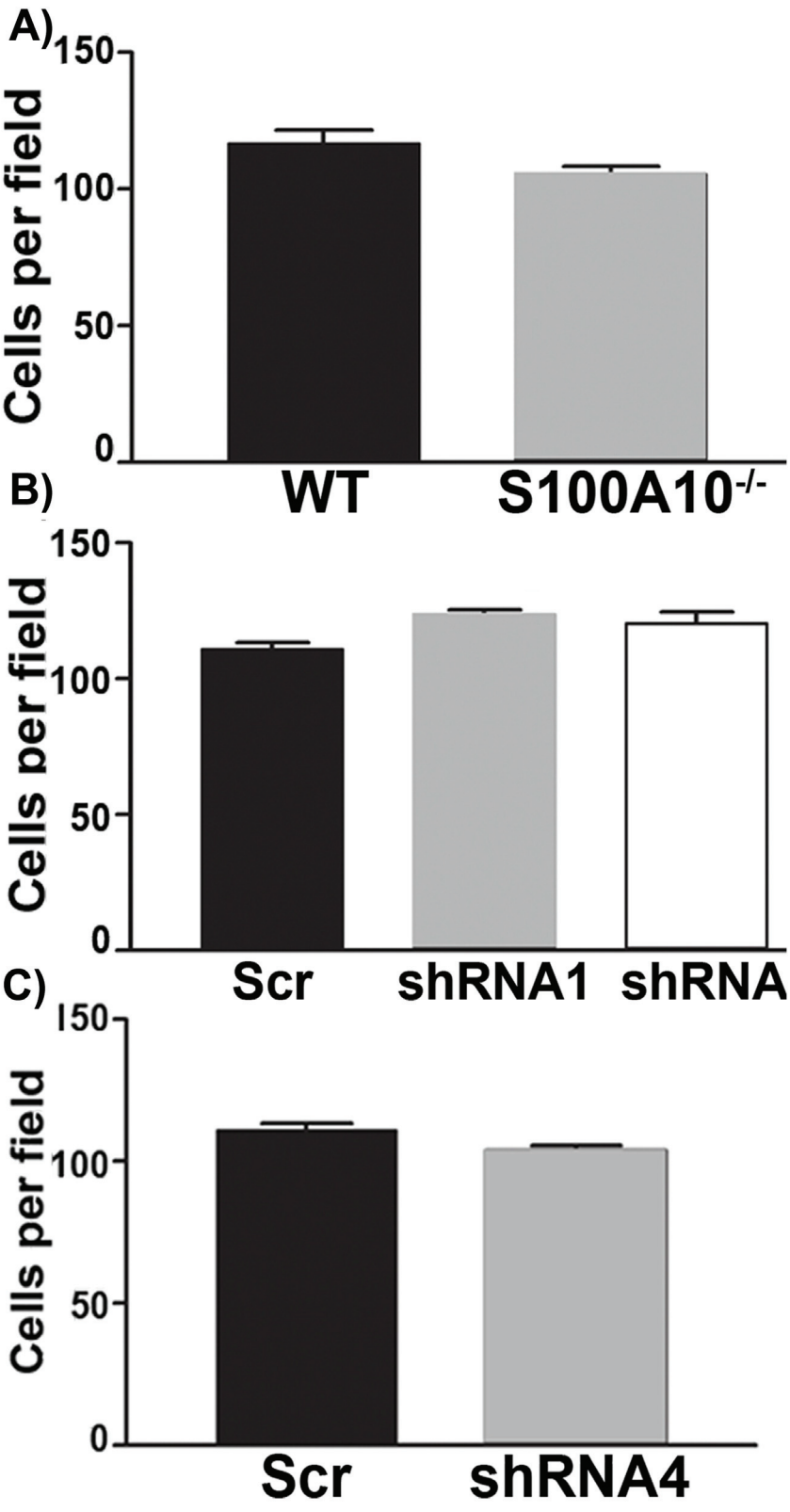
A)
150
100
50
0
Cells per field
WT
S100A10-/-
B)
150
100
50
0
Cells per field
Scr
shRNA1
shRNA
C)
150
100
50
0
Cells per field
Scr
shRNA4

CHAPTER 4: DISCUSSION

Our observation that S100A10$^{-/-}$ mice accumulate fibrin in their tissues is consistent with a role for S100A10 in Pm generation and fibrinolysis. However, fibrin clot accumulation in tissue is a dynamic process that is regulated by both the rate of clot formation (coagulation) and clot dissolution (fibrinolysis). Therefore, fibrin accumulation in the tissues could also be explained by increased coagulation in the S100A10$^{-/-}$ mouse. Since the PT, aPTT and thrombin generation assays, which directly measure coagulation, were identical for the WT and S100A10$^{-/-}$ mice, it is unlikely that enhanced coagulation is responsible for the increased accumulation of fibrin in the tissues of S100A10$^{-/-}$ mice.

To directly measure endogenous fibrinolysis *in vivo,* we injected mice with ^{125}I-fibrinogen followed by injection of batroxobin. Batroxobin is a thrombin-like enzyme which cleaves the fibrinopeptide A from fibrinogen and activates factor XIII only to a slight degree.[316] Compared to thrombin-formed fibrin, batroxobin-formed fibrin is more readily lysed by Pm, since it only cross-links fibrin to a minor extent. Furthermore, unlike thrombin, batroxobin does not activate platelets.[317] Under our experimental conditions, batroxobin rapidly converts ^{125}I-fibrinogen to ^{125}I-fibrin which is removed from the blood and retained in the tissues in the form of clots. Pm which is activated by the endothelium of the tissues digests the ^{125}I-fibrin and these degradation products are released into the blood. Our observation that the S100A10$^{-/-}$ mice have higher tissue and lower blood radioactivity levels than the WT mice suggests that the S100A10$^{-/-}$ mice have lower rates

of fibrinolysis *in vivo*. Similarly, another group used the batroxobin model system for analysis of fibrinolysis in mice deficient in the thrombin activatable fibrinolysis inhibitor (TAFI). They reported a reduction of radioactivity in the lungs of TAFI$^{-/-}$ mice, consistent with an increase in fibrinolytic activity in these mice.[318]

Tail bleeding times have typically been used to provide a measure of hemostasis *in vivo*, and tail bleeding times in mice are sensitive to both alterations in coagulation[319] or fibrinolysis.[319] Our observation that bleeding time is reduced in S100A10$^{-/-}$ mice, compared to WT mice, is consistent with the decreased fibrinolysis exhibited by the S100A10$^{-/-}$ mice. Bleeding time has been shown to be significantly increased in the Pg$^{-/-}$ mice compared to WT mice[320] whereas another group found no difference.[321] The interpretation of the Pg$^{-/-}$ mouse data was complicated by the possible role of Pg in platelet function.[320] However, S100A10 has not been detected in platelets, suggesting that loss of S100A10 is unlikely to affect platelet function.[322] In support of the decreased bleed time being due to decreased fibrinolysis is the report that textilinin-1, a potent Pm inhibitor from Pseudonaja textilis venom, dramatically decreases the bleeding time.[319]

Similarly, the decreased re-bleeding time, exhibited by the S100A10$^{-/-}$ mice compared to the WT mice, could be due to increased stability of the fibrin clot due to decreased fibrinolytic attack. The decreased fibrinolytic attack could be mediated by the generation of Pm by the assembly of tPA and Pg on the plasma clot surface or by Pm generated as a consequence of the assembly of tPA and Pg on the surface of the endothelium. Our

observation that t-PA dependent plasma clot lysis by WT and S100A10$^{-/-}$ mice is identical would rule out the possibility that neither the assembly of tPA and Pg on the fibrin clot and the generation of Pm by the plasma clot are altered by S100A10 depletion. Therefore, the central defect in the S100A10$^{-/-}$ mice likely involves Pm generation by the endothelium.

Matrigel is an extract of the Engleberth-Holm-Swarm tumor, and is composed of basement membrane proteins.[324] The Matrigel plug supports an intense vascular response when supplemented with angiogenic factors, such as bFGF, and is a well established procedure for measurement of angiogenic responses in mice.[325] Our observation that the Matrigel plugs were poorly vascularized in S100A10$^{-/-}$ mice compared to WT mice suggests that depletion of S100A10 inhibits angiogenesis. Further evidence for the role of S100A10 in angiogenesis is provided by the significant reduction in vascularization of T241 tumors grown in the S100A10$^{-/-}$ mice compared to WT mice (Figure 23). A role for S100A10 in angiogenesis was also suggested by the dramatic loss in the ability of S100A10-depleted endothelial cells to migrate through Matrigel barriers (Figure 27).

Hajjar's group has recently developed an annexin A2$^{-/-}$ mouse.[208] The homozygous annexin A2$^{-/-}$ mice displayed deposition of fibrin in the microvasculature and incomplete clearance of injury-induced arterial thrombi. Our results support a subsequent publication from Hajjar's group reporting that the loss of annexin A2 also results in the loss of

S100A10 in these mice[145] (Figure 19E). The concomitant loss of S100A10 with annexin A2 depletion was also consistent with the reports from several other laboratories.[148,326-329] Since the levels of S100A10 were reduced in the annexin $A2^{-/-}$ mice it is unclear if the fibrin deposition observed in the annexin $A2^{-/-}$ mice was due to annexin A2 or S100A10 depletion (or both). Interestingly, we observed that compared to WT endothelial cells, the $S100A0^{-/-}$ endothelial cells had similar total levels of annexin A2 but the cell surface annexin A2 levels were depleted (Figure 19). This suggested that S100A10 might be necessary for the transport of annexin A2 to the cell surface.[160] However, the loss of cell surface annexin A2 in $S100A10^{-/-}$ endothelial cells made it difficult to assess the function of annexin A2 in the $S100A10^{-/-}$ cells. We therefore utilized two different approaches to address the issue of whether annexin A2 played a significant role in endothelial cell-dependent fibrinolysis. First, since annexin A2 requires proteolytic processing and cleavage at Lys-307 to form a carboxyl-terminal Pg binding site[200], we examined the molecular weight forms of annexin A2 at the endothelial cell surface by western blotting. Although native annexin A2 was easily detected, we were unable to detect any lower molecular weight (truncated) forms of annexin A2 (Figure 19C-E). Similarly, we have been unable to detect any truncated annexin A2 on the surface of macrophages that are actively generating Pm,[142] on the surface of hyperfibrinolytic leukemic promyelocytes[207] and on the surface of cancer cells.[39] The truncated form of annexin A2 (Ser-1-Lys-307) has, to the best of our knowledge, never been directly demonstrated on any cell surface. Interesting, similar to our suggestion that annexin A2 does not play a role on the surface of endothelial cells, it has been suggested that macrophage cell surface annexin A2 most likely serves as a cell-surface binding partner of S100A10, but does not directly bind

Pg.[330] Second, TIME cells depleted of S100A10 showed dramatic losses in both Pg binding (50%) and Pm generation (60%) even though the surface annexin A2 levels of the WT and S100A10-depleted cells are similar (Figure 19). Third, the loss in Pg binding and Pm generation is similar between the S100A10-depleted TIME cells and the annexin A2 depleted TIME cells despite the fact that the annexin A2 depleted TIME cells are actually depleted in both cell surface annexin A2 and cell surface S100A10, i.e. the loss in cell surface annexin A2 does not appear to effect Pg binding or Pm generation under these experimental conditions. Therefore, we propose that annexin A2 functions to stabilize S100A10 and to localize S100A10 to the cell surface of endothelial cells but does not play a direct role in fibrinolysis by endothelial cells (figure 29).

In conclusion, our studies with the S100A10$^{-/-}$ mouse establish an important role for S100A10 in endothelial cell-dependent fibrinolysis and angiogenesis. At the cellular level, S100A10 is responsible for much of the Pg binding and Pm generation of murine and human microvascular endothelial cells.

Figure 29. Model depicting the role of S100A10 in endothelial cell plasmin generation. The predominant form of S100A10 at the endothelial cell surface is as a heterotetramer, AIIt, which consists of two copies each of the annexin A2 and S100A10 subunits.[143] The annexin A2 subunit acts as a regulatory subunit which utilizes its phospholipid-binding sites to anchor S100A10 to the cell surface. The S100A10 subunit binds tPA and Pg at the carboxyl-terminal lysine residue.[95,115] The co-localization of tPA and Pg results in accelerated cleavage of Pg by tPA resulting in Pm generation and fibrinolytic activity.

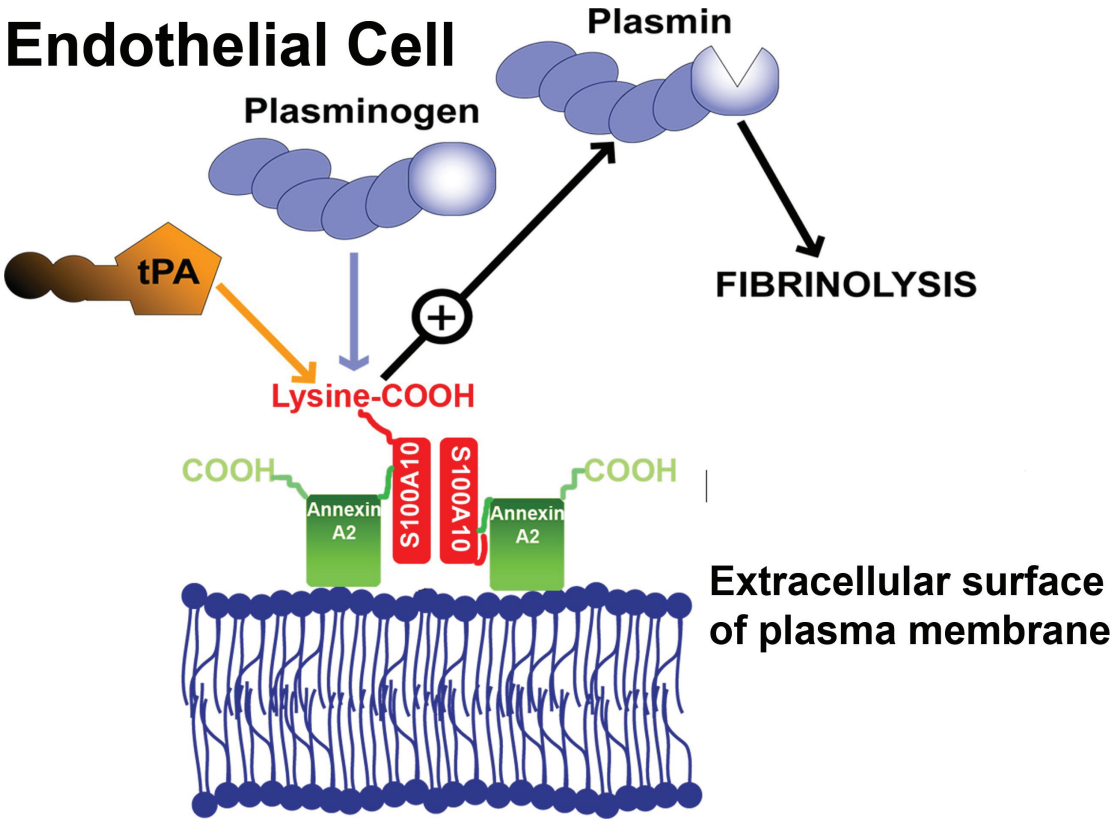
Endothelial Cell
Plasmin
Plasminogen
tPA
FIBRINOLYSIS
Lysine-COOH
COOH
Annexin A2
S100A10
S100A10
Annexin A2
COOH
Extracellular surface of plasma membrane

CHAPTER 5: CONCLUSION

5.1 Conclusion

We have demonstrated that S100A10 plays a critical role in fibrinolysis *in vivo*. S100A10$^{-/-}$ mice displayed significant levels of fibrin deposition in several organs. S100A10$^{-/-}$ mice had an impaired ability to clear batroxobin induced fibrin clots, indicating that *in vivo* fibrinolysis was impaired in the S100A10$^{-/-}$ mice. Despite demonstrating unaltered clotting parameters and components, the S100A10$^{-/-}$ mice also formed more stable clots, evidenced by the increased stability of clots formed in the tail-clip assay, suggesting that loss of S100A10 mediated plasmin activation results in increased fibrin clot stability. We also performed *in vitro* experiments with endothelial cells to further investigate the *in vivo* observations. Using S100A10$^{-/-}$ murine microvascular endothelial cells along with S100A10 and annexin A2 depleted TIME cells, we observed that loss of S100A10 results in decreased Pg binding and subsequent plasmin activation. Interestingly, we failed to observe any truncated annexin A2, which has been suggested to be necessary for AIIt dependent Pg binding, on the cell surface. We also observed that the presence of annexin A2 alone on the surface of human endothelial cells did not contribute to Pg binding and activation, suggesting that S100A10 is required for AIIt dependent Pg binding and activation. Furthermore, we demonstrated that S100A10 contributes to angiogenesis. Endothelial cells in S100A10$^{-/-}$ mice failed to invade into matrigel plugs *in vivo* and T241 tumors in S100A10$^{-/-}$ mice were poorly vascularized when compared to tumors grown in WT mice. Depletion of S100A10

severely impaired endothelial cell Pg-dependent invasion through a matrigel barrier *in vitro*. In conclusion, our studies with the S100A10$^{-/-}$ mouse establish an important role for S100A10 in endothelial cell-dependent fibrinolysis and angiogenesis. At the cellular level, S100A10 is responsible for a large portion of the Pg binding and Pm generation of murine and human microvascular endothelial cells.

5.2 Future directions.

The work presented in this thesis establishes a role for S100A10 in regulating fibrinolysis. However, the data raises further questions relating to the role played by AIIt and its individual components in a variety processes, providing several interesting possibilities for future directions for this project. We have shown that S100A10 is important in activating fibrinolysis *in vivo* and *in vitro*. Further experiments investigating the role S100A10 plays in preventing pathologies associated with impaired fibrinolysis would provide further biological significance to the data presented. For example, investigating whether S100A10-/- mice are more susceptible to atherosclerosis induced by a high cholesterol diet would be of interest. Additionally, experiments investigating whether administration of S100A10 protein by injection would promote clot dissolution in mice would be useful in determining whether S100A10 has any therapeutic effects. Preliminary data presented in Appendix B expands on whether AIIt-Hcy interactions participate in the contribution of Hcy to the development of cardiovascular disease. This preliminary data provides a plethora of future directions. I observed that AIIt incubated with Hcy and HTL had a reduced ability to activate plasminogen. An interesting experiment would be to

observe whether Hcy and/or HTL alters the ability of AIIt to bind to Pg and/or tPA. Analyzing these interactions using surface plasmon resonance would help elucidate the mechanism by which Hcy and HTL alter AIIt Pg activation. The literature describes an interaction between the annexin A2 monomer and Hcy[202,291], yet does not address a potential interaction between Hcy and AIIt *in vivo*, which may be more relevant to impaired fibrinolysis. Placing mice on a hyperhomocysteinemic diet and analyzing the AIIt from these mice for homocysteinylation would elucidate the nature of this potential interaction. Investigating the ability of the AIIt from mice on a hyperhomocysteinemic diet to activate plasminogen would also provide insight into whether elevated homocysteine serum levels alter the ability of AIIt to initiate fibrinolysis. In order to determine the nature of the Hcy-AIIt and HTL-AIIt interactions, AIIt incubated with Hcy or HTL could be analyzed by mass spectrometry to determine which amino acid residues may be modified by Hcy. AIIt isolated from murine lungs following a hyperhomocysteinemic diet could also be subjected to mass spectrometry in order to investigate the nature of the interaction *in vivo*.

Preliminary results also indicate that AIIt participates in Hcy mediated p-ERK signaling in endothelial cells. Further experiments need to be performed in order to elucidate the role AIIt plays in each of this signaling event. Additional experiments using S100A10 and other annexin A2 shRNA depleted TIME cells will clarify whether S100A10, annexin A2 or AIIt are involved in this response. Addition of AIIt and its individual components to the cells will provide evidence as to whether cell surface AIIt, S100A10 or annexin A2 are

required for Hcy mediated signaling since the proteins will interact with the extracellular membrane without entering the cells. Additionally, it would be interesting to investigate whether gene expression in response to Hcy is altered in the absence of AIIt. Of particular interest are MMP-9, tissue factor and adhesion molecules which can be induced by Hcy.[281,288,300,331-333] I also observed that p-ERK signaling was altered by loss of AIIt. Similar experiments could therefore also be conducted to further investigate the role AIIt plays in plasmin signaling and how loss of AIIt and its protein components alters the endothelial cell response to the presence of plasmin.

Another interesting preliminary observation was that tissue factor was not detectable in annexin A2 and S100A10 depleted TIME cells. This result was very surprising and additional experiments would be very interesting to determine whether this result was due to cell culture conditions. Additional agents known to induce tissue factor expression would also be useful in determining whether these cells are capable of tissue factor expression. Experiments using additional endothelial cell lines and other cell types known to express tissue factor would investigate whether this phenomena is restricted to TIME cells. If it is a broad phenomena amongst endothelial cell lines, researching whether AIIt is responsible for tissue factor expression and stability would be helpful in explaining the preliminary observation. Using the S100A10$^{-/-}$ and annexin A2$^{-/-}$ mice, experiments analyzing tissue factor expression and activity in various tissues and and cell types would be useful in determining whether the observed loss of tissue factor in TIME cells also occurred *in vivo.*

The work described in this thesis establishes a role for S100A10 in the regulation of fibrinolysis. However, further work is necessary to determine whether S100A10 is a feasible therapeutic target in the treatment of thrombotic disorders.

APPENDIX A: MANUSCRIPT

This appendix contains manuscript for the first publication created with work presented in this thesis. It was accepted for publication on July 1st, 2011 in the journal Blood. Manuscript references have not been included. All experiments were performed by Alexi Surette, except where indicated.

This research was originally published in *Blood*. Surette AP, Madureira PA, Phipps KD, Miller VA, Svenningsson P, Waisman DM. Regulation of fibrinolysis by S100A10 *in vivo*. *Blood*. 2011;118(11):3172-81 © the American Society of Hematology.

Regulation of fibrinolysis by S100A10 in vivo

Running title: S100A10 and fibrinolysis

Alexi P. Surette[1], Patricia A. Madureira[1], Kyle D. Phipps[1], Victoria A. Miller[1], Per Svenningsson[3] and David M. Waisman[1,2]

[1]Department of Biochemistry & Molecular Biology, [2]Department of Pathology, Dalhousie University, Halifax, Nova Scotia, B3H 4R2, [3]Center for Molecular Medicine, Karolinska Institutet, SE-171 77 Stockholm.

Corresponding author:

David M. Waisman

Department of Biochemistry and Molecular Biology

Dalhousie University

Halifax, Nova Scotia

david.waisman@dal.ca

(Ph) 902-494-1803

(Fax) 902-494-1355

Abstract word count: 200

Text word count: 4989

Figure count: 6

Table count: 1

Reference count: 47

Abstract

Endothelial cells form the inner lining of vascular networks and maintain blood fluidity by inhibiting blood coagulation and promoting blood clot dissolution (fibrinolysis). Plasmin, the primary fibrinolytic enzyme, is generated by the cleavage of the plasma protein, plasminogen, by its activator, tissue plasminogen activator (tPA). This reaction is regulated by plasminogen receptors at the surface of the vascular endothelial cells. Previous studies have identified the plasminogen receptor protein, S100A10 as a key regulator of plasmin generation by cancer cells and macrophages. Here we examine the role of S100A10 and its annexin A2 binding partner in endothelial cell function using a homozygous S100A10-null mouse. Compared to wild-type mice, S100A10-null mice displayed increased deposition of fibrin in the vasculature and reduced clearance of batroxobin-induced vascular thrombi, suggesting a role for S100A10 in fibrinolysis *in vivo*. Compared to WT cells, endothelial cells from S100A10-null mice demonstrated a 40% reduction in plasminogen binding and plasmin generation *in vitro*. Furthermore, S100A10-deficient endothelial cells demonstrated impaired neovascularization of Matrigel plugs *in vivo* suggesting a role for S100A10 in angiogenesis. These results establish an important role for S100A10 in the regulation of fibrinolysis and angiogenesis *in vivo*, suggesting S100A10 plays a critical role in endothelial cell function.

Introduction

Blood clots are continually forming in the vasculature due to activation of the coagulation process by sluggish blood flow, the presence of tissue debris in the blood, collagen or lipids or because of damage to small blood vessels and capillaries[1,2]. In various diseases such as atherosclerosis, damage to the normally smooth vascular surface also results in the generation of blood clots. The endothelial cells that form the inner lining of the blood vessels are responsible for ensuring vascular patency by removing these potentially dangerous blood clots. To achieve this goal, the endothelial cells convert the plasma zymogen, plasminogen, to the active serine protease plasmin. The primary function of plasmin is to maintain vascular patency by degrading the fibrin-rich blood clots, a process called fibrinolysis[3,4]. Fibrinolysis is a normal vascular process that occurs continuously

and is required to prevent naturally occurring blood clots from growing and causing vascular occlusions which would result in heart attack and stroke[5]. Fundamental to the process of fibrinolysis are the proteins that colocalize plasminogen with its activators to the endothelial cell surface, thereby stimulating the formation of plasmin in a tightly localized and highly regulated fashion[6]. Among the protein and nonprotein plasminogen receptors that have been identified are a subset of plasminogen receptors that utilize their carboxyl-terminal lysine residue to interact with the kringle domains of plasminogen and tPA[7-12]. Several of these plasminogen receptors, such as α-enolase[13], histone H2B[14], PLG-RTK[15] and S100A10[16] have recently been the focus of detailed studies highlighting the importance of plasminogen receptors in the regulation of cellular plasmin generation.

S100A10 is present on the surface of endothelial and other cells in a heterotetrameric complex with its binding partner, annexin A2[17,18]. The complex, called the annexin A2 heterotetramer (AIIt), is composed of a dimer of S100A10 that links together two molecules of annexin A2. Our laboratory has demonstrated that the phospholipid-binding sites of annexin A2 anchor S100A10 to the cell surface whereas the carboxyl-terminal lysine of the S100A10 subunits provide the binding sites for tPA (Kd = 0.45 μM), plasminogen (Pg) (Kd = 1.81 μM) and plasmin (Pm) (Kd = 0.36 μM)[19]. The annexin A2 subunit may also play a role in Pg binding. However, the binding of Pg to annexin A2 is absolutely dependent on the cleavage of annexin A2 at Lys-307[20], an event which has not been demonstrated to occur on the cell surface *in vivo.* The role of S100A10 in Pg binding and Pm regulation has been verified by a series of studies which have examined S100A10 function in the absence of annexin A2 *in vitro*. For example, removal of the carboxyl-terminal lysine from S100A10 attenuates its binding to tPA and Pg, establishing this region of S100A10 as the tPA and Pg binding site[21]. The binding of Pg to S100A10 also induces an activator-susceptible conformation in Pg which facilitates the activation of Pg by tPA[19]. Furthermore, S100A10 protects Pm from its physiological inhibitor, α2-antiplasmin and also protects tPA from its inhibitor, PAI-1[22].

Using an *in vitro* assay that measures the rate of conversion of Pg to Pm by tPA, it was shown that recombinant S100A10 stimulated the rate of tPA-dependent activation of Pg

by about 46-fold compared to a stimulation of 2-fold by recombinant annexin A2 and 77-fold by recombinant AIIt[22]. Interestingly, the formation of a complex between S100A10 and a peptide comprising the first fifteen amino acids of annexin A2, representing the S100A10-binding site of annexin A2, demonstrated similar activity to recombinant AIIt, suggesting that the binding of annexin A2 to S100A10 stimulates S100A10-dependent Pg activation[22]. Other studies have used site-directed mutagenesis to study the role of S100A10 within the heterotetrameric complex. For example, a mutant recombinant AIIt, composed of the wild-type annexin A2 and a S100A10 subunit deletion mutant missing the carboxyl-terminal lysine residue, possessed about 12% of the wild-type activity[22] and also failed to bind Pg[19], confirming that the carboxyl-terminal lysine residue of S100A10 is the Pg binding site within AIIt[19]. It has also been shown that physiologically relevant concentrations of plasma carboxypeptidase N and thrombin-activated fibrinolysis inhibitor (TAFI) are capable of completely ablating the enhancement of Pg activation by AIIt. These enzymes specifically catalyze the removal of the carboxy-terminal lysine residues of S100A10[21]. These results suggest that S100A10 is a potent activator of cellular Pm generation and that physiological mechanisms exist to terminate S100A10-stimulated Pm production and thereby protect cells from the deleterious effect of Pm overproduction.

S100A10 was originally identified as an important regulator of Pm generation by endothelial and cancer cells *in* vitro[17,23-25]. Depletion of S100A10 by RNA interference results in the loss of 65-95% of cancer cell Pm generation[23,24]. The loss of S100A10 from the extracellular surface of HT1080 fibrosarcoma cells also corresponded to a decrease in cellular invasiveness and metastatic potential, suggesting a role for S100A10 in tumor growth and metastasis *in vivo*[23]. Recently, it was reported that macrophage recruitment in response to an inflammatory stimulus was markedly decreased in S100A10-deficient mice compared to wild-type mice. This established that S100A10 is a major mediator of the Pm-dependent component of the inflammatory response *in vivo*[16]. Interestingly, although a role for S100A10 in Pm regulation has been well documented, an *in vivo* role for S100A10 in endothelial cell function has not been investigated.

Here we use the recently developed homozygous S100A10-null mouse to investigate the role of S100A10 in endothelial cell function *in vivo*. We report that S100A10 plays a key role in the fibrinolytic and angiogenic response of endothelial cells *in vivo*.

Materials and Methods

A detailed description of the routine methods is presented in the supplemental data. Only non-routine procedures and specialized materials are described here.

Mice

The S100A10-null ($S100A10^{-/-}$) mice, on a 129SV × a C57BL/6 background, were graciously provided by Svenningsson *et al.* [26]. Experimental mice were typically 6 to 8 weeks of age and of mixed gender. All animal experiments were performed in accordance with protocols approved by the University Committee on Laboratory Animals (UCLA) at Dalhousie University.

Isolation of Primary Murine Microvascular Cells

Lungs were collected from five mice, finely diced, digested with Liberase Blendzyme (Roche), and passed through a 100 μm filter (BD Biosciences). Endothelial cells were then isolated by magnetic bead separation using CD146 microbeads (Miltenyi Biotec). Purity was measured by Dil-Ac-LDL (Biomedical Technologies).

Cell culture

Primary endothelial cells and telomerase immortalized microvascular endothelial (TIME) cells were cultured with EBM-2 media (Lonza). Primary endothelial cells between passages 4 and 8 were used in all studies. T241 fibrosarcoma were a generous gift from Dr. Y. Cao (Karolinska Instiute) and were cultured in complete DMEM (Gibco).

Plasmids

pSUPER-retro plasmids were constructed as previously described.[207] Briefly, TIME cells were transduced with a retroviral shRNA system using shRNA specific for two sequences of S100A10 (shRNA 1 and shRNA 5), one sequence of annexin A2 (shRNA 4) and a control shRNA scramble sequence (shRNA Scramble).

Transfections

In order to establish S100A10 and annexin A2 knockdown cell lines, Phoenix packaging cells plated in 25 cm^3 flasks were transfected with 4 μg of the pSUPER-retro plasmids described above using the Lipofectamine 2000 transfection reagent (Invitrogen) according to the manufacturer's instructions. 48 hours after transfection the TIME cells were infected with the Phoenix cell supernatants. 48 hours after infection the S100A10 and annexin A2 knockdown cells were selected with 2 μg/ml of puromycin for a minimum of one week.

Analysis of Protein Expression

Proteins were analyzed by Western immunoblot as described in detail in the supplemental data.

Plasminogen activation

Cells were trypsinized with EDTA-free trypsin and washed 3X with DPBS. $1x10^5$ cells were then incubated with 5 nM tPA for 20 minutes at 4 ºC in incubation buffer (HBSS containing 3 mM $CaCl_2$, and 1 mM $MgCl_2$). The cells were then washed 3X with incubation buffer and incubated with 0.5 μM Glu-Pg and 250 μM Pm substrate S2251 (Chromogenix, Diapharma Group). The uPA Pg activation assay was performed as previously described[334] using 25 nM uPA (Sigma) instead of tPA and is described in detail

in the supplemental data. The rate of plasmin generation was measured at absorbance 405 nm every minute for 2 hours using a BioTek ELx808 plate reader.

Plasminogen binding assays

Preparation of FITC-Pg is described elsewhere.[142] Cells were washed and cultured in the absence of serum for 2 hours prior to assay. Cells were trypsinized with EDTA-free trypsin and washed 3X with DPBS. For carboxypeptidase B (CpB) (Worthington Biochemical) treatment, cells were incubated for 20 minutes at 37 ºC in the presence of 5 U/ml CpB. Cells were then incubated with 200 nM FITC Glu-Pg, with or without ε-ACA (100 mM), for 1 hour at 4 ºC in HBSS (1 mM $MgCl_2$ and 3 mM $CaCl_2$). Pg binding was measured by FACS analysis .

Cell surface biotinylation

Cell surface protein levels were analyzed by cell surface biotinylation as described in detail in the supplemental data.

Fibrin deposition

Levels of fibrin deposition were determined as previously described[27].

Histochemistry and Immunohistochemistry

Masson's trichrome and immunohistochemical staining of tissues are described in detail in the supplemental data.

Batroxobin-induced fibrin deposition

WT and S100A10$^{-/-}$ C57BL/6 mice were injected with 25 μCi ^{125}I-fibrinogen (MP

Biomedicals) followed by 25 U/kg batroxobin (Pentapharm) using tail vein catheters (Braintree Scientific). Two hours later, blood and tissues were collected and weighed. Gamma counts for the tissues and blood were measured with a Beckman LS 5000TA scintillation counter and corrected for weight.

Neoangiogenesis assay

750 µL Growth Factor-reduced Matrigel (BD Biosciences) with 200 ng/ml basic fibroblast growth factor (bFGF) (Invitrogen) and 60 U/mL heparin (Calbiochem) added was injected subcutaneously into WT and S100A10$^{-/-}$ C57BL/6 mice. After 7 days, the Matrigel plug was removed and embedded in Tissue Tek Cryo-OCT (Andwin Scientific). Sections were blocked with horse serum (1:20; Gibco) and incubated with an antibody against CD31 (1:250; BD Biosciences) or normal mouse IgG1 (as control; BD Biosciences) at room temperature overnight. Sections were then stained with Alexa-Fluor 488 conjugated rabbit anti-rat (1:2500; Invitrogen) and DAPI. Vessel density was quantified using Image J v1.42q software (National Institutes of Health).

T241 tumor angiogenesis

T241 tumors were established by subcutaneous injection of 2x10^6 cells, suspended in 100µL DMEM (Gibco), containing 10% FBS (Hyclone), in the right flank of female 6-8week old mice. Tumors were removed from the mice after 3 weeks and embedded in Tissue Tek Cryo-OCT (Andwin Scientific). Sections were blocked with horse serum (1:20; Gibco) and incubated with an antibody against CD31 (1:250; BD Biosciences) or normal mouse IgG1 (as control; BD Biosciences) at room temperature overnight. Sections were then stained with Alexa-Fluor 488 conjugated rabbit anti-rat (1:2500; Invitrogen) and DAPI. Vessel density was quantified using Image J v1.42q software (National Institutes of Health).

Matrigel invasion and cell migration

Murine WT or S100A10$^{-/-}$ endothelial cells and control or S100A10-depleted TIME cells were loaded (1x10^5 cells/well) into the upper layer of Transwell chambers, coated with Matrigel (invasion assays) or uncoated (migration assays) (BD Biosciences). Pg (0.5 μM), which was prepared as previously described28, and CpB (5 U/mL) were added to serum-free media in the upper chamber where indicated while media with 20% FBS was added to the bottom chamber as chemoattractant. After 48 hours, cells on the underside of the membrane were stained with hematoxylin and eosin (Sigma-Aldrich) and counted.

Coagulation Assays-The prothrombin time (PT) and activated partial thromboplastin time (aPTT) were determined using an ACL TOP (Beckman Coulter) while platelet levels were determined using an LH 755 analyzer (Beckman Coulter). Citrated blood collected from the mice was used for all coagulation assays. Clot lysis assay is described in supplemental data.

Tail Vein Clip Assay

WT and S100A10$^{-/-}$ C57BL/6 mice were anaesthetized with isoflurane and the bottom 3 mm of the tail was clipped off with a scalpel and the bleeding tail was placed in 37 °C saline. Time until bleeding stoppage and re-bleeding was recorded.

Statistics

Statistical significance was determined by Student's t test or one-way ANOVA with Tukey's multiple comparisons. Results were regarded as significant if 2-tailed P values were less than 0.05. All data are expressed as mean ± SD.

Results

S100A10$^{-/-}$ mice accumulate fibrin in their tissues

S100A10 has been proposed to be an important regulator of cellular Pm generation[17]. Mice with inactivation of the Pg gene do not generate Pm and develop spontaneous fibrin deposition in the tissues due to impaired fibrinolysis[29,30]. Therefore, we compared the fibrin content of freshly isolated tissues from WT and S100A10$^{-/-}$ mice. Tissues homogenates were prepared and the fibrin levels were determined by Western blot analysis using an anti-fibrin antibody. As shown in Figure 1A, tissues from S100A10$^{-/-}$ mice contain significantly higher amounts of fibrin that their WT litter mates. Quantification of band intensity revealed 1.8-fold increases of fibrin in lung, 2.2 fold increase in liver, 4 fold increase in kidney and 4.4 fold increase spleen from the S100A10$^{-/-}$ mice compared with WT controls. Fibrin immunohistochemistry of tissue sections demonstrated areas of fibrin deposition in the S100A10$^{-/-}$ lung (Figure 1A), liver (Figure 1B), spleen (Figure 1C) and kidney (Figure 1D) while fibrin positive staining was not observed in sections from the WT mice. Since this increased accumulation of fibrin in the tissues of the S100A10$^{-/-}$ mice could be due to either enhanced coagulation or reduced fibrinolytic activity, we further investigated the potential role of S100A10 in coagulation and fibrinolysis. The PT and aPTT values were identical between the WT and S100A10$^{-/-}$ mice (Supplemental Figure S1A,B), suggesting that S100A10 depletion does not affect the coagulation pathway.

S100A10$^{-/-}$ mice have impaired fibrinolysis

To evaluate fibrinolysis in WT and S100A10$^{-/-}$ mice, ^{125}I-fibrinogen was injected via the tail vein into WT and S100A10$^{-/-}$ mice. After 5 minutes, fibrin clot formation was initiated by the tail vein injection of batroxobin[31] and after 2 hours, blood and tissues were collected and total radioactivity was determined. We observed that the tissues of the S100A10$^{-/-}$ mice had significantly greater accumulation of ^{125}I-label than the WT mice

and less ^{125}I-label in the blood (Figure 2). For example, the residual radioactivity in the lung tissue of the S100A10$^{-/-}$ mouse was 2.5-fold higher than the WT lung tissue and 5-fold lower in the blood. The dramatic loss in the ability of the S100A10$^{-/-}$ mouse to degrade a batroxobin-induced clot could be due to a loss in plasma components of the fibrin clot lysis system or the fibrinolytic activity of the endothelium. Therefore, we compared the plasma components of the fibrinolytic system. The platelet and protein levels of plasma Pg and fibrinogen of WT and S100A10$^{-/-}$ mice were similar (Supplemental Figure S1 C,D). Plasma clots prepared from WT and S100A10$^{-/-}$ mice were then evaluated for their susceptibility to tPA-mediated clot lysis. We observed that neither the time to clot nor the time of clot lysis differed between the WT and S100A10$^{-/-}$ mice (Supplemental Figure S1E,F). Additionally, no differences were observed in antiplasmin levels, plasmin-antiplasmin (PAP) complex levels and thrombin potential between the WT and S100A10$^{-/-}$ mice (Supplemental Figure S1 G,H,I). These results are consistent with a loss of fibrinolytic activity of the endothelium in the S100A10$^{-/-}$ mouse.

Tail bleeding-rebleeding assay

A short segment of the tail of WT and S100A10$^{-/-}$ mice was clipped and the time until cessation of bleeding was determined. We observed that mice lacking S100A10 had a 4-fold reduction in the bleeding time after the tail clip compared to the WT mice (Figure 3A). Since we observed a decrease in fibrinolysis in the S100A10$^{-/-}$ mouse (Figure 2B), and a similar coagulation rate (Supplemental Figure S1A,B), the observed reduction in bleeding time by the S100A10$^{-/-}$ mice was likely due to decreased fibrinolysis of the tail clip-induced blood clot. We also observed that the time between cessation of bleeding and the initiation of subsequent episodes of bleeding, the rebleeding time, was of shorter duration and also occurred with less frequency with the S100A10$^{-/-}$ mice (Table 1). This suggested that the clots formed by the S100A10$^{-/-}$ mice were more stable than the WT mice, presumably again due to a decreased rate of fibrinolysis.

We also examined the tails of the mice for other differences that might explain the variations in the bleeding and rebleeding values. Sections of the tails were stained for collagen with Masson's Trichrome (Figure 3B,C) and obvious qualitative differences were not observed, thus suggesting that the collagen levels and architecture of the tails were similar. Since the tail collagen is the major platelet adhesive substratum for initiation of coagulation, these results further support our data suggesting that decreased fibrinolytic activity bt the endothelium of the S100A10$^{-/-}$ mice was responsible for the decreased bleeding times. Sections of the tail from the WT and S100A10$^{-/-}$ mice were also stained for S100A10 (Figure 3D,E). As expected, S100A10 did not stain the tail section obtained from the S100A10$^{-/-}$ mouse (Figure 3E) while S100A10 staining in observed throughout the WT sections, including on the endothelium of the vessels (Figure 3D).

Generation of plasmin by isolated endothelial cells from WT and S100A10$^{-/-}$ mice.

We investigated the possibility that the fibrinolytic defect displayed by the S100A10$^{-/-}$ mice was due to endothelial cell dysfunction. Lung endothelial cells from WT and S100A10$^{-/-}$ mice were isolated. Total annexin A2 levels were unaffected by loss of S100A10 (Figure 4A) while cell-surface annexin A2 was depleted in the S100A10$^{-/-}$ cells (Figure 4C). In contrast, the cell surface levels of annexin A2 in the endothelial cell line, TIME, were unaffected by S100A10 depletion (Figure 4D), while total annexin A2 levels were also unaltered (Figure 4B). Compared to the WT mice, the endothelial cells from the S100A10$^{-/-}$ mice displayed 40% less Pg binding (Figure 4E) and Pm generation (Figure 4G). We also observed that human endothelial cells that were depleted of S100A10 by RNA interference also bound about 50% less Pg (Figure 4E) and generated 60% less Pm with both tPA (Figure 4H) and uPA (Figure 4I). Pretreatment of the cells with carboxypeptidase B significantly decreased Pg binding and activation, suggesting that these processes are dependent in large part on carboxyl-terminal lysine on the Pg receptors. In this regard, S100A10 was responsible for 76% and 55% of the carboxyl-terminal dependent Pg binding of the murine and human endothelial cells, respectively.

This also suggests that although S100A10 is the dominant Pg-binding protein in endothelial cells, other carboxyl-terminal lysine containing Pg receptors also contribute to endothelial cell Pg binding and Pm generation.

We also examined the possible contribution of annexin A2 to endothelial cell Pm regulation. Depletion of annexin A2 by RNA interference reduced TIME cell Pg binding by about 50% and Pm generation with tPA and uPA by around 60% (Supplemental Figure S2B,C,D). These values were similar to the loss in Pg binding and Pm generation observed for S100A10-depleted TIME cells (Figure 4F,H,I). As expected, the depletion of TIME cell annexin A2 by the annexin A2 shRNA also resulted in S100A10 depletion (Supplemental Figure S2A). Thus, the similarity between the loss in Pg binding and Pm generation between TIME cells depleted of S100A10 by S100A10 shRNAs, but possessing unaltered levels of annexin A2 (Figure 4F,H) and those depleted of both annexin A2 and S100A10 by the annexin A2 shRNA (Supplemental Figure S2B,C) suggested that annexin A2 did not significantly contribute to TIME cell Pg binding and Pm generation under these experimental conditions. Annexin A2 binds Pg via a mechanism that is absolutely dependent on the exposure of a new carboxyl-terminal lysine. The exposure of this lysine residue requires proteolytic processing and the loss of 29 amino acid residues (about 3200 Da)[20]. Therefore, if annexin A2 played a significant role in Pm generation by the TIME cells, it would be expected that the truncated annexin A2 would be the predominant form of annexin A2 on the cell surface of TIME cells. Although we easily detected intact cell surface annexin A2, we were unable to detect any truncated annexin A2 at the cell surface (Figure 4D).

S100A10$^{-/-}$ mice display reduced angiogenesis

Pm, by virtue of its role in the degradation of extracellular matrix proteins, plays an important role in angiogenesis and Pg$^{-/-}$ mice show significant defects in angiogenesis[32]. To examine the possible role of S100A10 in angiogenesis, we implanted WT and S100A10$^{-/-}$ mice with Matrigel plugs containing bFGF. When known angiogenic factors,

such as bFGF, are mixed with Matrigel and injected subcutaneously into mice, endothelial cells migrate into the Matrigel plug and form vessel-like structures. We observed that the Matrigel plugs obtained from the WT mice contained 4.7 fold more positive endothelial staining when compared to the plugs obtained from the S100A10$^{-/-}$ mice (Figure 5A,B). When T241 tumors grown in the WT and S100A10$^{-/-}$ mice were stained for the endothelial cell marker CD31, we observed 1.7 fold more positive staining in the tumors grown in the WT mice compared to those grown in the S100A10$^{-/-}$ mouse (Figure 5C,D). These results suggest that angiogenesis was severely compromised in the S100A10$^{-/-}$ mice.

Endothelial cells from S100A10$^{-/-}$ mice show impaired chemotaxis through Matrigel

The simplest explanation for the inability of the S100A10-depleted endothelial cells to vascularize the Matrigel plug was due to the reduced capacity of these cells to generate Pm and clear a path through the Matrigel plug. We therefore directly examined the ability of the WT and S100A10-null endothelial cells to migrate through a Matrigel layer. These experiments used Boyden chambers in which Pg and endothelial cells isolated from WT or S100A10-null mice were placed in the upper chamber, the insert between chambers was coated with Matrigel, and serum was added to the lower chamber to act as a chemoattractant. We observed that in response to the chemoattractant, 74% fewer S100A10-null endothelial cells migrated across the Matrigel barrier than WT endothelial cells (Figure 5E). Carboxypeptidase B treatment decreased migration across the Matrigel barrier of both WT and S100A10-null cells. We also observed that 55% fewer S100A10-depleted TIME cells migrated across the Matrigel barrier than control TIME cells (Figure 5F) and that carboxypeptidase B treatment also decreased migration across the Matrigel barrier of both control and S100A10-depleted TIME cells. Interestingly, the chemotaxis of the WT endothelial cells was enhanced in the presence of Pg. A comparison of the chemotaxis of the S100A10-null cells in the presence or absence of Pg suggested that S100A10 was responsible for 100% of this Pg-dependent chemotaxis of the S100A10-

null cells and similarly for 75% of the Pg dependent chemotaxis of the S100A10-depleted TIME cells. These results suggest that S100A10 plays a key role in the regulation of endothelial cell surface protease activity. Loss of annexin A2 resulted in similar decrease in Pg dependent invasion through a matrigel barrier (Supplemental Figure 2E).

When chemotaxis assays were repeated in the absence of a Matrigel barrier, the migration of endothelial cells from WT and S100A10-null mice through the inserts was indistinguishable (Figure 5G) as was the migration of the S100A10 depleted TIME cells (Figure 5H). This result establishes that the ability of the S100A10$^{-/-}$ endothelial cells to migrate in response to a chemotactic stimulus was unaffected by genetic ablation of S100A10.

Discussion

Our observation that S100A10$^{-/-}$ mice accumulate fibrin in their tissues is consistent with a role for S100A10 in Pm generation and fibrinolysis. However, fibrin clot accumulation in tissue is a dynamic process that is regulated by both the rate of clot formation (coagulation) and clot dissolution (fibrinolysis). Therefore, fibrin accumulation in the tissues could also be explained by increased coagulation in the S100A10$^{-/-}$ mouse. Since the PT and aPTT assays, which directly measure coagulation, were identical for the WT and S100A10$^{-/-}$ mice, it is unlikely that enhanced coagulation is responsible for the increased accumulation of fibrin in the tissues of S100A10$^{-/-}$ mice.

To directly measure endogenous fibrinolysis *in vivo,* we injected mice with ^{125}I-fibrinogen followed by injection of batroxobin. Batroxobin is a a thrombin-like enzyme which cleaves mainly the fibrinopeptide A from fibrinogen and activates factor XIII only to a slight degree[33]. Compared to thrombin-formed fibrin, batroxobin-formed fibrin is more readily lysed by Pm, since it only cross-links fibrin to a minor extent. Furthermore, unlike thrombin, batroxobin does not activate platelets[34]. Under our experimental conditions, batroxobin rapidly converts ^{125}I-fibrinogen to ^{125}I-fibrin which is removed

from the blood and retained in the tissues. Pm which is produced by the endothelium of the tissues digests the ^{125}I-fibrin and these degradation products are released into the blood. Our observation that the S100A10$^{-/-}$ mice have higher tissue and lower blood radioactivity levels than the WT mice suggests that the S100A10$^{-/-}$ mice have lower rates of fibrinolysis *in vivo*. Similarly, another group used the batroxobin model system for analysis of fibrinolysis in mice deficient in the thrombin activatable fibrinolysis inhibitor (TAFI). They reported a reduction of radioactivity in the lungs of TAFI$^{-/-}$ mice, consistent with an increase in fibrinolytic activity in these mice[35].

Tail bleeding times have typically been used to provide a measure of hemostasis *in vivo*, and tail bleeding times in mice are sensitive to both alterations in coagulation[36] or fibrinolysis[37]. Our observation that bleeding time is reduced in S100A10$^{-/-}$ mice, compared to WT mice, is consistent with the decreased fibrinolysis exhibited by the S100A10$^{-/-}$ mice. Bleeding time has been shown to be significantly increased in the Pg$^{-/-}$ mice compared to WT mice[38] whereas another group found no difference[39]. The interpretation of the Pg$^{-/-}$ mouse data was complicated by the possible role of Pg in platelet function[38]. However, S100A10 has not been detected in platelets, suggesting that loss of S100A10 is unlikely to affect platelet function[40]. In support of the decreased bleed time being due to decreased fibrinolysis is the report that textilinin-1, a potent Pm inhibitor from Pseudonaja textilis venom, dramatically decreases the bleeding time[37].

Similarly, the decreased rebleeding time, exhibited by the S100A10$^{-/-}$ mice compared to the WT mice, could be due to increased stability of the fibrin clot due to decreased fibrinolytic attack. The decreased fibrinolytic attack could be mediated by the generation of Pm by the assembly of tPA and Pg on the plasma clot surface or by Pm generated as a consequence of the assembly of tPA and Pg on the surface of the endothelium. Our observation that t-PA dependent plasma clot lysis by WT and S100A10$^{-/-}$ mice is identical would rule out the possibility that neither the assembly of tPA and Pg on the fibrin clot and the generation of Pm by the plasma clot are altered by S100A10 depletion. Therefore, the central defect in the S100A10$^{-/-}$ mice likely involves Pm generation by the

endothelium.

Matrigel is an extract of the Engleberth-Holm-Swarm tumor, and is composed of basement membrane proteins. The Matrigel plug supports an intense vascular response when supplemented with angiogenic factors, such as bFGF, and is a well established procedure for measurement of angiogenic responses in mice. Our observation that the Matrigel plugs were poorly vascularized by the S100A10$^{-/-}$ mice compared to WT mice suggests that depletion of S100A10 inhibits angiogenesis. Further evidence for the role of S100A10 in angiogenesis is provided by the significant reduction in endothelial cells within T241 tumors grown in the S100A10$^{-/-}$ mice compared to normal tumor vascularization in the WT mice. A role for S100A10 in angiogenesis was also suggested by the dramatic loss in the ability of S100A10-depleted endothelial cells to migrate through Matrigel barriers (Figure 5).

Hajjar's group has recently developed an annexin A2$^{-/-}$ mouse[27]. The homozygous annexin A2$^{-/-}$ mice displayed deposition of fibrin in the microvasculature and incomplete clearance of injury-induced arterial thrombi. Our results support a subsequent publication from Hajjar's group reporting that the loss of annexin A2 also results in the loss of S100A10 in these mice[41] (Supplementary Figure S2A). The concomitant loss of S100A10 with annexin A2 depletion was also consistent with the reports from several other laboratories[42-46]. Since the levels of S100A10 were reduced in the annexin A2$^{-/-}$ mice it is unclear if the fibrin deposition observed in the annexin A2$^{-/-}$ mice was due to annexin A2 or S100A10 depletion (or both). Interestingly, we observed that compared to WT endothelial cells, the S100A0$^{-/-}$ endothelial cells had similar total levels of annexin A2 but the cell surface annexin A2 levels were depleted. This suggested that S100A10 might be necessary for the transport of annexin A2 to the cell surface[42]. However, the loss of cell surface annexin A2 in S100A10$^{-/-}$ endothelial cells made it difficult to assess the function of annexin A2 in the S100A10$^{-/-}$ cells. We therefore utilized two different approaches to address the issue of whether annexin A2 played a significant role in endothelial cell-dependent fibrinolysis. First, since annexin A2 requires proteolytic processing and

cleavage at Lys-307 to form a carboxyl-terminal Pg binding site, we examined the molecular weight forms of annexin A2 at the endothelial cell surface by western blotting. Although native annexin A2 was easily detected, we were unable to detect any lower molecular weight (truncated) forms of annexin A2 (Figure 4C,D and Supplemental Figure S2A). Similarly, we have been unable to detect any truncated annexin A2 on the surface of macrophages that are actively generating Pm16, on the surface of hyperfibrinolytic leukemic promyelocytes[25] and on the surface of cancer cells[23]. The truncated form of annexin A2 (Ser-1-Lys-307) has to the best of our knowledge never been directly demonstrated on any cell surface. Interesting, similar to our suggestion that annexin A2 does not play a role on the surface of endothelial cells, has been the suggestion that macrophage cell surface annexin A2 most likely serves as a cell-surface binding partner of S100A10, but does not directly bind Pg[47]. Second, TIME cells depleted of S100A10 showed dramatic losses in both Pg binding (50%) and Pm generation (60%) even though the surface annexin A2 levels of the WT and S100A10-depleted cells are similar (Figure 4). Third, the loss in Pg binding and Pm generation is similar between the S100A10-depleted TIME cells and the annexin A2 depleted TIME cells despite the fact that the annexin A2 depleted TIME cells are actually depleted in both cell surface annexin A2 and cell surface S100A10, i.e. the loss in cell surface annexin A2 does not appear to effect Pg binding or Pm generation under these experimental conditions. Therefore, we propose that annexin A2 functions to stabilize S100A10 and to localize S100A10 to the cell surface of endothelial cells but does not play a direct role in fibrinolysis by endothelial cells (figure 6).

In conclusion, our studies with the S100A10$^{-/-}$ mouse establish an important role for S100A10 in endothelial cell-dependent fibrinolysis and angiogenesis. At the cellular level, S100A10 is responsible for much of the Pg binding and Pm generation of murine and human microvascular endothelial cells.

Acknowledgements

This work was supported by the Heart and Stroke Foundation of New Brunswick and

Nova Scotia. We thank Patricia Colp from the Dalhousie University Histology and Research Services Laboratory for tissue processing.

Authorship

Contribution: APS designed and performed research, analyzed data, and wrote the manuscript. PAM generated the S100A10 and Annexin A2 depleted human endothelial cell lines and cell surface biotinylation. KDP and VAM performed research. PS provided the S100A10$^{-/-}$ mice and critically evaluated the manuscript. DMW. designed research, analyzed data, and wrote the manuscript.

Conflict of Interest Disclosure: The authors declare no conflict of interest

Correspondence: David M. Waisman, Department of Biochemistry & Molecular Biology and Department of Pathology, Dalhousie University, Halifax, Nova Scotia, B3H 4R2; email: david.waisman@dal.ca

Figure A1. Loss of S100A10 results in increased tissue fibrin deposition. Lung, liver, kidney and spleen tissues from 6 WT and S100A10$^{-/-}$ mice were collected, and the fibrin content of tissue lysates was determined by SDS-PAGE and Western blot analysis. 10 ng of each tissue were loaded. Quantification of fibrin deposition was normalized to WT levels. Immunohistochemistry for fibrin was performed on perfused sections of formalin fixed tissues. Sections were deparaffinized and incubated with anti-fibrin antibody followed by anti-rabbit HRP. Arrows indicate areas with fibrin deposition. Tissues observed were lung (A), liver (B), spleen (C) and kidney (D). Statistical analysis was performed using Student's t-test and and the data are expressed as the mean (±) SEM of 6 independent experiments (** $p < 0.01$, *** $p < 0.001$). Sections were mounted using Cytoseal 60 mounting media (Richard-Allen Scientific) and viewed using a 20×/0.5 NA objective lens. Images were captured by the Nikon Eclipse E600 microscope using a Nikon DXM1200F camera. Digital acquisition of the images was performed using ACT-1 v2.7 software (Nikon). Figures were generated using Adobe Photoshop CS3 v10 (Adobe Systems Incorporated).

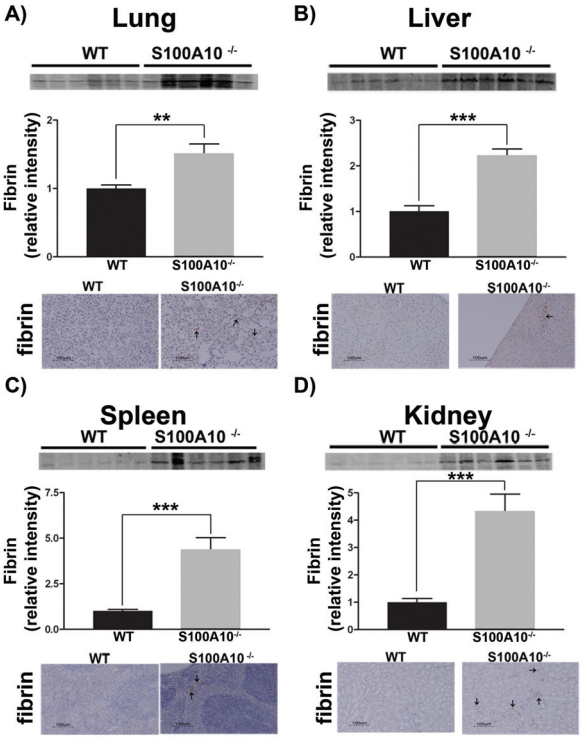
A)
Lung
WT
S100A10 -/-
Fibrin (relative intensity)
**
WT
S100A10-/-
fibrin
B)
Liver
***
C)
Spleen
D)
Kidney

Figure A2. S100A10$^{-/-}$ mice have impaired ability to clear induced fibrin clots. WT and S100A10$^{-/-}$ mice were injected with ^{125}I-fibrinogen and batroxobin. After 2 hours, tissues were collected, weighed and radioactivity was measure in a gamma counter. The data are expressed as counts per gram of tissue. Statistical analysis was performed using Student's t-test and and the data are expressed as the mean (±) SEM of 6 independent experiments (** $p < 0.01$, *** $p < 0.001$). Figures were generated using Adobe Photoshop CS3 v10 (Adobe Systems Incorporated).

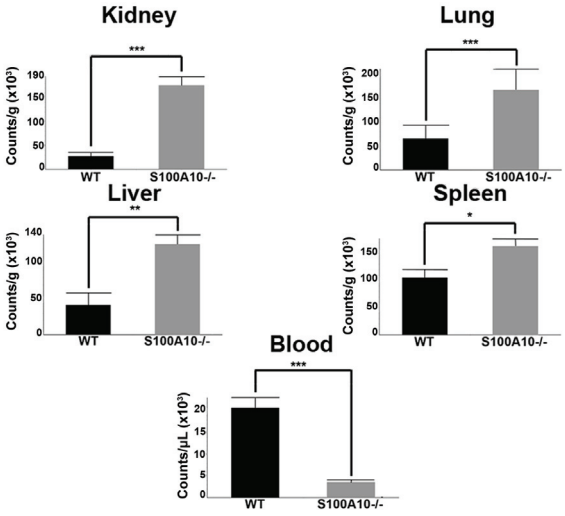
Kidney
***
Counts/g (x10³)
190
150
100
50
0
WT
S100A10-/-
Lung
***
Counts/g (x10³)
200
150
100
50
0
WT
S100A10-/-
Liver
**
Counts/g (x10³)
140
100
50
0
WT
S100A10-/-
Spleen
*
Counts/g (x10³)
150
100
50
0
WT
S100A10-/-
Blood
***
Counts/µL (x10³)
20
15
10
5
0
WT
S100A10-/-

Figure A3. Bleeding time in WT and S100A10$^{-/-}$ mice. The last 3 mm of the tail of anaesthetized WT and S100A10$^{-/-}$ mice was clipped using a scalpel blade. The clipped tails of the anaesthetized mice were placed in 37 ºC saline and the time for cessation of bleeding was recorded (A). Masson's trichrome stain was used to observe the morphology of tail sections from WT (B) and S100A10$^{-/-}$ (C) mice. Immunohistochemistry for S100A10 was also performed on tail sections from WT (D) and S100A10$^{-/-}$ (E) mice. Sections were deparaffinized and either subjected to Masson's trichrome or anti-S100A10 antibody followed by anti-goat HRP. Arrows indicate endothelial lining of vessels. Statistical analysis was performed using Student's t-test and the data are expressed as (±) SEM of 3 independent experiments (*** $p < 0.001$). Sections were mounted using Cytoseal 60 mounting media (Richard-Allen Scientific) and viewed using a 20×/0.5 NA objective lens. Images were captured by the Nikon Eclipse E600 microscope using a Nikon DXM1200F camera. Digital acquisition of the images was performed using ACT-1 v2.7 software (Nikon). Figures were generated using Adobe Photoshop CS3 v10 (Adobe Systems Incorporated).

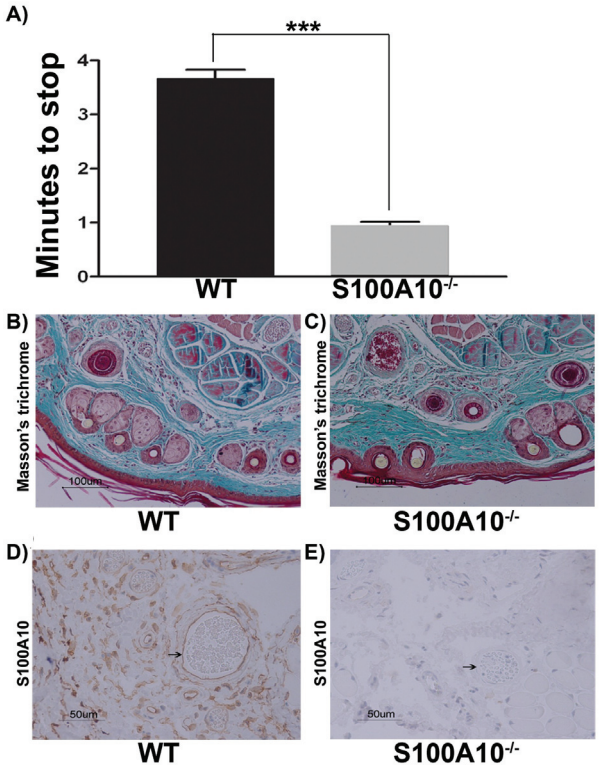
A)
***
Minutes to stop
4
3
2
1
0
WT
S100A10-/-
B)
Masson's trichrome
100um
WT
C)
Masson's trichrome
S100A10-/-
D)
S100A10
50um
WT
E)
S100A10
50um
S100A10-/-

Figure A4. Depletion of S100A10 results in decreased endothelial cell plasminogen binding and plasmin generation. In order to detect the total cellular levels of annexin A2 and S100A10, primary murine endothelial cells, isolated from WT or S100A10$^{-/-}$ mice (A), as well as control and S100A10 depleted TIME cells (B), were dissociated from culture flasks, lysed, subjected to SDS PAGE and immunoblotted with anti-actin (loading control), anti-annexin A2 or anti-S100A10 antibodies. Cell surface protein levels for primary murine endothelial cells (C) and TIME cells (D), as detected by cell-surface biotinylation, are shown. FITC-Pg binding to the primary murine endothelial cells (E) or TIME cells (F) was measured by FACS. Quantification of flow cytometric analysis of Pg binding was calculated using WinMDI software. Loss of S100A10 affected tPA dependent plasmin generation by primary murine endothelial cells (G) and TIME cells (H) along with uPA dependent plasmin generation by TIME cells (I). Statistical analysis was performed using Student's t-test (E,G) or ANOVA (F,H) (* $p < 0.1$, *** $p < 0.001$). Figures were generated using Adobe Photoshop CS3 v10 (Adobe Systems Incorporated). TIME cell shRNA knockdown cell lines were created by Dr Patricia Madureira.

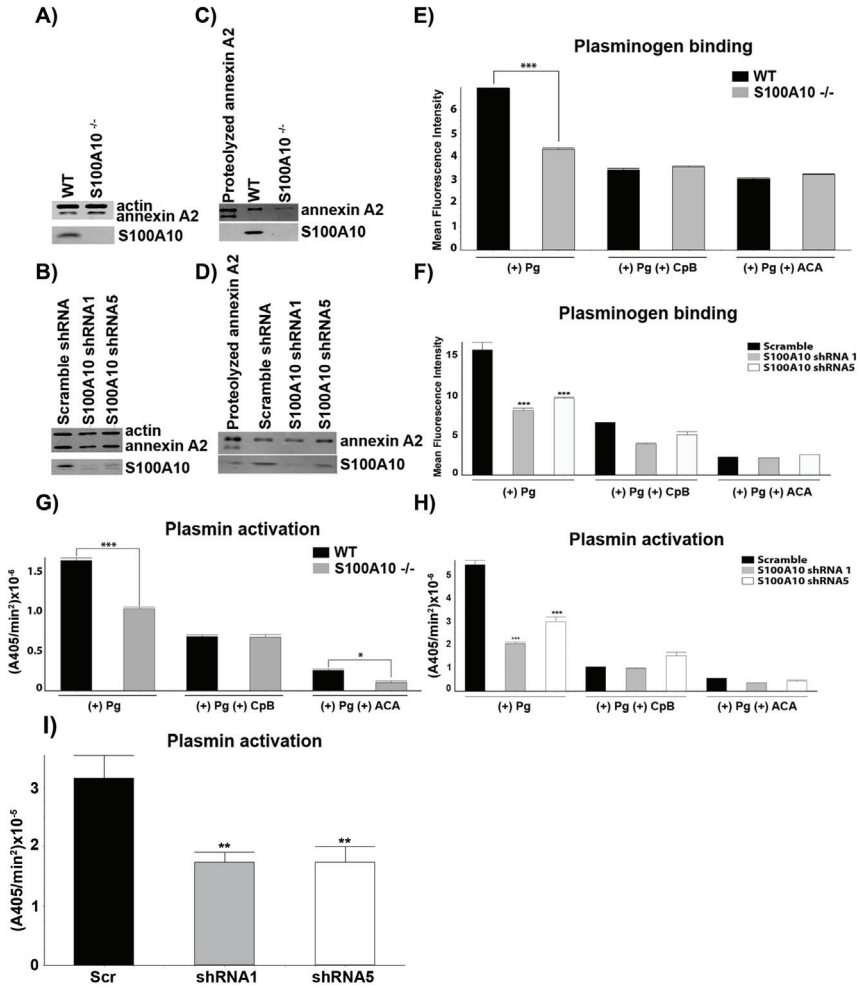
A)
WT
S100A10 -/-
actin
annexin A2
S100A10
C)
Proteolyzed annexin A2
WT
S100A10 -/-
annexin A2
S100A10
E)
Plasminogen binding
WT
S100A10 -/-
Mean Fluorescence Intensity
(+) Pg
(+) Pg (+) CpB
(+) Pg (+) ACA
B)
Scramble shRNA
S100A10 shRNA1
S100A10 shRNA5
actin
annexin A2
S100A10
D)
Proteolyzed annexin A2
Scramble shRNA
S100A10 shRNA1
S100A10 shRNA5
annexin A2
S100A10
F)
Plasminogen binding
Scramble
S100A10 shRNA 1
S100A10 shRNA5
Mean Fluorescence Intensity
(+) Pg
(+) Pg (+) CpB
(+) Pg (+) ACA
G)
Plasmin activation
WT
S100A10 -/-
(A405/min²)x10⁻⁶
(+) Pg
(+) Pg (+) CpB
(+) Pg (+) ACA
H)
Plasmin activation
Scramble
S100A10 shRNA 1
S100A10 shRNA5
(A405/min²)x10⁻⁶
(+) Pg
(+) Pg (+) CpB
(+) Pg (+) ACA
I)
Plasmin activation
(A405/min²)x10⁻⁵
Scr
shRNA1
shRNA5

Figure A5. Role of S100A10 in plasmin dependent Matrigel invasion. WT and S100A10$^{-/-}$ mice were implanted with a Matrigel plug containing 200 ng/ml basic fibroblast growth factor and 60 U/ml heparin. CD31 staining (green) of endothelial cells shows decreased invasion into the matrigel plug in S100A10$^{-/-}$ mice (A). Nuclei were stained with DAPI (blue). Tissue surrounding the matrigel plug is visible in the S100A10$^{-/-}$ sections. Quantification of positive CD31 staining of 20X fields from 3 separate matrigel plugs was performed using Image J software (B). T241 fibrosarcoma cells were injected *s.c.* into WT and S100A10$^{-/-}$. Tumors were collected after 3 weeks. CD31 staining (green) of endothelial cells shows decreased levels of endothelial cells in tumors collected from the S100A10$^{-/-}$ mice (C). Nuclei were stained with DAPI (blue). Quantification of positive CD31 staining of 20X fields from 3 separate tumors was performed using Image J software (D). Sections were mounted using Vectashield mounting medium (Vector Laboratories) and viewed using a 20×/0.5 NA objective lens. Images were captured by the Zeiss Axioplan 2 microscope using a Spot 2 digital camera. Digital acquisition of the images was performed using Axiovision 4.7 (Zeiss). Primary WT or S100A10$^{-/-}$ murine endothelial cells (E,G) or control or S100A10 depleted TIME cells (F,H) were added to the top chamber of Transwell chambers in the presence of media and in the presence or absence of Pg (0.5 μM). Some chambers were coated with Matrigel (invasion assays) (E,F) or uncoated (migration assays) (G,H). The lower chambers contained media with 10% fetal bovine serum (FBS). Cells were incubated for 48 hours after which invading cells were stained with Haematoxylin and Eosin and counted. Data are expressed as mean number of cells per 40X field plus or minus SD of 3 independent experiments. Statistical analysis was performed using Student's t-test (B,D,E,G) or ANOVA (F,H) (*** $p<0.001$). In some experiments cells were pretreated with carboxypeptidase B (CpB, 5 U/ml), which was added to the upper chamber where indicated. Figures were generated using Adobe Photoshop CS3 v10 (Adobe Systems Incorporated). T241 tumors were grown by Dr Kyle Phipps.

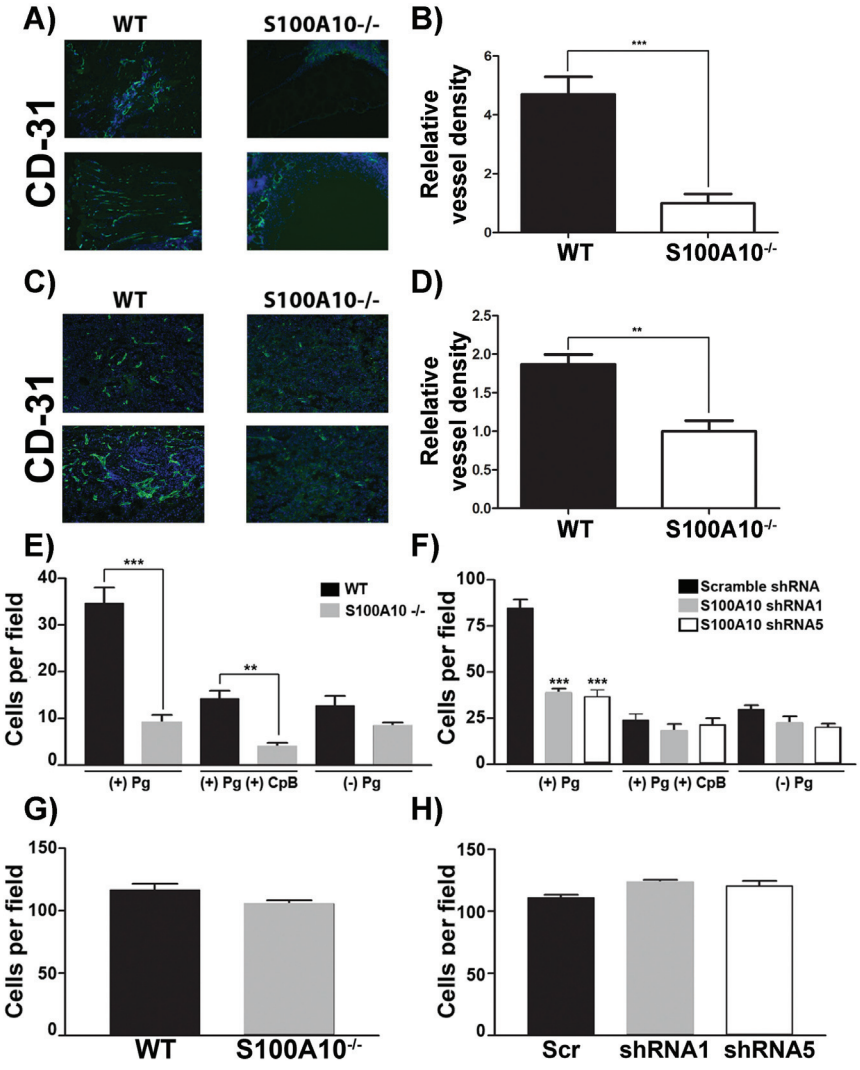
A)
WT
S100A10-/-
CD-31
B)
Relelative vessel density
***
WT
S100A10-/-
C)
WT
S100A10-/-
CD-31
D)
Relelative vessel density
**
WT
S100A10-/-
E)
***
**
WT
S100A10 -/-
Cells per field
(+) Pg
(+) Pg (+) CpB
(-) Pg
F)
Scramble shRNA
S100A10 shRNA1
S100A10 shRNA5
***
***
Cells per field
(+) Pg
(+) Pg (+) CpB
(-) Pg
G)
Cells per field
WT
S100A10-/-
H)
Cells per field
Scr
shRNA1
shRNA5

Figure A6. Model depicting the role of S100A10 in endothelial cell plasmin generation. The predominant form of S100A10 at the endothelial cell surface is as a heterotetramer, AIIt, which consists of two copies each of the annexin A2 and S100A10 subunits[22]. The annexin A2 subunit acts as a regulatory subunit which utilizes its phospholipid-binding sites to anchor S100A10 to the cell surface. The S100A10 subunit binds tPA and Pg at the carboxyl-terminal lysine residue[18,19]. The colocalization of tPA and Pg results in accelerated cleavage of Pg by tPA resulting in Pm generation and fibrinolytic activity.

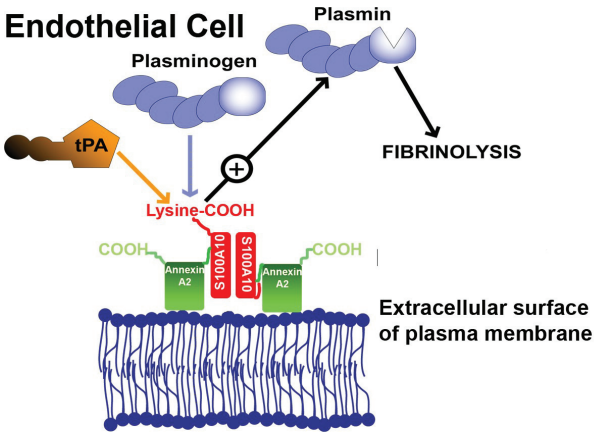
Endothelial Cell
Plasmin
Plasminogen
tPA
FIBRINOLYSIS
Lysine-COOH
COOH
Annexin A2
S100A10
S100A10
Annexin A2
COOH
Extracellular surface of plasma membrane

Table 1. Time of bleeding stops and starts.

	Stop	Start	Stop	Start	Stop	Start	Stop	Start	Stop	Start	Stop	Start	Stop	Start	Stop	Start	Stop	Start	Stop	Start
WT 1	3:30	4:50	7:40	9:36	10:23															
WT 2	3:09	3:20	4:15	5:40	6:11	8:20	9:11	11:10	12:10	13:20	14:15	15:01	21:00	22:30						
WT 3	3:38	4:55	7:11	7:40	8:35	8:50	11:47	12:25												
WT 4	3:30	5:54	6:28	7:20	8:05	9:00	9:41	11:36	12:03	13:50	14:39	15:50	17:04	18:12	18:40	18:56	23:23	26:12	27:33	29:13
WT 5	4:17	6:14	7:40	8:54	11:01	12:06	15:45	17:20	19:50	21:33										
WT 6	2:57	6:29	11:03	13:16	17:37	20:04	21:50													
-/- 1	0:45																			
-/- 2	0:50	2:30	4:00																	
-/- 3	0:51	4:30	5:00																	
-/- 4	0:58	10:40	11:02																	
-/- 5	1:15	6:08	7:07	11:30	11:58	17:00	17:17													
-/- 6	1:01	5:31	5:55																	

The last 3 mm of the mouse tail was clipped and the tail was placed in 37 ºC saline. Time until cessation and re-initiation of bleeding was recorded. Bleeding-re-bleeding was followed for 30 min.

Supplemental Methods

Analysis of protein expression

Cells were lysed with cell lysis buffer (1% NP-40, 150 mM NaCl, 20 mM Tris-HCl, 1 mM EDTA, 1 mM EGTA, and protease inhibitor cocktail (1:500; Sigma-Aldrich)). 20 μg total protein was loaded into each well and was resolved by 12% SDS-polyacrylamide gel electrophoresis (PAGE) and electroblotted onto nitrocellulose membranes. Proteolyzed annexin A2 was generated as previously described[16].Membranes were incubated with antibodies for S100A10 (BD Biosciences), annexin A2 (BD Biosciences), and actin (loading control; Sigma) and the secondary IRdye-800 antibody (LI-COR Biosciences). Antibody complexes were viewed on the Odyssey IR imaging system (LI-COR Biosciences).

Cell surface biotinylation

Endothelial cells (5 x 10^6) were washed with incubation buffer (IB; 20 mM HEPES, 3 mM $CaCl_2$, 1 mM $MgCl_2$, and 150 mM NaCl) and incubated with 1 mM Sulfo-NHS-SS-biotin (Pierce) in IB for 30 minutes at room temperature. Cells were lysed in lysis buffer (see western blot analysis above) on ice for 10 minutes and 100 μg total protein was incubated with 30 μL of Dynabeads M-280 streptavidin (Invitrogen) for 2 hours at 4 ^oC with rotation and then washed 5X with lysis buffer. Beads were resuspended in 2X SDS-PAGE loading buffer, and the supernatant collected, subjected to SDS-PAGE followed by western blot analysis for S100A10 and annexin A2.

Histochemistry and immunohistochemistry

Tissues were fixed in 10% formalin and embedded in paraffin. Paraffin sections were deparaffinized, blocked with horse serum (1:20; Invitrogen) and incubated with rabbit anti-fibrin(ogen) (F0111; Dako), S100A10 (BAF2377 ;R&D Systems), or normal mouse IgG1 (as control; BD Biosciences) at room temperature overnight. Sections were then incubated for 1 hour at room temperature with Horseradish peroxidase (HRP) conjugated

antibodies specific for rabbit or goat (Santa Cruz). Subsequently, a peroxidase diaminobenzidine detection system (Dako North America) was applied according to the manufacturer's instructions. Sections were counterstained with hematoxylin. Sections were mounted using Cytoseal 60 mounting media (Richard-Allen Scientific) and viewed using either a 40×/0.75 NA or 10×/0.3 NA objective lens. Images were captured by the Nikon Eclipse E600 microscope using a Nikon DXM1200F camera. Digital acquisition of the images was performed using ACT-1 v2.7 software (Nikon). Figures were generated using Adobe Photoshop CS3 v10 (Adobe Systems Incorporated).

uPA dependent plasmin activation.

Plasmin activation with uPA was performed as previously described[48]. Briefly, TIME cells were trypsinized with EDTA-free trypsin and washed 3X with DPBS. Cells were then washed with 0.05M glycine, pH 3.0, 0.1 M NaCl for 3 minutes followed by neutralization with an equal volume of 0.5 M HEPES, pH 7.5, 0.1 M NaCl to dissociate potential endogenously bound ligands. $1x10^5$ cells were then incubated with 25 nM uPA for 30 minutes at 37 ^oC in DPBS containing 0.2% BSA The cells were then washed 3X DPBS with 0.2% BSA and incubated with 0.5 μM Glu-Pg and 250 μM Pm substrate S2251 (Chromogenix, Diapharma Group) in 0.05 M Tris-HCl, pH 7.4, 0.1 M NaCl, 0.01% Tween 80. The rate of plasmin generation was measured at absorbance 405 nm every minute for 2 hours using a BioTek ELx808 plate reader.

Clot lysis assay.

In vitro clot lysis was determined using a modification of the APTT assay. In a 96-well, flat bottom plate, 50 μL citrated plasma, 50 μL APTT reagent (STA®-PTT A, Stago) and 100μL HBS-Tw80 (40 mM HEPES pH 7.0, 150 mM NaCl and 0.01% Tween 80) were added to wells containing 2.5 μL of 5.8 μM sc-tPA (Genentech). Duplicate reactions were carried out in well lacking sc-tPA. After incubation at 37 °C for 3 minutes, 100 μL of 25 mM CaCl2 was added, the solution mixed and absorbance was monitored at 405 nm every minute for 60 minutes using a BioTek ELx808 plate reader. Clot lysis time was

defined as the time required to achieve the absorbance that was one-half of the difference between the maximum absorbance reached after clotting and the minimum absorbance value achieved after complete lysis.

Antiplasmin activity and plasmin-antiplasmin levels

Antiplasmin activity was assessed using Coamatic © Plasmin Inhibitor chromogenic kit (generously provided by Diapharma, West Chester OH), following manufacturer's direction. The assay was calibrated using standardized human plasma, HemosIL Calibration plasma (Instrumentation Laboratory, Lexington, MA). Plasmin-antiplasmin levels were determined using Imuclone® PAP ELISA (American Diagnostica Inc, Montréal QC) following manufacturer's direction.

Thrombin Potential Assay

Endogenous Thrombin Potential was determined using Technothrombin ® TGA (Vienna, Austria), utilizing a modification of the procedure as directed by the manufacturer, briefly, murine plasma samples were diluted ½ with TGA-buffer prior to addition of the trigger reagent and substrate.

Supplemental figure A1. Comparison of clotting parameters and components. Murine blood was obtained by cardiac puncture and treated with sodium citrate to prevent clotting. The activated partial thrombospondin time (aPTT) (A), prothrombin time (PT) (B), platelet levels (C) and fibrinogen and Pg levels (D), clotting time (E), clot lysis time (F), antiplasmin activity (G), plasmin-antiplasmin levels (H) and endogenous thombin potential (I) in the S100A10$^{-/-}$ mice were observed to be the comparable with their WT counterparts. Figures were generated using Adobe Photoshop CS3 v10 (Adobe Systems Incorporated). Assays for A,E,F,G,H and I were performed by Victoria Miller with samples collected and prepared by Alexi Surette.

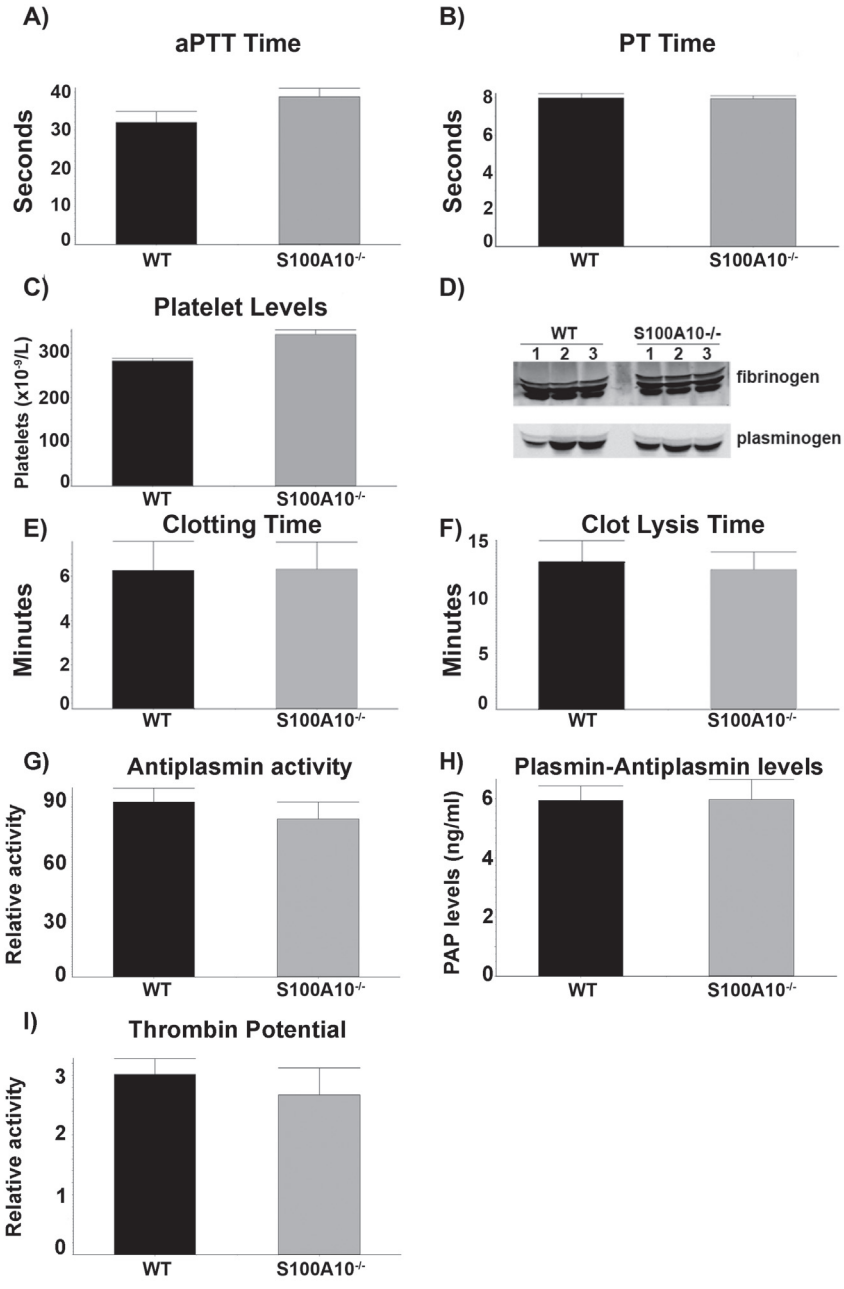
A)
aPTT Time
Seconds
40
30
20
10
0
WT
S100A10-/-
B)
PT Time
Seconds
8
6
4
2
0
WT
S100A10-/-
C)
Platelet Levels
Platelets (x10-9/L)
300
200
100
0
WT
S100A10-/-
D)
WT
S100A10-/-
1 2 3
1 2 3
fibrinogen
plasminogen
E)
Clotting Time
Minutes
6
4
2
0
WT
S100A10-/-
F)
Clot Lysis Time
Minutes
15
10
5
0
WT
S100A10-/-
G)
Antiplasmin activity
Relative activity
90
60
30
0
WT
S100A10-/-
H)
Plasmin-Antiplasmin levels
PAP levels (ng/ml)
6
4
2
0
WT
S100A10-/-
I)
Thrombin Potential
Relative activity
3
2
1
0
WT
S100A10-/-

Supplemental figure A2. Loss of annexin A2 results in depletion of S100A10 levels and resulting decreased plasmin activation. TIME cell annexin A2 levels were depleted using an shRNA construct. Western blot analysis was performed to observe total and cell surface annexin A2 and S100A10 protein levels in TIME cells (A). FITC-Pg binding to the annexin A2 depleted TIME cells (B) was measured by FACS. Quantification of flow cytometric analysis of Pg binding was calculated using WinMDI software. Loss of annexin A2 affected tPA dependent plasmin generation (C) and uPA dependent plasmin generation (D) by TIME cells. Control or annexin A2 depleted TIME cells were added to the top chamber of Transwell chambers in the presence of media and in the presence or absence of Pg (0.5 μM). Some chambers were coated with Matrigel (invasion assays) (E) or uncoated (migration assays) (F). Cells were incubated for 48 hours after which invading cells were stained with Haematoxylin and Eosin and counted. Data are expressed as mean number of cells per 40X field plus or minus SD of 3 independent experiments. Statistical analysis was performed using Student's t-test (*** $p<0.001$). In some experiments cells were pretreated with carboxypeptidase B (CpB, 5 U/ml), which was added to the upper chamber where indicated. Figures were generated using Adobe Photoshop CS3 v10 (Adobe Systems Incorporated).

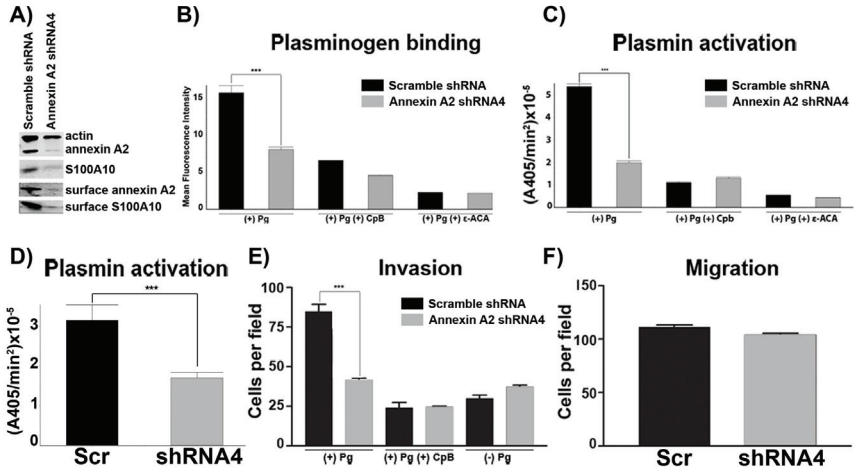
A)
Scramble shRNA
Annexin A2 shRNA4
actin
annexin A2
S100A10
surface annexin A2
surface S100A10
B)
Plasminogen binding
Mean Fluorescence Intensity
Scramble shRNA
Annexin A2 shRNA4
(+) Pg
(+) Pg (+) CpB
(+) Pg (+) ε-ACA
C)
Plasmin activation
(A405/min²)x10⁻⁵
Scramble shRNA
Annexin A2 shRNA4
(+) Pg
(+) Pg (+) Cpb
(+) Pg (+) ε-ACA
D)
Plasmin activation
(A405/min²)x10⁻⁵
Scr
shRNA4
E)
Invasion
Cells per field
Scramble shRNA
Annexin A2 shRNA4
(+) Pg
(+) Pg (+) CpB
(-) Pg
F)
Migration
Cells per field
Scr
shRNA4

APPENDIX B: COPYRIGHT

This research was originally published in *Blood*. Surette AP, Madureira PA, Phipps KD, Miller VA, Svenningsson P, Waisman DM. Regulation of fibrinolysis by S100A10 *in vivo*. *Blood*. 2011;118(11):3172-81 © the American Society of Hematology.

The following exert was obtained from the website http://bloodjournal.hematologylibrary.org/site/misc/rights.xhtml, detailing permission to reprint:

Authors have permission to do the following after their article has been published in *Blood*, either in print or online as a First Edition Paper.

- Reprint the article in print collections of the author's own writing.
- Present the work orally in its entirety.
- **Use the article in theses and/or dissertation**.
- Reproduce the article for use in courses the author is teaching. If the author is employed by an academic institution, that institution may also reproduce the article for course teaching.
- Distribute photocopies of the article to colleagues, but only for noncommercial purposes.
- Reuse figures and tables created by the author in future works.
- Post a copy of the article on the author's personal website, departmental website, and/or the university intranet. A hyperlink to the article on the *Blood* website must be included.

The author must include the following citation when citing material that appeared in the print edition of *Blood*:

"This research was originally published in *Blood*. Author(s). Title. *Blood*. Year;Vol:pp-pp. © the American Society of Hematology."

APPENDIX C: PRELIMINARY RESULTS

This appendix contains data from preliminary experiments conducted investigating the role AIIt plays in plasmin and homocysteine triggered endothelial cell signaling and on the effect homocysteine has on AIIt dependent Pg activation.

B.1 AIIt is required for homocysteine and plasmin signaling in endothelial cells.

Homocysteine has previously been demonstrated to trigger the phosphorylation of the ERK.[281] In order to investigate whether AIIt was necessary for Hcy mediated phosphorylation of ERK, annexin A2 depleted TIME cells were treated with 100 μM Hcy. We observed that depletion of annexin A2 in TIME cells resulted in loss of p-ERK signaling following Hcy treatment (Figure B1). AIIt was also shown to be required for plasmin triggered p-ERK signaling in TIME cells since depletion of S100A10 (Figure B2A) and annexin A2 (Figure B2B) prevented phosphorylation of ERK following plasmin treatment. In addition to p-ERK signaling in response to plasmin treatment, p-JNK and p-p38 signaling was also absent in annexin A2 depleted TIME cells while present in scramble control TIME cells (Figure B2B). We have yet to investigate whether these plasmin induced signaling events are also absent in S100A10 depleted TIME cells. Incubation of the annexin A2 depleted TIME cells with bovine AIIt restored plasmin mediated p-ERK signaling, suggesting that AIIt at the cell surface is responsible for plasmin mediated signaling in TIME cells (Figure B2C). Incubation with AIIt alone did not activate p-ERK (Figure B2C), suggesting that the restoration in p-ERK was due to the presence of plasmin and AIIt. In contrast to previously published reports on plasmin mediated signaling in monocytes,[301,335] plasmin proteolytic activity did not appear to be required for plasmin mediated signaling in TIME cells since treatment of plasmin with aprotinin did not prevent plasmin mediated signaling (Figure B2D). Signaling potential, however, is not lost in annexin A2 depleted TIME cells, as LPS and fetal bovine serum (FBS) triggered signaling in these cells (Figure B2E,F). LPS signals through TLR-4,[336]

indicating that loss of AIIt is not required for all signaling through TLR-4. Plasmin and Hcy may therefore utilize AIIt to signal through TLR-4 differently than LPS or require another trans-membrane protein to transduce a signal into the cell. FBS contains an abundance of growth factors that can induce signaling pathways. AIIt may therefore not be required for growth factor signaling. However, since FBS contains several factors that elicit signaling pathways,[337,338] it is impossible to determine whether all FBS mediated signaling events are unaffected by loss of AIIt.

Tissue factor expression is increased in response to several stimuli, including plasmin,[339] Hcy[333] and thrombin,[340] which trigger signaling events similar to those observed in Figure B2. Interestingly, loss of AIIt in TIME cells also results in depletion of tissue factor protein levels (Figure B3A) and measurable tissue factor activity (Figure B3B). As expected, induction of tissue factor protein levels by thrombin and Hcy were observed in scramble control TIME cells. However, loss of AIIt prevented this induction (Figure B3C). It is unknown whether tissue factor protein expression is inducible in AIIt depleted TIME cells under different conditions, whether loss of AIIt results in loss of tissue factor in other endothelial cells and other cell types, and whether loss of AIIt prevents expression or is involved in tissue factor protein stability.

B.2 Effect of homocysteine on AIIt dependent plasminogen activation.

Incubation of AIIt with Hcy, Hci and HTL each decreased AIIt dependent Pg activation in the presence of tPA by 50% (Figure B4). As mentioned in future directions, additional work is being conducted to investigate the mechanism by which Hcy and HTL affect AIIt dependent Pg activation.

Figure B1. Homocysteine triggered p-ERK signaling requires annexin A2.

TIME cells were treated with 100μM homocysteine for the indicated time. Total cell extracts were obtained and proteins analyzed by Western Blot. The data shows that loss of annexin A2 results in loss of p-ERK signaling in response to homocysteine. Tubulin and total ERK levels serve as loading controls.

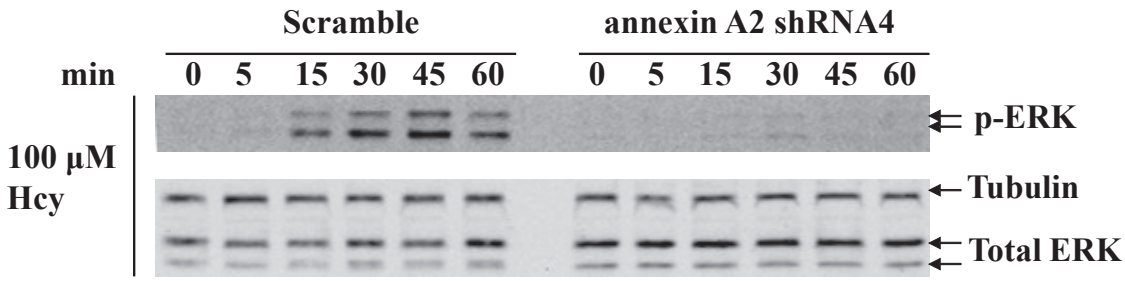
Scramble
annexin A2 shRNA4
min
0 5 15 30 45 60
0 5 15 30 45 60
100 μM
Hcy
p-ERK
Tubulin
Total ERK

Figure B2. AIIt is required for plasmin triggered signaling in TIME cells.

S100A10 and annexin A2 (AIIt) depleted TIME cells were treated with plasmin (0.43 CTA/mL) for the indicated periods of time. Total cell lysates were analyzed by Western Blot. The data show that loss of S100A10 prevents plasmin induced p-ERK signaling (A) and loss of annexin A2 prevents plasmin incuded p-ERK, p-p38 and p-jnk signaling (B). Pretreatment of annexin A2 depleted TIME cells with bovine AIIt restored plasmin mediated p-ERK signaling (C). Inhibition of plasmin activity with aprotinin failed to prevent plasmin triggered p-ERK signaling (D). Depletion of TIME cell annexin A2 did not affect LPS induced p-ERK and p-p38 signaling (E) or FBS induced p-ERK (F).

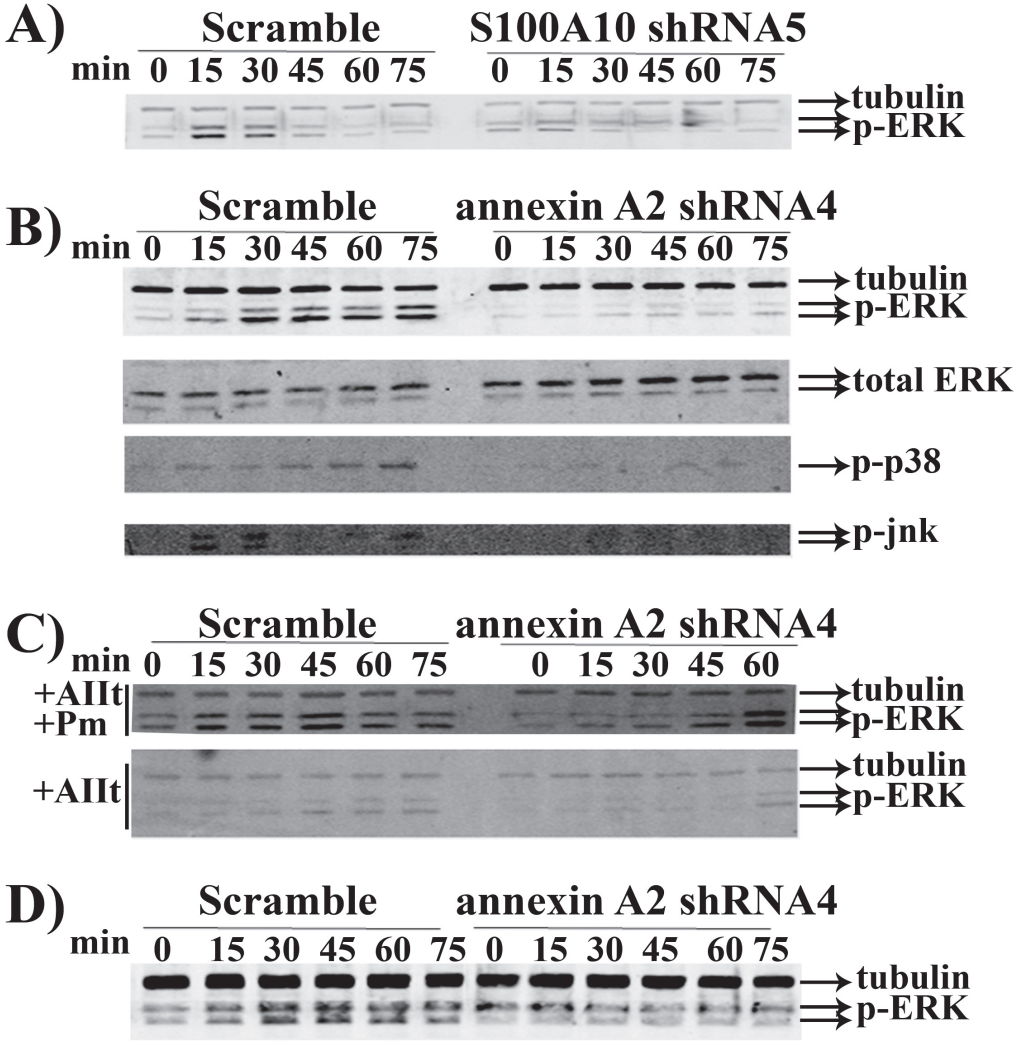
A)
Scramble
S100A10 shRNA5
min 0 15 30 45 60 75 0 15 30 45 60 75
tubulin
p-ERK
B)
Scramble
annexin A2 shRNA4
min 0 15 30 45 60 75 0 15 30 45 60 75
tubulin
p-ERK
total ERK
p-p38
p-jnk
C)
Scramble
annexin A2 shRNA4
min 0 15 30 45 60 75 0 15 30 45 60
+AIIt
+Pm
tubulin
p-ERK
+AIIt
tubulin
p-ERK
D)
Scramble
annexin A2 shRNA4
min 0 15 30 45 60 75 0 15 30 45 60 75
tubulin
p-ERK

Figure B3. Tissue factor expression and activity is reduced in AIIt depleted TIME cells. Western Blot analysis of total cell lysates from S100A10 and annexin A2 depleted TIME cells revealed that loss of S100A10 and annexin A2 resulted in loss of tissue factor (TF) (A). A TF activity assay revealed that loss of S100A10 and annexin A2 resulted in decreased TF activity (B) (***<0.001). Annexin A2 depleted TIME cells were incubated with thrombin (4 U/mL) or Hcy (100 μM) for the indicated period of time. Loss of annexin A2 prevented thrombin and Hcy induced TF expression (C).

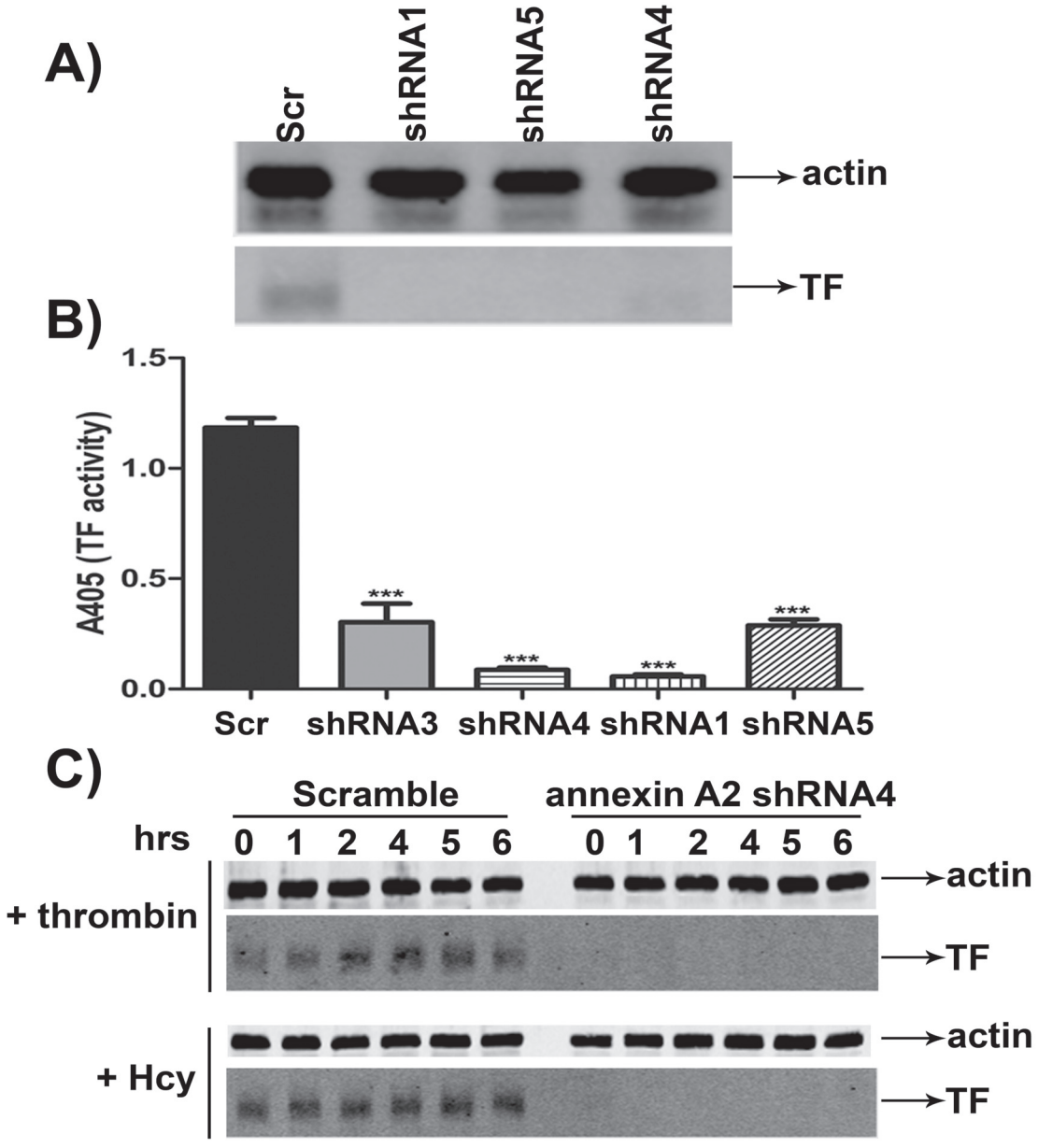
A)
Scr
shRNA1
shRNA5
shRNA4
actin
TF
B)
A405 (TF activity)
1.5
1.0
0.5
0.0
***
***
***
***
Scr
shRNA3
shRNA4
shRNA1
shRNA5
C)
Scramble
annexin A2 shRNA4
hrs
0 1 2 4 5 6
0 1 2 4 5 6
+ thrombin
actin
TF
+ Hcy
actin
TF

Figure B4. Effect of homocysteine and homocysteine-thiolactone on AIIt dependent plasminogen activation. Prior to incubation with Pg, tPA and S2251, AIIt was incubated with 5 mM homocysteine (Hcy), homocystine (Hci) or cysteine (Cys) (A) or with 1 mM homocysteine thiolactone (HTL) (B) overnight at 37 °C (* indicates AIIt that was not incubated overnight at 37 °C to determine whether incubation of AIIt overnight at 37 °C altered Pg activation). Incubation of AIIt with Hcy and HTL resulted over 50% decreased Pg activation (***$p<0.001$).

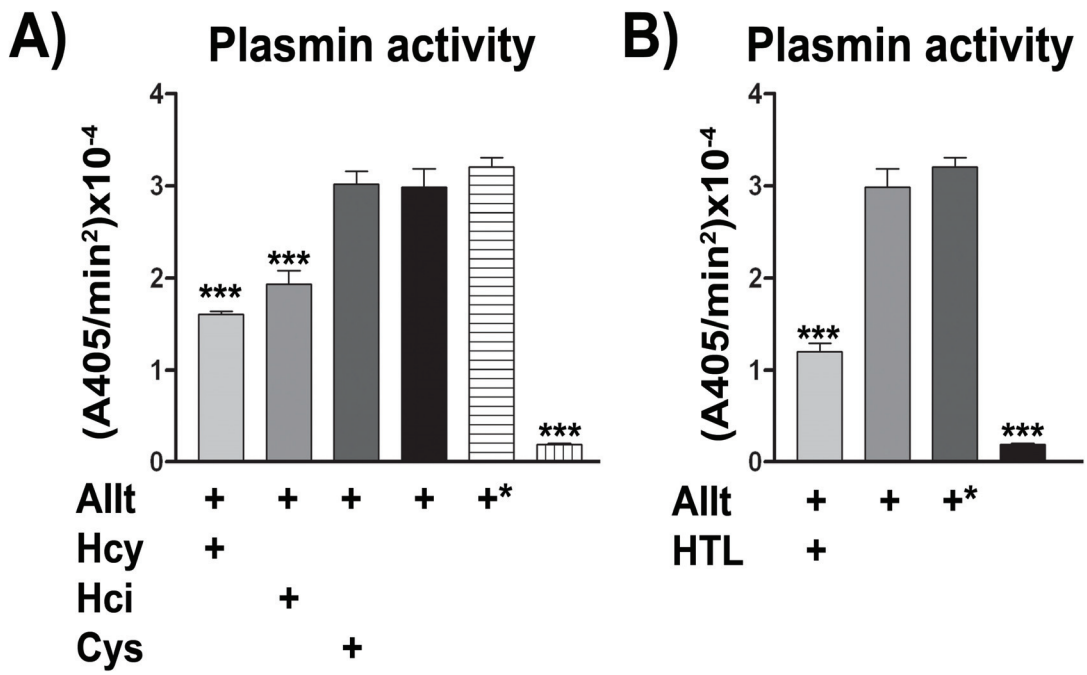
A)
Plasmin activity
(A405/min²)x10⁻⁴
4
3
2
1
0
***
***
***
Allt + + + + +*
Hcy +
Hci +
Cys +
B)
Plasmin activity
(A405/min²)x10⁻⁴
4
3
2
1
0
***
***
Allt + + +*
HTL +

REFERENCES

1. Owens AP 3rd, Mackman N. Tissue factor and thrombosis: The clot starts here. *Thromb. Haemost*. 2010;104(3):432-439.

2. Lord ST. Fibrinogen and fibrin: scaffold proteins in hemostasis. *Curr. Opin. Hematol*. 2007;14(3):236-241.

3. Gailani D, Renné T. Intrinsic Pathway of Coagulation and Arterial Thrombosis. *Arteriosclerosis, Thrombosis, and Vascular Biology*. 2007;27(12):2507 -2513.

4. GAILANI D, RENNÉ T. The intrinsic pathway of coagulation: a target for treating thromboembolic disease? *Journal of Thrombosis and Haemostasis*. 2007;5(6):1106-1112.

5. Vogler EA, Siedlecki CA. Contact Activation of Blood Plasma Coagulation. *Biomaterials*. 2009;30(10):1857-1869.

6. Wagner DD, Burger PC. Platelets in inflammation and thrombosis. *Arterioscler. Thromb. Vasc. Biol*. 2003;23(12):2131-2137.

7. Gentry PA. Comparative aspects of blood coagulation. *The Veterinary Journal*. 2004;168(3):238-251.

8. Forrester JS, Litvack F, Grundfest W. Initiating Events of Acute Coronary Arterial Occlusion. *Annu. Rev. Med.* 1991;42(1):35-45.

9. Brass L. Understanding and evaluating platelet function. *Hematology Am Soc Hematol Educ Program*. 2010;2010:387-396.

10. Borissoff JI, Spronk HMH, ten Cate H. The hemostatic system as a modulator of atherosclerosis. *N. Engl. J. Med*. 2011;364(18):1746-1760.

11. Ay C, Dunkler D, Marosi C, et al. Prediction of venous thromboembolism in cancer patients. *Blood*. 2010;116(24):5377 -5382.

12. Furie B, Furie BC. Mechanisms of thrombus formation. *N. Engl. J. Med*. 2008;359(9):938-949.

13. Collen D. The Plasminogen (Fibrinolytic) System. *Thromb. Haemost.* 1999;82(2):259-270.

14. Castellino FJ, McCance SG. The kringle domains of human plasminogen. *Ciba Found. Symp*. 1997;212:46-60; discussion 60-65.

15. An SS, Carreño C, Marti DN, et al. Lysine-50 is a likely site for anchoring the plasminogen N-terminal peptide to lysine-binding kringles. *Protein Sci*. 1998;7(9):1960-1969.

16. Weisel JW, Nagaswami C, Korsholm B, Petersen LC, Suenson E. Interactions of plasminogen with polymerizing fibrin and its derivatives, monitored with a photoaffinity cross-linker and electron microscopy. *J. Mol. Biol*. 1994;235(3):1117-1135.

17. Ponting CP, Holland SK, Cederholm-Williams SA, et al. The compact domain conformation of human Glu-plasminogen in solution. *Biochim. Biophys. Acta*. 1992;1159(2):155-161.

18. Gong Y, Kim SO, Felez J, et al. Conversion of Glu-plasminogen to Lys-plasminogen is necessary for optimal stimulation of plasminogen activation on the endothelial cell surface. *J. Biol. Chem.* 2001;276(22):19078-19083.

19. Mulichak AM, Tulinsky A, Ravichandran KG. Crystal and molecular structure of human plasminogen kringle 4 refined at 1.9-A resolution. *Biochemistry.* 1991;30(43):10576-10588.

20. Mathews II, Vanderhoff-Hanaver P, Castellino FJ, Tulinsky A. Crystal structures of the recombinant kringle 1 domain of human plasminogen in complexes with the ligands epsilon-aminocaproic acid and trans-4-(aminomethyl)cyclohexane-1-carboxylic Acid. *Biochemistry.* 1996;35(8):2567-2576.

21. Chang Y, Mochalkin I, McCance SG, et al. Structure and ligand binding determinants of the recombinant kringle 5 domain of human plasminogen. *Biochemistry.* 1998;37(10):3258-3271.

22. Wu TP, Padmanabhan K, Tulinsky A, Mulichak AM. The refined structure of the epsilon-aminocaproic acid complex of human plasminogen kringle 4. *Biochemistry.* 1991;30(43):10589-10594.

23. Wahl ML, Kenan DJ, Gonzalez-Gronow M, Pizzo SV. Angiostatin's molecular mechanism: aspects of specificity and regulation elucidated. *J. Cell. Biochem*. 2005;96(2):242-261.

24. Salonen EM, Saksela O, Vartio T, et al. Plasminogen and tissue-type plasminogen activator bind to immobilized fibronectin. *J. Biol. Chem*. 1985;260(22):12302-12307.

25. Liotta LA, Goldfarb RH, Brundage R, et al. Effect of plasminogen activator (urokinase), plasmin, and thrombin on glycoprotein and collagenous components of basement membrane. *Cancer Res*. 1981;41(11 Pt 1):4629-4636.

26. Silverstein RL, Nachman RL. Thrombospondin-plasminogen interactions: modulation of plasmin generation. *Semin. Thromb. Hemost*. 1987;13(3):335-342.

27. Bonnefoy A, Legrand C. Proteolysis of subendothelial adhesive glycoproteins (fibronectin, thrombospondin, and von Willebrand factor) by plasmin, leukocyte cathepsin G, and elastase. *Thromb. Res*. 2000;98(4):323-332.

28. Ellis V. Plasminogen activation at the cell surface. *Curr. Top. Dev. Biol*. 2003;54:263-312.

29. Miles LA, Plow EF. Receptor mediated binding of the fibrinolytic components, plasminogen and urokinase, to peripheral blood cells. *Thromb. Haemost*. 1987;58(3):936-942.

30. Hajjar KA. Cellular receptors in the regulation of plasmin generation. *Thromb. Haemost*. 1995;74(1):294-301.

31. Wang H, Doll JA, Jiang K, et al. Differential Binding of Plasminogen, Plasmin, and Angiostatin4.5 to Cell Surface {beta}-Actin: Implications for Cancer-Mediated Angiogenesis. *Cancer Res*. 2006;66(14):7211-7215.

32. Herren T, Burke TA, Jardi M, Felez J, Plow EF. Regulation of plasminogen binding to neutrophils. *Blood*. 2001;97(4):1070-1078.

33. Ploplis VA, Carmeliet P, Vazirzadeh S, et al. Effects of disruption of the plasminogen gene on thrombosis, growth, and health in mice. *Circulation*. 1995;92(9):2585-2593.

34. Ploplis VA, French EL, Carmeliet P, Collen D, Plow EF. Plasminogen deficiency differentially affects recruitment of inflammatory cell populations in mice. *Blood*. 1998;91(6):2005-2009.

35. Plow EF, Herren T, Redlitz A, Miles LA, Hoover-Plow JL. The cell biology of the plasminogen system. *FASEB J*. 1995;9(10):939-945.

36. Ploplis VA, French EL, Carmeliet P, Collen D, Plow EF. Plasminogen deficiency differentially affects recruitment of inflammatory cell populations in mice. *Blood*. 1998;91(6):2005-2009.

37. Tarui T, Majumdar M, Miles LA, Ruf W, Takada Y. Plasmin-induced migration of endothelial cells. A potential target for the anti-angiogenic action of angiostatin. *J. Biol. Chem*. 2002;277(37):33564-33570.

38. Choi K-S, Fogg DK, Yoon C-S, Waisman DM. p11 regulates extracellular plasmin production and invasiveness of HT1080 fibrosarcoma cells. *FASEB J*. 2003;17(2):235-246.

39. Lijnen HR. Plasmin and matrix metalloproteinases in vascular remodeling. *Thromb. Haemost*. 2001;86(1):324-333.

40. Davis GE, Pintar Allen KA, Salazar R, Maxwell SA. Matrix metalloproteinase-1 and -9 activation by plasmin regulates a novel endothelial cell-mediated mechanism of collagen gel contraction and capillary tube regression in three-dimensional collagen matrices. *J. Cell. Sci*. 2001;114(Pt 5):917-930.

41. Rømer J, Bugge TH, Pyke C, et al. Plasminogen and wound healing. *Nat. Med*. 1996;2(7):725.

42. Szabo I, Simon M Jr, Hunyadi J. Plasmin promotes keratinocyte migration and phagocytic-killing accompanied by suppression of cell proliferation which may facilitate re-epithelialization of wound beds. *Clin. Dev. Immunol*. 2004;11(3-4):233-240.

43. Bezerra JA, Bugge TH, Melin-Aldana H, et al. Plasminogen deficiency leads to impaired remodeling after a toxic injury to the liver. *Proc. Natl. Acad. Sci. U.S.A*. 1999;96(26):15143-15148.

44. Hoover-Plow J, Ellis J, Yuen L. In vivo plasminogen deficiency reduces fat accumulation. *Thromb. Haemost*. 2002;87(6):1011-1019.

45. Green KA, Nielsen BS, Castellino FJ, Rømer J, Lund LR. Lack of plasminogen leads to milk stasis and premature mammary gland involution during lactation. *Developmental Biology*. 2006;299(1):164-175.

46. Lijnen HR, Carmeliet P, Bouché A, et al. Restoration of thrombolytic potential in plasminogen-deficient mice by bolus administration of plasminogen. *Blood*. 1996;88(3):870-876.

47. Busuttil SJ, Drumm C, Ploplis VA, Plow EF. Endoluminal arterial injury in plasminogen-deficient mice. *J. Surg. Res.* 2000;91(2):159-164.

48. Carmeliet P, Moons L, Ploplis V, Plow E, Collen D. Impaired arterial neointima formation in mice with disruption of the plasminogen gene. *J. Clin. Invest.* 1997;99(2):200-208.

49. Drew AF, Tucker HL, Kombrinck KW, et al. Plasminogen is a critical determinant of vascular remodeling in mice. *Circ. Res.* 2000;87(2):133-139.

50. Bugge TH, Kombrinck KW, Flick MJ, et al. Loss of fibrinogen rescues mice from the pleiotropic effects of plasminogen deficiency. *Cell*. 1996;87(4):709-719.

51. Danø K, Behrendt N, Høyer-Hansen G, et al. Plasminogen activation and cancer. *Thromb. Haemost*. 2005;93(4):676-681.

52. Palumbo JS, Talmage KE, Liu H, et al. Plasminogen supports tumor growth through a fibrinogen-dependent mechanism linked to vascular patency. *Blood*. 2003;102(8):2819-2827.

53. Bugge TH, Lund LR, Kombrinck KK, et al. Reduced metastasis of Polyoma virus middle T antigen-induced mammary cancer in plasminogen-deficient mice. *Oncogene*. 1998;16(24):3097-3104.

54. Ranson M, Andronicos NM, O'Mullane MJ, Baker MS. Increased plasminogen binding is associated with metastatic breast cancer cells: differential expression of plasminogen binding proteins. *Br. J. Cancer.* 1998;77(10):1586-1597.

55. Menell JS, Cesarman GM, Jacovina AT, et al. Annexin II and bleeding in acute promyelocytic leukemia. *N. Engl. J. Med*. 1999;340(13):994-1004.

56. Lacroix R, Sabatier F, Mialhe A, et al. Activation of plasminogen into plasmin at the surface of endothelial microparticles: a mechanism that modulates angiogenic properties of endothelial progenitor cells in vitro. *Blood*. 2007;110(7):2432-2439.

57. Oh C-W, Hoover-Plow J, Plow EF. The role of plasminogen in angiogenesis in vivo. *J. Thromb. Haemost*. 2003;1(8):1683-1687.

58. Plow EF, Ploplis VA, Busuttil S, Carmeliet P, Collen D. A role of plasminogen in atherosclerosis and restenosis models in mice. *Thromb. Haemost*. 1999;82 Suppl 1:4-7.

59. Melchor JP, Pawlak R, Strickland S. The tissue plasminogen activator-plasminogen proteolytic cascade accelerates amyloid-beta (Abeta) degradation and inhibits Abeta-induced neurodegeneration. *J. Neurosci*. 2003;23(26):8867-8871.

60. Busso N, Péclat V, Van Ness K, et al. Exacerbation of antigen-induced arthritis in urokinase-deficient mice. *J. Clin. Invest.* 1998;102(1):41-50.

61. McColl BK, Baldwin ME, Roufail S, et al. Plasmin Activates the Lymphangiogenic Growth Factors VEGF-C and VEGF-D. *J Exp Med*. 2003;198(6):863-868.

62. Robbins KC, Summaria L. Plasminogen and plasmin. *Meth. Enzymol*. 1976;45:257-273.

63. Violand BN, Castellino FJ. Mechanism of the urokinase-catalyzed activation of human plasminogen. *J. Biol. Chem*. 1976;251(13):3906-3912.

64. Coughlin PB. Antiplasmin: the forgotten serpin? *FEBS J*. 2005;272(19):4852-4857.

65. Lijnen HR. Gene targeting in hemostasis. Alpha2-antiplasmin. *Front. Biosci*. 2001;6:D239-247.

66. Wiman B, Collen D. On the mechanism of the reaction between human alpha 2-antiplasmin and plasmin. *J. Biol. Chem*. 1979;254(18):9291-9297.

67. Schaller J, Gerber SS. The plasmin-antiplasmin system: structural and functional aspects. *Cell. Mol. Life Sci*. 2011;68(5):785-801.

68. Lijnen HR, Van Hoef B, De Cock F, Collen D. Effect of fibrin-like stimulators on the activation of plasminogen by tissue-type plasminogen activator (t-PA)--studies with active site mutagenized plasminogen and plasmin resistant t-PA. *Thromb. Haemost*. 1990;64(1):61-68.

69. Loscalzo J. Structural and kinetic comparison of recombinant human single- and two-chain tissue plasminogen activator. *J. Clin. Invest*. 1988;82(4):1391-1397.

70. Collen D, Lijnen HR. Basic and clinical aspects of fibrinolysis and thrombolysis. *Blood*. 1991;78(12):3114-3124.

71. Byeon IJ, Llinás M. Solution structure of the tissue-type plasminogen activator kringle 2 domain complexed to 6-aminohexanoic acid an antifibrinolytic drug. *J. Mol. Biol*. 1991;222(4):1035-1051.

72. Binder BR, Mihaly J, Prager GW. uPAR-uPA-PAI-1 interactions and signaling: a vascular biologist's view. *Thromb. Haemost*. 2007;97(3):336-342.

73. Conese M, Blasi F. Urokinase/urokinase receptor system: internalization/degradation of urokinase-serpin complexes: mechanism and regulation. *Biol. Chem. Hoppe-Seyler.* 1995;376(3):143-155.

74. Danø K, Rømer J, Nielsen BS, et al. Cancer invasion and tissue remodeling--cooperation of protease systems and cell types. *APMIS*. 1999;107(1):120-127.

75. Pepper MS. Role of the Matrix Metalloproteinase and Plasminogen Activator-Plasmin Systems in Angiogenesis. *Arterioscler Thromb Vasc Biol*. 2001;21(7):1104-1117.

76. Mazar AP. The urokinase plasminogen activator receptor (uPAR) as a target for the diagnosis and therapy of cancer. *Anticancer Drugs*. 2001;12(5):387-400.

77. Petersen LC. Kinetics of reciprocal pro-urokinase/plasminogen activation--stimulation by a template formed by the urokinase receptor bound to poly(D-lysine). *Eur. J. Biochem*. 1997;245(2):316-323.

78. Ellis V, Scully MF, Kakkar VV. Plasminogen activation initiated by single-chain urokinase-type plasminogen activator. Potentiation by U937 monocytes. *J. Biol. Chem*. 1989;264(4):2185-2188.

79. Binder BR, Christ G, Gruber F, et al. Plasminogen activator inhibitor 1: physiological and pathophysiological roles. *News Physiol. Sci*. 2002;17:56-61.

80. Nykjaer A, Conese M, Christensen EI, et al. Recycling of the urokinase receptor upon internalization of the uPA:serpin complexes. *EMBO J*. 1997;16(10):2610-2620.

81. Orth K, Madison EL, Gething MJ, Sambrook JF, Herz J. Complexes of tissue-type plasminogen activator and its serpin inhibitor plasminogen-activator inhibitor type 1 are internalized by means of the low density lipoprotein receptor-related protein/alpha 2-macroglobulin receptor. *Proc. Natl. Acad. Sci. U.S.A*. 1992;89(16):7422-7426.

82. Vaughan DE. PAI-1 and atherothrombosis. *J. Thromb. Haemost*. 2005;3(8):1879-1883.

83. Kwon M, MacLeod TJ, Zhang Y, Waisman DM. S100A10, annexin A2, and annexin a2 heterotetramer as candidate plasminogen receptors. *Front. Biosci*. 2005;10:300-325.

84. Ranson M, Andronicos NM. Plasminogen binding and cancer: promises and pitfalls. *Front. Biosci*. 2003;8:s294-304.

85. Miles LA, Hawley SB, Baik N, et al. Plasminogen receptors: the sine qua non of cell surface plasminogen activation. *Front. Biosci*. 2005;10:1754-1762.

86. Redlitz A, Plow EF. Receptors for plasminogen and t-PA: an update. *Baillieres Clin. Haematol*. 1995;8(2):313-327.

87. Félez J, Miles LA, Fábregas P, et al. Characterization of cellular binding sites and interactive regions within reactants required for enhancement of plasminogen activation by tPA on the surface of leukocytic cells. *Thromb. Haemost*. 1996;76(4):577-584.

88. Miles LA, Dahlberg CM, Plescia J, et al. Role of cell-surface lysines in plasminogen binding to cells: identification of alpha-enolase as a candidate plasminogen receptor. *Biochemistry*. 1991;30(6):1682-1691.

89. Andronicos NM, Chen EI, Baik N, et al. Proteomics-based discovery of a novel, structurally unique, and developmentally regulated plasminogen receptor, Plg-RKT, a major regulator of cell surface plasminogen activation. *Blood*. 2010;115(7):1319-1330.

90. Hembrough TA, Li L, Gonias SL. Cell-surface cytokeratin 8 is the major plasminogen receptor on breast cancer cells and is required for the accelerated activation of cell-associated plasminogen by tissue-type plasminogen activator. *J. Biol. Chem*. 1996;271(41):25684-25691.

91. Herren T, Burke TA, Das R, Plow EF. Identification of histone H2B as a regulated plasminogen receptor. *Biochemistry*. 2006;45(31):9463-9474.

92. MacLeod TJ, Kwon M, Filipenko NR, Waisman DM. Phospholipid-associated annexin A2-S100A10 heterotetramer and its subunits: characterization of the interaction with tissue plasminogen activator, plasminogen, and plasmin. *J. Biol. Chem*. 2003;278(28):25577-25584.

93. Cesarman GM, Guevara CA, Hajjar KA. An endothelial cell receptor for plasminogen/tissue plasminogen activator (t-PA). II. Annexin II-mediated enhancement of t-PA-dependent plasminogen activation. *J. Biol. Chem*. 1994;269(33):21198-21203.

94. Kassam G, Choi KS, Ghuman J, et al. The role of annexin II tetramer in the activation of plasminogen. *J. Biol. Chem*. 1998;273(8):4790-4799.

95. Das R, Burke T, Plow EF. Histone H2B as a functionally important plasminogen receptor on macrophages. *Blood*. 2007;110(10):3763-3772.

96. Pluskota E, Soloviev DA, Bdeir K, Cines DB, Plow EF. Integrin alphaMbeta2 orchestrates and accelerates plasminogen activation and fibrinolysis by neutrophils. *J. Biol. Chem*. 2004;279(17):18063-18072.

97. Bergmann S, Rohde M, Hammerschmidt S. Glyceraldehyde-3-Phosphate Dehydrogenase of Streptococcus pneumoniae Is a Surface-Displayed Plasminogen-Binding Protein. *Infect Immun*. 2004;72(4):2416-2419.

98. Miles LA, Andronicos NM, Baik N, Parmer RJ. Cell-Surface Actin Binds Plasminogen and Modulates Neurotransmitter Release from Catecholaminergic Cells. *The Journal of Neuroscience*. 2006;26(50):13017 -13024.

99. Kanalas JJ. Analysis of plasmin binding and urokinase activation of plasminogen bound to the Heymann nephritis autoantigen, gp330. *Arch. Biochem. Biophys.* 1992;299(2):255-260.

100. Miles LA, Dahlberg CM, Plescia J, et al. Role of cell-surface lysines in plasminogen binding to cells: identification of alpha-enolase as a candidate plasminogen receptor. *Biochemistry.* 1991;30(6):1682-1691.

101. Borza DB, Morgan WT. Acceleration of plasminogen activation by tissue plasminogen activator on surface-bound histidine-proline-rich glycoprotein. *J. Biol. Chem.* 1997;272(9):5718-5726.

102. Andronicos NM, Chen EI, Baik N, et al. Proteomics-based discovery of a novel, structurally unique, and developmentally regulated plasminogen receptor, Plg-RKT, a major regulator of cell surface plasminogen activation. *Blood*. 2010;115(7):1319-1330.

103. Wang W, Boffa MB, Bajzar L, Walker JB, Nesheim ME. A study of the mechanism of inhibition of fibrinolysis by activated thrombin-activable fibrinolysis inhibitor. *J. Biol. Chem*. 1998;273(42):27176-27181.

104. Swaisgood CM, Schmitt D, Eaton D, Plow EF. In vivo regulation of plasminogen function by plasma carboxypeptidase B. *J. Clin. Invest*. 2002;110(9):1275-1282.

105. Eaton DL, Malloy BE, Tsai SP, Henzel W, Drayna D. Isolation, molecular cloning, and partial characterization of a novel carboxypeptidase B from human plasma. *J. Biol. Chem*. 1991;266(32):21833-21838.

106. Foley JH, Cook PF, Nesheim ME. Kinetics of activated thrombin-activatable fibrinolysis inhibitor (TAFIa)-catalyzed cleavage of C-terminal lysine residues of fibrin degradation products and removal of plasminogen-binding sites. *J. Biol. Chem*. 2011;286(22):19280-19286.

107. Redlitz A, Tan AK, Eaton DL, Plow EF. Plasma carboxypeptidases as regulators of the plasminogen system. *J. Clin. Invest*. 1995;96(5):2534-2538.

108. Bouma BN, Marx PF, Mosnier LO, Meijers JC. Thrombin-activatable fibrinolysis inhibitor (TAFI, plasma procarboxypeptidase B, procarboxypeptidase R, procarboxypeptidase U). *Thromb. Res*. 2001;101(5):329-354.

109. Gerke V, Moss SE. Annexins: from structure to function. *Physiol. Rev.* 2002;82(2):331-371.

110. Futter CE, White IJ. Annexins and endocytosis. *Traffic*. 2007;8(8):951-958.

111. Aunis D, Langley K. Physiological aspects of exocytosis in chromaffin cells of the adrenal medulla. *Acta Physiol. Scand*. 1999;167(2):89-97.

112. Hayes MJ, Moss SE. Annexins and disease. *Biochem. Biophys. Res. Commun*. 2004;322(4):1166-1170.

113. Gilmore WS, Olwill S, McGlynn H, Alexander HD. Annexin A2 expression during cellular differentiation in myeloid cell lines. *Biochem. Soc. Trans*. 2004;32(Pt 6):1122-1123.

114. Takagi H, Asano Y, Yamakawa N, Matsumoto I, Kimata K. Annexin 6 is a putative cell surface receptor for chondroitin sulfate chains. *J. Cell. Sci*. 2002;115(Pt 16):3309-3318.

115. Kirilenko A, Golczak M, Pikula S, Buchet R, Bandorowicz-Pikula J. GTP-induced membrane binding and ion channel activity of annexin VI: is annexin VI a GTP biosensor? *Biophys. J*. 2002;82(5):2737-2745.

116. Kim KM, Kim DK, Park YM, Kim CK, Na DS. Annexin-I inhibits phospholipase A2 by specific interaction, not by substrate depletion. *FEBS Lett*. 1994;343(3):251-255.

117. Waisman DM. Annexin II tetramer: structure and function. *Mol. Cell. Biochem*. 1995;149-150:301-322.

118. Gerke V. Tyrosine protein kinase substrate p36: a member of the annexin family of Ca2+/phospholipid-binding proteins. *Cell Motil. Cytoskeleton*. 1989;14(4):449-454.

119. Kumble KD, Vishwanatha JK. Immunoelectron microscopic analysis of the intracellular distribution of primer recognition proteins, annexin 2 and phosphoglycerate kinase, in normal and transformed cells. *J. Cell. Sci*. 1991;99 (Pt 4):751-758.

120. Kristoffersen EK, Matre R. Surface annexin II on placental membranes of the fetomaternal interface. *Am. J. Reprod. Immunol*. 1996;36(3):141-149.

121. Hajjar KA, Jacovina AT, Chacko J. An endothelial cell receptor for plasminogen/tissue plasminogen activator. I. Identity with annexin II. *J. Biol. Chem*. 1994;269(33):21191-21197.

122. Kwon M, MacLeod TJ, Zhang Y, Waisman DM. S100A10, annexin A2, and annexin a2 heterotetramer as candidate plasminogen receptors. *Front. Biosci*. 2005;10:300-325.

123. Vishwanatha JK, Jindal HK, Davis RG. The role of primer recognition proteins in DNA replication: association with nuclear matrix in HeLa cells. *J. Cell. Sci*. 1992;101 (Pt 1):25-34.

124. Eberhard DA, Karns LR, VandenBerg SR, Creutz CE. Control of the nuclear-cytoplasmic partitioning of annexin II by a nuclear export signal and by p11 binding. *J. Cell. Sci*. 2001;114(Pt 17):3155-3166.

125. Zokas L, Glenney JR. The calpactin light chain is tightly linked to the cytoskeletal form of calpactin I: studies using monoclonal antibodies to calpactin subunits. *The Journal of Cell Biology*. 1987;105(5):2111 -2121.

126. Harder T, Gerke V. The annexin II2p11(2) complex is the major protein component of the triton X-100-insoluble low-density fraction prepared from MDCK cells in the presence of Ca2+. *Biochim. Biophys. Acta*. 1994;1223(3):375-382.

127. Sargiacomo M, Sudol M, Tang Z, Lisanti M. Signal transducing molecules and glycosyl-phosphatidylinositol-linked proteins form a caveolin-rich insoluble complex in MDCK cells. *The Journal of Cell Biology*. 1993;122(4):789 -807.

128. Cavallo-Medved D, Sloane BF. Cell-surface cathepsin B: understanding its functional significance. *Curr. Top. Dev. Biol.* 2003;54:313-341.

129. Burger A, Berendes R, Liemann S, et al. The crystal structure and ion channel activity of human annexin II, a peripheral membrane protein. *J. Mol. Biol*. 1996;257(4):839-847.

130. Shao C, Zhang F, Kemp MM, et al. Crystallographic analysis of calcium-dependent heparin binding to annexin A2. *J. Biol. Chem*. 2006;281(42):31689-31695.

131. Sullivan DM, Wehr NB, Fergusson MM, Levine RL, Finkel T. Identification of oxidant-sensitive proteins: TNF-alpha induces protein glutathiolation. *Biochemistry.* 2000;39(36):11121-11128.

132. Glenney JR Jr, Tack BF. Amino-terminal sequence of p36 and associated p10: identification of the site of tyrosine phosphorylation and homology with S-100. *Proc. Natl. Acad. Sci. U.S.A*. 1985;82(23):7884-7888.

133. Jost M, Gerke V. Mapping of a regulatory important site for protein kinase C phosphorylation in the N-terminal domain of annexin II. *Biochim. Biophys. Acta*. 1996;1313(3):283-289.

134. Zheng L, Foley K, Huang L, et al. Tyrosine 23 phosphorylation-dependent cell-surface localization of annexin A2 is required for invasion and metastases of pancreatic cancer. *PLoS ONE*. 2011;6(4):e19390.

135. Gould KL, Woodgett JR, Isacke CM, Hunter T. The protein-tyrosine kinase substrate p36 is also a substrate for protein kinase C in vitro and in vivo. *Mol. Cell. Biol*. 1986;6(7):2738-2744.

136. Rescher U, Ludwig C, Konietzko V, Kharitonenkov A, Gerke V. Tyrosine phosphorylation of annexin A2 regulates Rho-mediated actin rearrangement and cell adhesion. *J Cell Sci*. 2008;121(13):2177-2185.

137. Gerke V, Weber K. Identity of p36K phosphorylated upon Rous sarcoma virus transformation with a protein purified from brush borders; calcium-dependent binding to non-erythroid spectrin and F-actin. *EMBO J*. 1984;3(1):227-233.

138. Biener Y, Feinstein R, Mayak M, et al. Annexin II is a novel player in insulin signal transduction. Possible association between annexin II phosphorylation and insulin receptor internalization. *J. Biol. Chem*. 1996;271(46):29489-29496.

139. Jiang Y, Chan JL, Zong CS, Wang LH. Effect of tyrosine mutations on the kinase activity and transforming potential of an oncogenic human insulin-like growth factor I receptor. *J. Biol. Chem*. 1996;271(1):160-167.

140. Brambilla R, Zippel R, Sturani E, et al. Characterization of the tyrosine phosphorylation of calpactin I (annexin II) induced by platelet-derived growth factor. *Biochem. J*. 1991;278 (Pt 2):447-452.

141. Luo W, Yan G, Li L, et al. Epstein-Barr virus latent membrane protein 1 mediates serine 25 phosphorylation and nuclear entry of annexin A2 via PI-PLC-PKCalpha/PKCbeta pathway. *Mol. Carcinog*. 2008;47(12):934-946.

142. Lauvrak SU, Hollås H, Døskeland AP, et al. Ubiquitinated annexin A2 is enriched in the cytoskeleton fraction. *FEBS Lett*. 2005;579(1):203-206.

143. Caplan JF, Filipenko NR, Fitzpatrick SL, Waisman DM. Regulation of annexin A2 by reversible glutathionylation. *J. Biol. Chem*. 2004;279(9):7740-7750.

144. Filipenko NR, Waisman DM. The C terminus of annexin II mediates binding to F-actin. *J. Biol. Chem*. 2001;276(7):5310-5315.

145. Filipenko NR, Kang HM, Waisman DM. Characterization of the Ca2+-binding sites of annexin II tetramer. *J. Biol. Chem*. 2000;275(49):38877-38884.

146. Kassam G, Manro A, Braat CE, et al. Characterization of the heparin binding properties of annexin II tetramer. *J. Biol. Chem*. 1997;272(24):15093-15100.

147. Choi KS, Fitzpatrick SL, Filipenko NR, et al. Regulation of plasmin-dependent fibrin clot lysis by annexin II heterotetramer. *J. Biol. Chem*. 2001;276(27):25212-25221.

148. O'Connell PA, Surette AP, Liwski RS, Svenningsson P, Waisman DM. S100A10 regulates plasminogen-dependent macrophage invasion. *Blood*. 2010;116(7):1136-1146.

149. Kassam G, Le BH, Choi KS, et al. The p11 subunit of the annexin II tetramer plays a key role in the stimulation of t-PA-dependent plasminogen activation. *Biochemistry.* 1998;37(48):16958-16966.

150. Deora AB, Kreitzer G, Jacovina AT, Hajjar KA. An annexin 2 phosphorylation switch mediates p11-dependent translocation of annexin 2 to the cell surface. *J. Biol. Chem.* 2004;279(42):43411-43418.

151. He K-L, Deora AB, Xiong H, et al. Endothelial cell annexin A2 regulates polyubiquitination and degradation of its binding partner S100A10/p11. *J. Biol. Chem*. 2008;283(28):19192-19200.

152. Puisieux A, Ji J, Ozturk M. Annexin II up-regulates cellular levels of p11 protein by a post-translational mechanisms. *Biochem. J.* 1996;313 (Pt 1):51-55.

153. Emans N, Gorvel JP, Walter C, et al. Annexin II is a major component of fusogenic endosomal vesicles. *J. Cell Biol*. 1993;120(6):1357-1369.

154. Zobiack N, Rescher U, Ludwig C, Zeuschner D, Gerke V. The annexin 2/S100A10 complex controls the distribution of transferrin receptor-containing recycling endosomes. *Mol. Biol. Cell*. 2003;14(12):4896-4908.

155. Morel E, Gruenberg J. The p11/S100A10 light chain of annexin A2 is dispensable for annexin A2 association to endosomes and functions in endosomal transport. *PLoS ONE*. 2007;2(10):e1118.

156. Harder T, Gerke V. The subcellular distribution of early endosomes is affected by the annexin II2p11(2) complex. *J. Cell Biol*. 1993;123(5):1119-1132.

157. Morel E, Gruenberg J. Annexin A2 binding to endosomes and functions in endosomal transport are regulated by tyrosine 23 phosphorylation. *J. Biol. Chem*. 2009;284(3):1604-1611.

158. Chasserot-Golaz S, Vitale N, Umbrecht-Jenck E, et al. Annexin 2 promotes the formation of lipid microdomains required for calcium-regulated exocytosis of dense-core vesicles. *Mol. Biol. Cell*. 2005;16(3):1108-1119.

159. Lorusso A, Covino C, Priori G, et al. Annexin2 coating the surface of enlargeosomes is needed for their regulated exocytosis. *EMBO J*. 2006;25(23):5443-5456.

160. Gerke V, Creutz CE, Moss SE. Annexins: linking Ca2+ signalling to membrane dynamics. *Nat. Rev. Mol. Cell Biol*. 2005;6(6):449-461.

161. Morel E, Parton RG, Gruenberg J. Annexin A2-dependent polymerization of actin mediates endosome biogenesis. *Dev. Cell*. 2009;16(3):445-457.

162. Hayes MJ, Shao D-M, Grieve A, et al. Annexin A2 at the interface between F-actin and membranes enriched in phosphatidylinositol 4,5,-bisphosphate. *Biochim. Biophys. Acta*. 2009;1793(6):1086-1095.

163. Yamada A, Irie K, Hirota T, et al. Involvement of the annexin II-S100A10 complex in the formation of E-cadherin-based adherens junctions in Madin-Darby canine kidney cells. *J. Biol. Chem*. 2005;280(7):6016-6027.

164. McVoy LA, Kew RR. CD44 and annexin A2 mediate the C5a chemotactic cofactor function of the vitamin D binding protein. *J. Immunol*. 2005;175(7):4754-4760.

165. Chung CY, Murphy-Ullrich JE, Erickson HP. Mitogenesis, cell migration, and loss of focal adhesions induced by tenascin-C interacting with its cell surface receptor, annexin II. *Mol. Biol. Cell*. 1996;7(6):883-892.

166. Benaud C, Gentil BJ, Assard N, et al. AHNAK interaction with the annexin 2/S100A10 complex regulates cell membrane cytoarchitecture. *J. Cell Biol*. 2004;164(1):133-144.

167. Borthwick LA, McGaw J, Conner G, et al. The formation of the cAMP/protein kinase A-dependent annexin 2-S100A10 complex with cystic fibrosis conductance regulator protein (CFTR) regulates CFTR channel function. *Mol. Biol. Cell*. 2007;18(9):3388-3397.

168. Muimo R. Regulation of CFTR function by annexin A2-S100A10 complex in health and disease. *Gen. Physiol. Biophys*. 2009;28 Spec No Focus:F14-19.

169. Harrist AV, Ryzhova EV, Harvey T, González-Scarano F. Anx2 interacts with HIV-1 Gag at phosphatidylinositol (4,5) bisphosphate-containing lipid rafts and increases viral production in 293T cells. *PLoS ONE*. 2009;4(3):e5020.

170. Valapala M, Vishwanatha JK. Lipid raft endocytosis and exosomal transport facilitate extracellular trafficking of Annexin A2. *J Biol Chem*. 2011. Available at: http://www.ncbi.nlm.nih.gov/pubmed/21737841. Accessed August 6, 2011.

171. Zhao W-Q, Waisman DM, Grimaldi M. Specific localization of the annexin II heterotetramer in brain lipid raft fractions and its changes in spatial learning. *J. Neurochem*. 2004;90(3):609-620.

172. Mohammad HS, Kurokohchi K, Yoneyama H, et al. Annexin A2 expression and phosphorylation are up-regulated in hepatocellular carcinoma. *Int. J. Oncol*. 2008;33(6):1157-1163.

173. Hou Y, Yang L, Mou M, et al. Annexin A2 regulates the levels of plasmin, S100A10 and Fascin in L5178Y cells. *Cancer Invest*. 2008;26(8):809-815.

174. Ohno Y, Izumi M, Kawamura T, et al. Annexin II represents metastatic potential in clear-cell renal cell carcinoma. *Br. J. Cancer.* 2009;101(2):287-294.

175. Zhong L-ping, Wei K-jie, Yang X, et al. Increased expression of Annexin A2 in oral squamous cell carcinoma. *Arch. Oral Biol*. 2009;54(1):17-25.

176. Bao H, Jiang M, Zhu M, et al. Overexpression of Annexin II affects the proliferation, apoptosis, invasion and production of proangiogenic factors in multiple myeloma. *Int. J. Hematol*. 2009;90(2):177-185.

177. Singh P. Role of Annexin-II in GI cancers: interaction with gastrins/progastrins. *Cancer Lett*. 2007;252(1):19-35.

178. Zhang L, Fogg DK, Waisman DM. RNA interference-mediated silencing of the S100A10 gene attenuates plasmin generation and invasiveness of Colo 222 colorectal cancer cells. *J. Biol. Chem*. 2004;279(3):2053-2062.

179. Erikson E, Erikson RL. Identification of a cellular protein substrate phosphorylated by the avian sarcoma virus-transforming gene product. *Cell*. 1980;21(3):829-836.

180. Hayes MJ, Moss SE. Annexin 2 has a dual role as regulator and effector of v-Src in cell transformation. *J. Biol. Chem*. 2009;284(15):10202-10210.

181. Rescher U, Ludwig C, Konietzko V, Kharitonenkov A, Gerke V. Tyrosine phosphorylation of annexin A2 regulates Rho-mediated actin rearrangement and cell adhesion. *J. Cell. Sci*. 2008;121(Pt 13):2177-2185.

182. Tanaka T, Akatsuka S, Ozeki M, et al. Redox regulation of annexin 2 and its implications for oxidative stress-induced renal carcinogenesis and metastasis. *Oncogene*. 2004;23(22):3980-3989.

183. Li Q, Ke F, Zhang W, et al. A role for the annexin A2 amino-terminal peptide in the plasmin-induced activation of human peripheral monocytes. *Mol. Immunol*. 2010;47(14):2405-2410.

184. Laumonnier Y, Syrovets T, Burysek L, Simmet T. Identification of the annexin A2 heterotetramer as a receptor for the plasmin-induced signaling in human peripheral monocytes. *Blood*. 2006;107(8):3342-3349.

185. Li Q, Laumonnier Y, Syrovets T, Simmet T. Plasmin triggers cytokine induction in human monocyte-derived macrophages. *Arterioscler. Thromb. Vasc. Biol*. 2007;27(6):1383-1389.

186. Rescher U, Gerke V. S100A10/p11: family, friends and functions. *Pflugers Arch*. 2008;455(4):575-582.

187. Donato R. S100: a multigenic family of calcium-modulated proteins of the EF-hand type with intracellular and extracellular functional roles. *Int. J. Biochem. Cell Biol*. 2001;33(7):637-668.

188. Santamaria-Kisiel L, Rintala-Dempsey AC, Shaw GS. Calcium-dependent and -independent interactions of the S100 protein family. *Biochem. J*. 2006;396(2):201-214.

189. Donato R. Functional roles of S100 proteins, calcium-binding proteins of the EF-hand type. *Biochim. Biophys. Acta*. 1999;1450(3):191-231.

190. Hiratsuka S, Watanabe A, Sakurai Y, et al. The S100A8-serum amyloid A3-TLR4 paracrine cascade establishes a pre-metastatic phase. *Nat. Cell Biol*. 2008;10(11):1349-1355.

191. Glenney J. Phospholipid-dependent Ca2+ binding by the 36-kDa tyrosine kinase substrate (calpactin) and its 33-kDa core. *J. Biol. Chem*. 1986;261(16):7247-7252.

192. Réty S, Sopkova J, Renouard M, et al. The crystal structure of a complex of p11 with the annexin II N-terminal peptide. *Nat. Struct. Biol*. 1999;6(1):89-95.

193. Gerke V, Weber K. The regulatory chain in the p36-kd substrate complex of viral tyrosine-specific protein kinases is related in sequence to the S-100 protein of glial cells. *EMBO J*. 1985;4(11):2917-2920.

194. Glenney JR Jr, Tack BF. Amino-terminal sequence of p36 and associated p10: identification of the site of tyrosine phosphorylation and homology with S-100. *Proc. Natl. Acad. Sci. U.S.A*. 1985;82(23):7884-7888.

195. Saris CJ, Kristensen T, D'Eustachio P, et al. cDNA sequence and tissue distribution of the mRNA for bovine and murine p11, the S100-related light chain of the protein-tyrosine kinase substrate p36 (calpactin I). *J. Biol. Chem*. 1987;262(22):10663-10671.

196. Zokas L, Glenney JR Jr. The calpactin light chain is tightly linked to the cytoskeletal form of calpactin I: studies using monoclonal antibodies to calpactin subunits. *J. Cell Biol*. 1987;105(5):2111-2121.

197. Yang X, Popescu NC, Zimonjic DB. DLC1 interaction with S100A10 mediates inhibition of in vitro cell invasion and tumorigenicity of lung cancer cells through a RhoGAP-independent mechanism. *Cancer Res*. 2011;71(8):2916-2925.

198. Bailleux A, Wendum D, Audubert F, et al. Cytosolic phospholipase A2-p11 interaction controls arachidonic acid release as a function of epithelial cell confluence. *Biochem. J*. 2004;378(Pt 2):307-315.

199. Girard C, Tinel N, Terrenoire C, et al. p11, an annexin II subunit, an auxiliary protein associated with the background K+ channel, TASK-1. *EMBO J*. 2002;21(17):4439-4448.

200. Okuse K, Malik-Hall M, Baker MD, et al. Annexin II light chain regulates sensory neuron-specific sodium channel expression. *Nature*. 2002;417(6889):653-656.

201. Borthwick LA, Neal A, Hobson L, et al. The annexin 2-S100A10 complex and its association with TRPV6 is regulated by cAMP/PKA/CnA in airway and gut epithelia. *Cell Calcium*. 2008;44(2):147-157.

202. Svenningsson P, Chergui K, Rachleff I, et al. Alterations in 5-HT1B receptor function by p11 in depression-like states. *Science*. 2006;311(5757):77-80.

203. Warner-Schmidt JL, Flajolet M, Maller A, et al. Role of p11 in cellular and behavioral effects of 5-HT4 receptor stimulation. *J. Neurosci*. 2009;29(6):1937-1946.

204. Mai J, Finley RL, Waisman DM, Sloane BF. Human Procathepsin B Interacts with the Annexin II Tetramer on the Surface of Tumor Cells. *Journal of Biological Chemistry.* 2000;275(17):12806 -12812.

205. Cavallo-Medved D, Mai J, Dosescu J, Sameni M, Sloane BF. Caveolin-1 mediates the expression and localization of cathepsin B, pro-urokinase plasminogen activator and their cell-surface receptors in human colorectal carcinoma cells. *J. Cell. Sci.* 2005;118(Pt 7):1493-1503.

206. Hajjar KA, Jacovina AT, Chacko J. An endothelial cell receptor for plasminogen/tissue plasminogen activator. I. Identity with annexin II. *J. Biol. Chem*. 1994;269(33):21191-21197.

207. Hajjar KA, Mauri L, Jacovina AT, et al. Tissue plasminogen activator binding to the annexin II tail domain. Direct modulation by homocysteine. *J. Biol. Chem*. 1998;273(16):9987-9993.

208. Fogg DK, Bridges DE, Cheung KK-T, et al. The p11 subunit of annexin II heterotetramer is regulated by basic carboxypeptidase. *Biochemistry*. 2002;41(15):4953-4961.

209. Falcone DJ, Borth W, Khan KM, Hajjar KA. Plasminogen-mediated matrix invasion and degradation by macrophages is dependent on surface expression of annexin II. *Blood*. 2001;97(3):777-784.

210. Zhang J, Guo B, Zhang Y, Cao J, Chen T. Silencing of the annexin II gene down-regulates the levels of S100A10, c-Myc, and plasmin and inhibits breast cancer cell proliferation and invasion. *Saudi Med J*. 2010;31(4):374-381.

211. Menell JS, Cesarman GM, Jacovina AT, et al. Annexin II and bleeding in acute promyelocytic leukemia. *N. Engl. J. Med*. 1999;340(13):994-1004.

212. O'Connell PA, Madureira PA, Berman JN, Liwski RS, Waisman DM. Regulation of S100A10 by the PML-RAR-{alpha} oncoprotein. *Blood*. 2011;117(15):4095-4105.

213. Ling Q, Jacovina AT, Deora A, et al. Annexin II regulates fibrin homeostasis and neoangiogenesis in vivo. *J. Clin. Invest*. 2004;113(1):38-48.

214. Hajjar KA, Guevara CA, Lev E, Dowling K, Chacko J. Interaction of the fibrinolytic receptor, annexin II, with the endothelial cell surface. Essential role of endonexin repeat 2. *J. Biol. Chem*. 1996;271(35):21652-21659.

215. Dejana E. Endothelial adherens junctions: implications in the control of vascular permeability and angiogenesis. *J. Clin. Invest.* 1996;98(9):1949-1953.

216. Speiser W, Anders E, Preissner KT, Wagner O, Müller-Berghaus G. Differences in coagulant and fibrinolytic activities of cultured human endothelial cells derived from omental tissue microvessels and umbilical veins. *Blood*. 1987;69(3):964-967.

217. Jackson CJ, Nguyen M. Human microvascular endothelial cells differ from macrovascular endothelial cells in their expression of matrix metalloproteinases. *Int. J. Biochem. Cell Biol.* 1997;29(10):1167-1177.

218. Gargett CE, Bucak K, Rogers PAW. Isolation, characterization and long-term culture of human myometrial microvascular endothelial cells. *Human Reproduction*. 2000;15(2):293 -301.

219. Andriopoulou P, Navarro P, Zanetti A, Lampugnani MG, Dejana E. Histamine induces tyrosine phosphorylation of endothelial cell-to-cell adherens junctions. *Arterioscler. Thromb. Vasc. Biol*. 1999;19(10):2286-2297.

220. Gong P, Angelini DJ, Yang S, et al. TLR4 signaling is coupled to SRC family kinase activation, tyrosine phosphorylation of zonula adherens proteins, and opening of the paracellular pathway in human lung microvascular endothelia. *J. Biol. Chem*. 2008;283(19):13437-13449.

221. Esser S, Lampugnani MG, Corada M, Dejana E, Risau W. Vascular endothelial growth factor induces VE-cadherin tyrosine phosphorylation in endothelial cells. *J. Cell. Sci*. 1998;111 (Pt 13):1853-1865.

222. FARQUHAR MG, PALADE GE. Junctional complexes in various epithelia. *J. Cell Biol*. 1963;17:375-412.

223. Lee DBN, Huang E, Ward HJ. Tight junction biology and kidney dysfunction. *American Journal of Physiology - Renal Physiology*. 2006;290(1):F20 -F34.

224. Shen W, Li S, Chung SH, et al. Tyrosine phosphorylation of VE-cadherin and claudin-5 is associated with TGF-β1-induced permeability of centrally derived vascular endothelium. *Eur. J. Cell Biol*. 2011;90(4):323-332.

225. Knust E. Regulation of epithelial cell shape and polarity by cell-cell adhesion (Review). *Mol. Membr. Biol*. 2002;19(2):113-120.

226. Lampugnani MG, Zanetti A, Breviario F, et al. VE-Cadherin Regulates Endothelial Actin Activating Rac and Increasing Membrane Association of Tiam. *Mol. Biol. Cell*. 2002;13(4):1175-1189.

227. Kouklis P, Konstantoulaki M, Malik AB. VE-cadherin-induced Cdc42 signaling regulates formation of membrane protrusions in endothelial cells. *J. Biol. Chem*. 2003;278(18):16230-16236.

228. Stamler J, Singel D, Loscalzo J. Biochemistry of nitric oxide and its redox-activated forms. *Science*. 1992;258(5090):1898 -1902.

229. Eto M, Barandiér C, Rathgeb L, et al. Thrombin suppresses endothelial nitric oxide synthase and upregulates endothelin-converting enzyme-1 expression by distinct pathways: role of Rho/ROCK and mitogen-activated protein kinase. *Circ. Res*. 2001;89(7):583-590.

230. Shaul PW. Endothelial nitric oxide synthase, caveolae and the development of atherosclerosis. *The Journal of Physiology*. 2003;547(1):21-33.

231. Lauer T, Kleinbongard P, Preik M, et al. Direct biochemical evidence for eNOS stimulation by bradykinin in the human forearm vasculature. *Basic Res. Cardiol*. 2003;98(2):84-89.

232. Riddell DR, Owen JS. Nitric oxide and platelet aggregation. *Vitam. Horm*. 1999;57:25-48.

233. Kubes P, Suzuki M, Granger DN. Nitric oxide: an endogenous modulator of leukocyte adhesion. *Proceedings of the National Academy of Sciences*. 1991;88(11):4651 -4655.

234. Stamler JS, Vaughan DE, Loscalzo J. Synergistic disaggregation of platelets by tissue-type plasminogen activator, prostaglandin E1, and nitroglycerin. *Circ. Res*. 1989;65(3):796-804.

235. Parkington HC, Coleman HA, Tare M. Prostacyclin and endothelium-dependent hyperpolarization. *Pharmacol. Res*. 2004;49(6):509-514.

236. Kelly LK, Wedgwood S, Steinhorn RH, Black SM. Nitric oxide decreases endothelin-1 secretion through the activation of soluble guanylate cyclase. *American Journal of Physiology - Lung Cellular and Molecular Physiology*. 2004;286(5):L984 -L991.

237. Schiffrin EL. Vascular endothelin in hypertension. *Vascul. Pharmacol*. 2005;43(1):19-29.

238. Pober JS, Sessa WC. Evolving functions of endothelial cells in inflammation. *Nat. Rev. Immunol*. 2007;7(10):803-815.

239. Birch KA, Ewenstein BM, Golan DE, Pober JS. Prolonged peak elevations in cytoplasmic free calcium ions, derived from intracellular stores, correlate with the extent of thrombin-stimulated exocytosis in single human umbilical vein endothelial cells. *J. Cell. Physiol*. 1994;160(3):545-554.

240. Teixeira MM, Williams TJ, Hellewell PG. Role of prostaglandins and nitric oxide in acute inflammatory reactions in guinea-pig skin. *Br. J. Pharmacol*. 1993;110(4):1515-1521.

241. Kiskin NI, Hellen N, Babich V, et al. Protein mobilities and P-selectin storage in Weibel-Palade bodies. *J. Cell. Sci*. 2010;123(Pt 17):2964-2975.

242. Bonfanti R, Furie BC, Furie B, Wagner DD. PADGEM (GMP140) is a component of Weibel-Palade bodies of human endothelial cells. *Blood*. 1989;73(5):1109-1112.

243. Middleton J, Neil S, Wintle J, et al. Transcytosis and surface presentation of IL-8 by venular endothelial cells. *Cell*. 1997;91(3):385-395.

244. Shen J, T-To SS, Schrieber L, King NJ. Early E-selectin, VCAM-1, ICAM-1, and late major histocompatibility complex antigen induction on human endothelial cells by flavivirus and comodulation of adhesion molecule expression by immune cytokines. *J. Virol*. 1997;71(12):9323-9332.

245. Lopez S, Prats N, Marco AJ. Expression of E-Selectin, P-Selectin, and Intercellular Adhesion Molecule-1 during Experimental Murine Listeriosis. *Am J Pathol*. 1999;155(4):1391-1397.

246. Schenkel AR, Mamdouh Z, Chen X, Liebman RM, Muller WA. CD99 plays a major role in the migration of monocytes through endothelial junctions. *Nat. Immunol*. 2002;3(2):143-150.

247. Albelda SM, Muller WA, Buck CA, Newman PJ. Molecular and cellular properties of PECAM-1 (endoCAM/CD31): a novel vascular cell-cell adhesion molecule. *The Journal of Cell Biology*. 1991;114(5):1059 -1068.

248. Vidal F, Colomé C, Martínez-González J, Badimon L. Atherogenic concentrations of native low-density lipoproteins down-regulate nitric-oxide-synthase mRNA and protein levels in endothelial cells. *Eur. J. Biochem*. 1998;252(3):378-384.

249. Badimon L, Storey RF, Vilahur G. Update on lipids, inflammation and atherothrombosis. *Thromb. Haemost*. 2011;105 Suppl 1:S34-42.

250. Chisolm GM, Steinberg D. The oxidative modification hypothesis of atherogenesis: an overview. *Free Radical Biology and Medicine*. 2000;28(12):1815-1826.

251. Tabas I. Macrophage apoptosis in atherosclerosis: consequences on plaque progression and the role of endoplasmic reticulum stress. *Antioxid. Redox Signal*. 2009;11(9):2333-2339.

252. Tonnesen MG, Feng X, Clark RA. Angiogenesis in wound healing. *J. Investig. Dermatol. Symp. Proc*. 2000;5(1):40-46.

253. Brodsky S, Chen J, Lee A, et al. Plasmin-dependent and -independent effects of plasminogen activators and inhibitor-1 on ex vivo angiogenesis. *Am. J. Physiol. Heart Circ. Physiol*. 2001;281(4):H1784-1792.

254. Carmeliet P, Jain RK. Molecular mechanisms and clinical applications of angiogenesis. *Nature*. 2011;473(7347):298-307.

255. Manalo DJ, Rowan A, Lavoie T, et al. Transcriptional regulation of vascular endothelial cell responses to hypoxia by HIF-1. *Blood*. 2005;105(2):659 -669.

256. Pugh CW, Ratcliffe PJ. Regulation of angiogenesis by hypoxia: role of the HIF system. *Nat Med*. 2003;9(6):677-684.

257. Simon AM, McWhorter AR. Vascular abnormalities in mice lacking the endothelial gap junction proteins connexin37 and connexin40. *Dev. Biol*. 2002;251(2):206-220.

258. Carmeliet P. Angiogenesis in health and disease. *Nat. Med*. 2003;9(6):653-660.

259. Pepper MS. Extracellular proteolysis and angiogenesis. *Thromb. Haemost*. 2001;86(1):346-355.

260. Lijnen HR, Collen D. Endothelium in hemostasis and thrombosis. *Prog Cardiovasc Dis*. 1997;39(4):343-350.

261. Esmon CT. Thrombomodulin as a model of molecular mechanisms that modulate protease specificity and function at the vessel surface. *FASEB J*. 1995;9(10):946-955.

262. Suzuki K, Kusumoto H, Deyashiki Y, et al. Structure and expression of human thrombomodulin, a thrombin receptor on endothelium acting as a cofactor for protein C activation. *EMBO J*. 1987;6(7):1891-1897.

263. Beckmann RJ, Schmidt RJ, Santerre RF, et al. The structure and evolution of a 461 amino acid human protein C precursor and its messenger RNA, based upon the DNA sequence of cloned human liver cDNAs. *Nucleic Acids Research*. 1985;13(14):5233 -5247.

264. Griffin JH, Fernández JA, Gale AJ, Mosnier LO. Activated protein C. *J. Thromb. Haemost*. 2007;5 Suppl 1:73-80.

265. Cines DB, Pollak ES, Buck CA, et al. Endothelial Cells in Physiology and in the Pathophysiology of Vascular Disorders. *Blood*. 1998;91(10):3527 -3561.

266. Colucci M, Balconi G, Lorenzet R, et al. Cultured human endothelial cells generate tissue factor in response to endotoxin. *J Clin Invest*. 1983;71(6):1893-1896.

267. Stähli BE, Camici GG, Steffel J, et al. Paclitaxel Enhances Thrombin-Induced Endothelial Tissue Factor Expression via c-Jun Terminal NH2 Kinase Activation. *Circulation Research*. 2006;99(2):149 -155.

268. Terry CM, Callahan KS. Protein kinase c regulates cytokine-induced tissue factor transcription and procoagulant activity in human endothelial cells. *Journal of Laboratory and Clinical Medicine*. 1996;127(1):81-93.

269. Zucker S, Mirza H, Conner CE, et al. Vascular endothelial groth factor induces tissue factor and matrix metalloproteinase production in endothelial cells: Conversion of prothrombin to thrombin results in progelatininase a activation and cell proliferation. *International Journal of Cancer.* 1998;75(5):780-786.

270. Yan S-F, Zou YS, Gao Y, et al. Tissue factor transcription driven by Egr-1 is a critical mechanism of murine pulmonary fibrin deposition in hypoxia. *Proceedings of the National Academy of Sciences*. 1998;95(14):8298 -8303.

271. Drake TA, Hannani K, Fei HH, Lavi S, Berliner JA. Minimally oxidized low-density lipoprotein induces tissue factor expression in cultured human endothelial cells. *Am J Pathol*. 1991;138(3):601-607.

272. Kataoka H, Hamilton JR, McKemy DD, et al. Protease-activated receptors 1 and 4 mediate thrombin signaling in endothelial cells. *Blood*. 2003;102(9):3224 -3231.

273. Pober JS, Lapierre LA, Stolpen AH, et al. Activation of cultured human endothelial cells by recombinant lymphotoxin: comparison with tumor necrosis factor and interleukin 1 species. *J. Immunol*. 1987;138(10):3319-3324.

274. Andrews RK, Berndt MC. Platelet adhesion: a game of catch and release. *J. Clin. Invest.* 2008. Available at: http://www.jci.org/articles/view/36883/pdf. Accessed August 12, 2011.

275. Li Z, Delaney MK, O'Brien KA, Du X. Signaling during platelet adhesion and activation. *Arterioscler. Thromb. Vasc. Biol*. 2010;30(12):2341-2349.

276. Wagner DD, Burger PC. Platelets in Inflammation and Thrombosis. *Arteriosclerosis, Thrombosis, and Vascular Biology*. 2003;23(12):2131 -2137.

277. Brass L. Understanding and evaluating platelet function. *Hematology Am Soc Hematol Educ Program*. 2010;2010:387-396.

278. Moshal KS, Sen U, Tyagi N, et al. Regulation of homocysteine-induced MMP-9 by ERK1/2 pathway. *Am. J. Physiol., Cell Physiol*. 2006;290(3):C883-891.

279. Undas A, Brozek J, Szczeklik A. Homocysteine and thrombosis: from basic science to clinical evidence. *Thromb. Haemost*. 2005;94(5):907-915.

280. Glushchenko AV, Jacobsen DW. Molecular targeting of proteins by L-homocysteine: mechanistic implications for vascular disease. *Antioxid. Redox Signal*. 2007;9(11):1883-1898.

281. Postea O, Koenen RR, Hristov M, Weber C, Ludwig A. Homocysteine up-regulates vascular transmembrane chemokine CXCL16 and induces CXCR6+ lymphocyte recruitment in vitro and in vivo. *J. Cell. Mol. Med*. 2008;12(5A):1700-1709.

282. McCully KS. Chemical pathology of homocysteine. IV. Excitotoxicity, oxidative stress, endothelial dysfunction, and inflammation. *Ann. Clin. Lab. Sci*. 2009;39(3):219-232.

283. Alkhoury K, Parkin SM, Homer-Vanniasinkam S, Graham AM. Chronic homocysteine exposure upregulates endothelial adhesion molecules and mediates leukocyte: endothelial cell interactions under flow conditions. *Eur J Vasc Endovasc Surg*. 2011;41(3):429-435.

284. Jacovina AT, Deora AB, Ling Q, et al. Homocysteine inhibits neoangiogenesis in mice through blockade of annexin A2-dependent fibrinolysis. *J. Clin. Invest*. 2009;119(11):3384-3394.

285. Lentz SR. Mechanisms of homocysteine-induced atherothrombosis. *J. Thromb. Haemost*. 2005;3(8):1646-1654.

286. Jacobsen DW, Catanescu O, Dibello PM, Barbato JC. Molecular targeting by homocysteine: a mechanism for vascular pathogenesis. *Clin. Chem. Lab. Med*. 2005;43(10):1076-1083.

287. Wotherspoon F, Laight DW, Shaw KM, Cummings MH. Review: Homocysteine, endothelial dysfunction and oxidative stress in type 1 diabetes mellitus. *The British Journal of Diabetes & Vascular Disease*. 2003;3(5):334 -340.

288. Papatheodorou L, Weiss N. Vascular oxidant stress and inflammation in hyperhomocysteinemia. *Antioxid. Redox Signal*. 2007;9(11):1941-1958.

289. Tyagi N, Sedoris KC, Steed M, et al. Mechanisms of homocysteine-induced oxidative stress. *Am. J. Physiol. Heart Circ. Physiol*. 2005;289(6):H2649-2656.

290. Stühlinger MC, Tsao PS, Her JH, et al. Homocysteine impairs the nitric oxide synthase pathway: role of asymmetric dimethylarginine. *Circulation*. 2001;104(21):2569-2575.

291. Looft-Wilson RC, Ashley BS, Billig JE, et al. Chronic diet-induced hyperhomocysteinemia impairs eNOS regulation in mouse mesenteric arteries. *Am. J. Physiol. Regul. Integr. Comp. Physiol*. 2008;295(1):R59-66.

292. Gu L, Hu X, Xue Z, et al. Potent homocysteine-induced ERK phosphorylation in cultured neurons depends on self-sensitization via system Xc-. *Toxicology and Applied Pharmacology*. 2010;242(2):209-223.

293. Tyagi N, Gillespie W, Vacek JC, et al. Activation of GABA-A receptor ameliorates homocysteine-induced MMP-9 activation by ERK pathway. *J. Cell. Physiol*. 2009;220(1):257-266.

294. Laumonnier Y, Syrovets T, Burysek L, Simmet T. Identification of the annexin A2 heterotetramer as a receptor for the plasmin-induced signaling in human peripheral monocytes. *Blood*. 2006;107(8):3342-3349.

295. Zhang J, McCrae KR. Annexin A2 mediates endothelial cell activation by antiphospholipid/anti-beta2 glycoprotein I antibodies. *Blood*. 2005;105(5):1964-1969.

296. Swisher JFA, Burton N, Bacot SM, Vogel SN, Feldman GM. Annexin A2 tetramer activates human and murine macrophages through TLR4. *Blood*. 2010;115(3):549-558.

297. Babiychuk EB, Draeger A. Annexins in cell membrane dynamics. Ca(2+)-regulated association of lipid microdomains. *J. Cell Biol*. 2000;150(5):1113-1124.

298. Fallahi-Sichani M, Linderman JJ. Lipid raft-mediated regulation of G-protein coupled receptor signaling by ligands which influence receptor dimerization: a computational study. *PLoS ONE*. 2009;4(8):e6604.

299. Karolczak K, Olas B. Mechanism of action of homocysteine and its thiolactone in hemostasis system. *Physiol Res*. 2009;58(5):623-633.

300. LAEMMLI UK. Cleavage of Structural Proteins during the Assembly of the Head of Bacteriophage T4. *Nature*. 1970;227(5259):680-685.

301. Towbin H, Staehelin T, Gordon J. Electrophoretic transfer of proteins from polyacrylamide gels to nitrocellulose sheets: procedure and some applications. *Proceedings of the National Academy of Sciences*. 1979;76(9):4350 -4354.

302. Kwon M, Yoon CS, Fitzpatrick S, et al. p22 is a novel plasminogen fragment with antiangiogenic activity. *Biochemistry*. 2001;40(44):13246-13253.

303. Khanna NC, Helwig ED, Ikebuchi NW, et al. Purification and characterization of annexin proteins from bovine lung. *Biochemistry*. 1990;29(20):4852-4862.

304. Ploplis VA, Carmeliet P, Vazirzadeh S, et al. Effects of disruption of the plasminogen gene on thrombosis, growth, and health in mice. *Circulation*. 1995;92(9):2585-2593.

305. Bugge TH, Flick MJ, Daugherty CC, Degen JL. Plasminogen deficiency causes severe thrombosis but is compatible with development and reproduction. *Genes Dev.* 1995;9(7):794-807.

306. Lenfors S, Gustafsson D. New model for in vivo studies of pharmacological interventions with endogenous fibrinolysis: effects of thrombin inhibitors. *Semin. Thromb. Hemost*. 1996;22(4):335-342.

307. Hantgan R, Fowler W, Erickson H, Hermans J. Fibrin assembly: a comparison of electron microscopic and light scattering results. *Thromb. Haemost*. 1980;44(3):119-124.

308. Niewiarowski S, Stewart GJ, Nath N, Sha AT, Lieberman GE. ADP, thrombin, and Bothrops atrox thrombinlike enzyme in platelet-dependent fibrin retraction. *Am. J. Physiol*. 1975;229(3):737-745.

309. Mao S-S, Holahan MA, Bailey C, et al. Demonstration of enhanced endogenous fibrinolysis in thrombin activatable fibrinolysis inhibitor-deficient mice. *Blood Coagul. Fibrinolysis*. 2005;16(6):407-415.

310. Dejana E, Quintana A, Callioni A, de Gaetano G. Bleeding time in laboratory animals. III - Do tail bleeding times in rats only measure a platelet defect? (the aspirin puzzle). *Thromb. Res*. 1979;15(1-2):199-207.

311. Flight SM, Johnson LA, Du QS, et al. Textilinin-1, an alternative anti-bleeding agent to aprotinin: Importance of plasmin inhibition in controlling blood loss. *Br. J. Haematol*. 2009;145(2):207-211.

312. Hoover-Plow J, Shchurin A, Hart E, et al. Genetic background determines response to hemostasis and thrombosis. *BMC Blood Disord*. 2006;6:6.

313. Matsuno H, Kozawa O, Niwa M, et al. Differential role of components of the fibrinolytic system in the formation and removal of thrombus induced by endothelial injury. *Thromb. Haemost*. 1999;81(4):601-604.

314. Murphy CT, Peers SH, Forder RA, et al. Evidence for the presence and location of annexins in human platelets. *Biochem. Biophys. Res. Commun*. 1992;189(3):1739-1746.

315. Benaud C, Gentil BJ, Assard N, et al. AHNAK interaction with the annexin 2/S100A10 complex regulates cell membrane cytoarchitecture. *J. Cell Biol*. 2004;164(1):133-144.

316. Puisieux A, Ji J, Ozturk M. Annexin II up-regulates cellular levels of p11 protein by a post-translational mechanisms. *Biochem. J*. 1996;313 (Pt 1):51-55.

317. van de Graaf SFJ, Hoenderop JGJ, Gkika D, et al. Functional expression of the epithelial Ca(2+) channels (TRPV5 and TRPV6) requires association of the S100A10-annexin 2 complex. *EMBO J*. 2003;22(7):1478-1487.

318. Chetcuti A, Margan SH, Russell P, et al. Loss of annexin II heavy and light chains in prostate cancer and its precursors. *Cancer Res*. 2001;61(17):6331-6334.

319. Miles LA, Parmer RJ. S100A10: a complex inflammatory role. *Blood*. 2010;116(7):1022-1024.

320. Ellis V, Whawell SA. Vascular smooth muscle cells potentiate plasmin generation by both urokinase and tissue plasminogen activator-dependent mechanisms: evidence for a specific tissue-type plasminogen activator receptor on these cells. *Blood*. 1997;90(6):2312-2322.

321. Li Q, Laumonnier Y, Syrovets T, Simmet T. Plasmin triggers cytokine induction in human monocyte-derived macrophages. *Arterioscler. Thromb. Vasc. Biol*. 2007;27(6):1383-1389.

322. Dauphinee SM, Karsan A. Lipopolysaccharide signaling in endothelial cells. *Lab. Invest*. 2006;86(1):9-22.

323. Johns DG, Webb RC, Charpie JR. Impaired ceramide signalling in spontaneously hypertensive rat vascular smooth muscle: a possible mechanism for augmented cell proliferation. *J. Hypertens*. 2001;19(1):63-70.

324. Pearson G, Robinson F, Beers Gibson T, et al. Mitogen-Activated Protein (MAP) Kinase Pathways: Regulation and Physiological Functions. *Endocrine Reviews*. 2001;22(2):153 -183.

325. Syrovets T, Jendrach M, Rohwedder A, Schüle A, Simmet T. Plasmin-induced expression of cytokines and tissue factor in human monocytes involves AP-1 and IKKbeta-mediated NF-kappaB activation. *Blood*. 2001;97(12):3941-3950.

326. Khajuria A, Houston DS. Induction of monocyte tissue factor expression by homocysteine: a possible mechanism for thrombosis. *Blood*. 2000;96(3):966-972.

327. Zhang JJ, Kelm RJ, Biswas P, Kashgarian M, Madri JA. PECAM-1 modulates thrombin-induced tissue factor expression on endothelial cells. *J. Cell. Physiol*. 2007;210(2):527-537.